Scalar Fields in Astrophysics

Thesis presented for the degree of Doctor of Philosophy to the University of Glasgow, 1992.

Gary Joseph Benson

Particle Theory Group
Department of Physics and Astronomy
University of Glasgow
Glasgow
Scotland

December 1992

ProQuest LLC.
789 East Eisenhower Parkway
P.O. Box 1346
Ann Arbor, MI 48106 – 1346

Abstract

This thesis is about the possible consequences of the existence of scalar particles on astrophysical objects, particularly neutron stars. The existence of such particles is hypothesized by certain developments in elementary particle theory. These particles are assumed to be *light*, having masses less than, or of approximately one electron volt. The stipulation that these particles are light is in no way discriminatory; it just so happens that over astrophysical distances lighter particles have far greater influence because of their greater range, i.e. their Compton wavelength, and so are more interesting in this context.

The introduction of this work will, after giving a brief historical summary of each subject, show how scalar fields arise in various theoretical contexts within the disciplines of particle physics and cosmology. It will also show how highly interlinked these disciplines are, and how developments in each drive and influence the other. Also included in the introduction will be a review of neutron stars and their properties and a summary of the methods of nuclear theory.

The first chapter consists of the construction of an explicit model of static neutron star and scalar field configurations. The properties of these configurations are discussed at length and then used to give bounds on the coupling of this hypothetical scalar field to ordinary matter. Certain technical difficulties arising from the presence of the scalar field are also discussed.

The second chapter consists of a study of the radial oscillations of the static configurations which were found in the preceding chapter. The equations of motion for the oscillations of the neutron star and scalar field are derived, after which the stability of the configurations is discussed with particular reference to the possibility of monopole scalar radiation. Lastly, an approximate calculation is made of the relaxation time of radial oscillations for a star which is radiating scalar waves.

The last chapter contains a simple model of gravitational collapse with a scalar field, constructed in the manner of the Oppenheimer–Snyder model. After integration of the Einstein equations for the interior, the problem of matching to an appropriate exterior is considered. It is found that, contrary to naive expectation, matching is greatly complicated by the presence of a scalar field;

both technical and conceptual problems are found to arise.

Finally, the necessary conditions and procedures for construction of more general exterior solutions, which this problem seems to require, are given and discussed.

Declaration

The work presented in this thesis was done entirely by myself, except where otherwise indicated by a reference. Chapter two was a collaboration between myself, my supervisor Professor R.G.Moorhouse and Professor A.B.Henriques of the Instituto Superior Técnico in Lisbon.

All the numerical work contained in this thesis was done entirely by myself, and so I must take responsibility for any errors in the numbers I have presented.

Gary Joseph Benson

Acknowledgements

I would like to thank my supervisor Professor Moorhouse for his help and timely advice over the past three years, which was always given in a gentle, friendly and positive manner. I only hope that I took this good advice in the spirit in which it was offered. Thanks also to Professor Henriques in Lisbon, who in the course of my studies visited Glasgow on a couple of occasions. It was a pleasure to meet and work with Alfredo, who offered his insights freely in a cooperative and gentlemanly manner. Thanks to the other theory staff also, in particular David Sutherland, and also to Colin Froggatt for tolerating my attempts at librarianship.

Thanks also to my fellow students with whom I have shared lunches, dinners, drinking sessions, football matches and games of pool with over the past three years. In no particular order; Carolyn, David, Amarjit, Alan, David, Helen, Ely, Simon, Gerry, Brian, Luke and David.

Thanks to the Science and Engineering Research Council for a postgraduate studentship.

Thanks to my first employer, whoever it is.

To Mum and Dad

Contents

3. Gravitational Collapse of Scalar Fields

3.1 Equations of Motion

3.2 Interior Solutions: Discussion

3.3 Exterior Solutions and Matching Conditions

3.4 Conclusion

Figure Captions

References

4. Overview and Conclusions

Introduction

Particle Physics, Cosmology, Neutron Stars and the role of Scalar Fields

The role of this introduction is to provide a solid motivation for the material studied in this thesis; that is, to show how scalar fields have arisen and been utilised in particle physics, and, furthermore, to show how this has repercussions in the field of cosmology. This is to provide something of a prelude and a motivation for the topic of the main body of this thesis, that is, to investigate how light scalars can alter the structure of compact objects, particularly neutron stars.

Particle physics, cosmology, their problems, and their necessary extensions concerning scalar fields will be reviewed first of all. Again, this is to provide motivation for the study of the scalar field in the astrophysical context. The 'astrophysical context' this thesis is chiefly concerned with, is neutron stars and in the final introductory section a review of the properties of neutron stars will be given, this time to provide some essential background information which will be of use later on. A review of some of the research concerning the equation of state of nuclear matter is also given since this is by far the most important ingredient used in the building of neutron star models.

0.1 Particle Physics

At the present time the most successful physical theory of fundamental particles and forces is the, rather aptly named, Standard Model. The successes of this theory have been phenomenal and are yet increasing due to the continued efforts of experimenters at CERN and other places.

So successful has the theory been that, in fact, there have been no clear–cut failures so far; despite this success, it is universally agreed by theoretical physicists that the Standard Model is in no way the final word on the subject of elementary particles.

To understand why this is so it necessary to review and criticise the Standard Model.

0.1.1 Gauge theories and the Standard Model

It is generally thought that any fundamental description of nature must be modelled in terms of a relativistic quantum field theory; the trouble is that there are too many possible choices of theory one can make. Within the class of all theories there exists a subclass known as *Gauge Theories* which occupy a very special position; so far, all known viable physical theories are of this type; Quantum Electrodynamics, the Standard Model and almost every plausible extension or would-be successor to these.

The Standard Model is a gauge theory; what this means is that there exists a special type of symmetry among the constituent fields of the action which give rise to a number of desirable properties, e.g. renormalizability. The origin of this type of symmetry goes back to the work of Hermann Weyl in the 1920s[1], who discovered an 'excellent' reason for the existence of the electromagnetic field. Consider the lagrangian density for a free electron

$$\mathcal{L} = \overline{\Psi}\left(i\gamma^{\mu}\partial_{\mu} - m\right)\Psi \tag{1}$$

Notice that this expression is invariant under the global phase transformation of the fields

$$\Psi \rightarrow e^{i\alpha}\Psi \qquad \overline{\Psi} \rightarrow e^{-i\alpha}\overline{\Psi} \tag{2}$$

[1]He was at this time chiefly involved in trying to unify general relativity with electromagnetism by means of scale invariance.

Weyl suggested that one should be able to do this at each point in space, i.e. putting $\alpha \rightarrow \alpha(x)$ and still maintain the invariance of the action. To do this requires the introduction of a 'compensating' field, A_μ, which is massless. After introducing kinetic terms for A_μ one has the action for quantum electrodynamics, A_μ being of course, the photon field.

Whether one agrees that this is an 'excellent' idea or not is irrelevant—it works!

In more mathematically sophisticated terms, the transformations in (2) are elements of a compact[2] abelian Lie group known as U(1). The extension to compact non-abelian groups was made in 1954 by Yang and Mills and remained for some time a mathematical curiosity until the idea was used by Glashow, Weinberg and Salam to build a candidate theory of the weak nuclear interaction, and later used by others to encompass the strong nuclear force.

The Standard Model is an $SU(3) \otimes SU(2) \otimes U(1)$ gauge theory which is spontaneously broken to $SU(3) \otimes U(1)$. The quantum numbers associated with the respective groups are termed color, weak isosopin and weak hypercharge. There are three types of field in the theory; the force–carrying gauge bosons of which there are twelve, consisting of eight gluons(strong), 3 vector bosons(weak) plus the photon which transform as $(8,1) \oplus (1,3) \oplus (1,1)$ under $SU(3) \otimes SU(2)$; fifteen 4-component complex spinor matter fields

$$\left[\begin{pmatrix} \nu_e \\ e^i \end{pmatrix}_L \; ; \; e_R \; ; \; \begin{pmatrix} u_i \\ d_i \end{pmatrix}_L \; ; \; u_{iR} \; ; \; d_{iR} \right] \tag{3}$$

which transform as $(1,2) \oplus (1,1) \oplus (3,2) \oplus (3,1) \oplus (3,1)$ under $SU(3) \otimes SU(2)$. There are three families of this type.

The last type is of course, the scalar fields; one complex isodoublet with four degrees of freedom, which has not been detected so far, and which, through the mechanism of spontaneous symmetry breaking(SSB) gives masses to the fermions through their mutual Yukawa couplings, and masses to the vector bosons, plus an extra longitudinal degree of freedom for the gauge bosons. Gauge bosons are naturally massless but the weak force is very short ranged, hence the need for masses.

[2]No one has yet found a use for non-compact gauge theories.

0.1.2 Quantum Chromodynamics

The Standard Model separates naturally into two quite distinct theories, quantum chromodynamics(QCD) and electro-weak theory(EW). The lagrangian density of QCD is

$$\mathcal{L}_{QCD} = \sum_f \overline{\Psi}_f \left(i\gamma^\mu D_\mu + m_f\right) \Psi_f - \frac{1}{2} Tr F_{\mu\nu} F^{\mu\nu} + \frac{g^2}{32\pi^2} \theta F.\tilde{F} \qquad (4)$$

where D is the covariant derivative and f stands for the different flavours of quarks having different masses and charges. The quarks are commonly known as up, down, charmed, strange, bottom and top. Up, charm and top have charge $+\frac{2}{3}$, while down, strange and bottom have charge $-\frac{1}{3}$. The up and down are the lightest, the heaviest, the top is as yet undiscovered.

The evidence that QCD is the correct theory of the strong interaction comes from two distinct sources; one is the 'hard' evidence from deep inelastic scattering, the other being the predictions of 'soft' QCD in the form of chiral symmetry breaking theorems and the static quark model.

One very important thing to bear in mind is that quarks are not observed as free particles, they are only seen as bound states, i.e. the known hadrons.

Deep inelastic scattering at high energy and momentum transfer provides us with very strong evidence that the hadrons are composed of more elementary entities, and moreover that these constituents are fermions. These experiments also tell us that these 'quarks' are not the only constituents—the quarks only account for half the momentum of the nucleon—but there exist other particles as well, the gluons.

The gluons are thought to be the carriers of the colour force, and so bind the nucleus together. The observational data produced in this type of experiment are correctly explained in terms of the parton model. The phenomenon known as Bjorken scaling, correctly interpreted in terms of the parton model gives the most direct evidence that hadrons are not elementary.

The non-relativistic quark model of the hadrons also provides evidence for QCD. In this theory all hadrons consist of quarks; mesons are quark–anti-quark bound states while baryons are three quark states. This model favours these

types of bound states only, and replicates the low lying spectra of the heavier mesons reasonably accurately i.e. the charmonium, $c\bar{c}$ and bottomium, $b\bar{b}$.

For example, in the quark model the ground state of the proton has spin-$\frac{1}{2}$ and is modelled as one up and two down quarks, giving charge $+1$, in a relative s-state of orbital angular momentum, with two of the quark spins 'pointing' up while the other 'points' down. Such thinking is overly simplistic—where are the gluons in this strongly interacting system?—but the model is a reasonably good first approximation to reality. Inspired by the surprising success of this naively attractive picture one feels motivated to give a more rigorous treatment, but it is extremely difficult to do much better; calculation of bound states in quantum field theory is notoriously difficult and lattice simulations are as yet in an early stage of development.

The 'naive' quark model also tells us that quarks have an extra quantum number, called color, associated with them. According to the model the wave-function of the quarks should be symmetric in space$\otimes$spin$\otimes$flavour. The Δ^{++} is interpreted as having three up quarks in an orbital s-state which violates the Pauli Principle unless one adds color. The number of 'colors' is suggested as three from the observation of the R-ratio and from the chiral symmetry prediction for the width of the decay $\Pi^o \rightarrow \gamma\gamma$. Anomaly cancellation constraints also suggest that there should be three families of quarks for each lepton family.

Chiral symmetry is a symmetry of low energy QCD. It originates when one assumes that the up and down quarks are massless. In this theory the pion is interpreted as a pseudo–Goldstone boson. Since chiral symmetry is only approximate, i.e. the up and down quarks being massive, yet light, the pion gets a small mass. This is thought to explain why the pion is much lighter than the next lightest meson, the rho. Chiral symmetry predicts that the gluons have spin-1 and much else in terms of the so-called 'soft pion theorems'.

0.1.3 Electro-weak Theory

The lagrangian density for the electro-weak theory is

$$\begin{aligned}\mathcal{L}_{EW} &= -\frac{1}{4}G^2 - \frac{1}{4}B^2 + \sum_i \left(\overline{\Psi}^i{}_L i\gamma^\mu D_\mu \Psi^i{}_L + \overline{\Psi}^i{}_R i\gamma^\mu D_\mu \Psi^i{}_R\right) + \\ &\quad |D_\mu \Phi|^2 - c\left(\Phi^*\Phi - \mu^2\right)^2 + \sum_{leptons} \left(\Lambda^i \left(\overline{\Psi}^i{}_L \Phi\right) \Psi^i{}_R + h.c.\right) + \\ &\quad \sum_{quarks} \left(\Lambda^{ij}{}_{(d)} \left(\overline{\Phi}^i{}_L \Phi\right) \Psi^{j(d)}{}_R + \Lambda^{ij}{}_{(u)} \left(\overline{\Psi}^i{}_L \sigma_2 \Phi^*\right) \Psi^{j(u)}{}_R + h.c.\right) \quad (5)\end{aligned}$$

where G and B are the kinetic terms for the SU(2) and U(1) gauge fields respectively(the physical $W^\pm, Z, \gamma$ are linear combinations of these). The subscripts L, R denote left and right handed fields respectively.

For spontaneous symmetry breaking to occur one requires $\mu^2 > 0$, then, instead of having massless gauge bosons with only transverse degrees of freedom, one gets massive vector bosons, three of the complex scalar doublet's degrees of freedom evaporating, to leave a massive neutral Higgs boson which couples to the vector bosons as gM_W, gM_Z and as $g\frac{m_f}{M_W}$ to the fermions, g being the SU(2) coupling constant. There are no right-handed neutrinos in the standard electro-weak theory.

The successes of the electro-weak lie primarily in the discovery of the vector bosons at exactly the predicted mass, and in the measurement of the width of the Z, which in turns implies that the number of generations of neutrinos is three.

The untested aspects of the theory lie in examining the self-coupling of the gauge bosons, hence testing the explicitly non-abelian features of the gauge theory, finding the top quark, which *must* exist, and finding the Higgs boson, of which there may be many or none. Of these aspects divulging the detailed structure of the Higgs sector is the most important.

Despite all these successes the Standard Model is seriously flawed; it is the best we have, and it does give the correct answers to all the questions we are capable of asking, but it provides remarkably few convincing explanations to the basic questions: Why are there three families? Why is charge quantized? Why are there no right-handed neutrinos? Are the forces of nature genuinely distinct, or are they the remnants of a single theory? and so on, and so on.

Given enough parameters, one can always fit a theory to the data but this is a very unsatisfying situation for anyone interested in finding the ultimate explanations.

For these reasons, theorists have been trying for a long time to find an all-encompassing theory with only a very small number of free parameters, which contains the standard model and in terms of which one may determine the large number of arbitrary parameters found therein. Ambitious attempts have been made towards this with the so-called theory of Grand-Unified Theories(GUTS).

Beyond any grand-unification lies the spectre of gravity, so long ignored by particle theorists. Eventually it too must be found a place in these grand schemes. In this case supergravity and strings are the main contenders as Theories of Everything(TOES).

Later on will be given an indication of how scalars may play an important role in the theory of strings and in the context of the unification program in general, but first it is fruitful and necessary to consider one of the problems of the Standard Model in some detail, since it has direct relevance to the possibility of light scalar particles and is also instructive in that it shows how particle theorists work in attempting to extend the Standard Model, but in a conceptually simple way.

This is of course the 'Strong CP problem' and its 'solution' via the axion.

0.1.4 The Strong CP Problem and the Axion

If one examines the last term of $\mathcal{L}_{QCD}$ one can see that it can give rise to CP violation in the strong interaction. This is because $F.\tilde{F}$ is odd under parity and even under charge-conjugation since $\tilde{F}$ is given by

$$\tilde{F}^{\mu\nu} = \epsilon^{\mu\nu\alpha\beta} F_{\alpha\beta} \tag{6}$$

where $\epsilon^{\mu\nu\alpha\beta}$ is the completely antisymmetric tensor in four dimensions. To proceed further it is necessary to make some manipulations of the θ-term.

It can be shown that $F.\tilde{F}$ can be written as $\partial_\mu K^\mu$ where

$$K^\mu = \epsilon^{\mu\nu\alpha\beta} A^a{}_\nu \left[F^a{}_{\alpha\beta} - \frac{g}{3} f^{abc} A^b{}_\alpha A^c{}_\beta \right] \tag{7}$$

This is known as the Chern-Simons current and it is gauge-dependent.

The contribution to the action of the θ-term can thus be written $\int \partial_\mu K^\mu$ which upon using Gauss's divergence theorem becomes $\int dS_\mu K^\mu$, where the bounding surface, S_μ, encloses an infinite volume. Such surface terms are usually discarded as they do not normally contribute to the action. However, in this case the contribution need not vanish since K^μ is not necessarily zero at infinity. One can however get rid of the θ term in the action by a chiral rotation of the fields, this in turn introduces a θ dependent, CP-violating phase into the quark mass matrix. This term in the quark mass matrix gives rise to an electric dipole moment for the neutron. Experimentally this is very small, necessitating that θ be very small also; $|\theta| < 10^{-9}$.

This is the strong CP-problem; θ is a strong interaction parameter, therefore its 'natural' scale is of the order of unity, but it is in fact minute. The fact that it is so small seems to suggest that it should be exactly zero, but there is no reason coming from QCD why this should be.

Peccei and Quinn suggested that the action should have an exact chiral symmetry—in which case the CP-violating piece of the mass matrix vanishes. To make the action invariant under this transformation they suggested introducing another Higgs doublet into the theory. This results in the theory having 2 charged and 3 neutral Higgs particles plus an 'axion' with a very small mass. Other variations on this idea include the KSVZ version which in addition to an extra doublet has a scalar and a heavy fermion, and the DFSZ variant which has two extra doublets plus a scalar.

All these ideas introduce an extremely light, extremely weakly interacting pseudo-scalar particle known generically as an 'axion'. The mass of the axion is approximately $10^{-2}/f(\mathrm{GeV})^2$ where f must be greater than 10^9GeV.

0.1.5 Extensions of the Standard Model

Other more substantial extensions to the Standard Model include GUTS and supersymmetric theories. The basic idea of the GUT scenario is that the gauge group of the Standard Model is a broken down remnant of a single, grand-unified group, G which contains the Standard Model group as a subgroup and which only has a single coupling constant. Because this larger symmetry is not manifest

means that it must be broken at some very high energy; this leads to problems of its own, the 'gauge hierarchy problem'.

Evidence for this hypothesis comes from the renormalization group flow of the Standard Model coupling constants. It is found that as we increase the energy of the particle interactions, the strong force becomes weaker while the weak force and electromagnetism become stronger. By extrapolation one finds that all the forces are of approximately equal strength at the colossal energy of 10^{15}GeV. This is the unification energy.

Supersymmetry(SUSY) is a symmetry between bosons and fermions, perhaps providing the essential link between the duality of 'force', which is mediated by bosons, and 'matter' which is in the form of fermions. This idea has a great deal of mathematical elegance and has been used over the years to do various things; to provide much needed cancellations in field theory calculations, to provide finiteness, to solve the gauge hierarchy problem and to sidestep the famous no-go theorem of Coleman and Mandula; that it was impossible to unify the compact Lie groups of gauge-invariant particle physics and the Poincare group of general relativity. Although very interesting, it would be inappropriate to go into too much detail about the myriad uses of SUSY. Nevertheless SUSY is a very beguiling idea; so far the concept of symmetry has been of profound importance to the model building process of particle physics and SUSY is in some sense the last remaining unexploited symmetry there is. Apart from the elegant theoretical reasons mentioned previously, there may actually be some evidence for the existence of SUSY. Recent calculations suggest that to truly unify the coupling constants of the Standard Model, i.e. to make them equal at exactly one point, supersymmetric contributions are required. In any case, we shall probably know once the next generation of colliders are built, SUSY predicts that at least one of the SUSY particles must be absolutely stable and reasonably light.

GUTS and SUSY have largely been superseded in recent years by interest in by far the most compelling candidate TOE so far invented, the Superstring. Before discussing strings it is worth quickly mentioning the first pioneering attempt at unification of fundamental forces, Kaluza-Klein theory. Interestingly enough, this theory and all modern extensions of it predict the existence of scalar particles in

four dimensions.

The original idea of Kaluza and Klein[3] was to unify general relativity and electromagnetism by encompassing them within a single theory of general relativity in five dimensions. In five dimensions there are twenty five gravitational potentials, the idea was then to reduce the apparent dimensionality of spacetime by 'rolling-up' one of the dimensions into a tube. The effective four dimensional theory now has sixteen gravitational potentials, four other potentials which are interpreted as electromagnetic potentials plus a single scalar field. Modern variations of this idea try to use even more dimensions and more exotic compactification manifolds than the cylinder used originally. These ideas are somewhat out of favour at present but it is interesting to note that the more popular TOES all use more than four dimensions, and hence all require compactification. Despite having little practical impact on the development of particle physics so far, Kaluza Klein theory is the true ancestor of all unification ideas.

0.1.6 String theory and the Dilaton

The most favoured candidate TOE at present is the Superstring. The basic idea of string theory is to replace the zero-dimensional point particles of quantum field theory with one-dimensional objects, strings. These strings then sweep out worldsheets in a background spacetime rather than wordlines. Analogously to an elastic membrane in classical mechanics, this worldsheet has many different modes of vibration or 'excitation', these modes of oscillation are interpreted as being different particle states. The 'higher harmonics' of the string all have masses of the order of the Planck mass, but the lowest modes are massless and can give rise to particles of spin 0, $\frac{1}{2}$, 1, $\frac{3}{2}$, 2, thus showing the possibility of unifying all particle interactions within a single theory. The existence of a spin-2 particle which seems to arise totally naturally, would seem to imply that the string can provide the first consistent quantum theory of gravity.

The action of the bosonic string is

$$\int d^2\xi \left(\sqrt{h}h^{ab}g_{\mu\nu}\partial_a X^\mu \partial_b X^\nu + \epsilon^{ab}B_{\mu\nu}\partial_a X^\mu \partial_b X^\nu + \sqrt{h}R^{(2)}\Phi\right) \tag{8}$$

[3]They worked independently some years apart from each other and had somewhat differing views on the interpretation of their work, but here I refer to them as co-authors for the sake of brevity.

$g_{\mu\nu}$ is the spacetime gravitational field, h is the target space metric and X is the string worldsheet vector. $B_{\mu\nu}$ is an antisymmetric tensor field which gives rise to a spacetime scalar in four dimensions which can be axion-like. Φ is the *dilaton* field.

There are two important constraints which the string must satisfy; one is reparametrisation invariance, which in the case of the bosonic string results in the background spacetime be 26 dimensional, and modular invariance which puts important constraints on the type of boson and fermion fields one can put on the worldsheet.

Several string models exist; the bosonic string, above, which lives in 26 dimensions, the supersymmetric string(superstring) which requires 10 dimensions and the most important from a phenomenological viewpoint, the heterotic superstring.

These theories all require more dimensions than the world really seems to have, and so need to be compactified in some way. This unfortunately has to be put in by hand as spacetime compactification seems to be a non-perturbative mechanism.

In any case to find what particle content string theory gives requires compactification and then a choice of vacuum. Unfortunately there are thousands of ways to do this but it is worth mentioning that the string can give rise to a 'flipped' SU(5)$\otimes$U(1) gauge theory which is a promising GUT[4] candidate.

The most interesting aspect of string theory from the point of view of this thesis is the existence of the last term in the string action, the dilaton, Φ. The dilaton is a universal prediction of string theory, all variations have it, and it seems to occupy a quite central role in the theory of the string. This is because the dilaton is multiplied with the Gauss–Bonnet two form, $R^{(2)}$, on the worldsheet. This term is sensitive to sheets of different genus, i.e. numbers of 'holes' or 'handles'. Since in string theory 'handles' are equivalent to the vertices of field theory, that is represent interactions, it follows that the dilaton determines the coupling constant.

Classically, and to all orders in perturbation theory the dilaton is massless,

[4]This is not actually unified in the original GUT sense.

but it is thought that it should obtain some mass since a massless scalar is ruled out cosmologically. What is more, this mass could possibly be very light. This is suggested by the hypothesized existence of a superconformal invariance linking the dilaton to the axion which was discussed previously. This invariance should only be broken by anomalies and so the dilaton mass should be reasonably closely linked to the mass of the axion, which is thought to be in the sub-eV range.

Of course, by reason of the vast choice of string theories there could be a very rich spectrum of light scalars but none are as well motivated as the dilaton.

0.2 Cosmology

Although not concerned with cosmology per se, it is not inappropriate to give a brief summary of present thinking since the links between comology and particle physics are very close and also since the best theory there is of modern cosmology actually seems to demand the existence of a scalar particle.

The question one first asks oneself when seeing the subjects of particle physics and cosmology linked is this: what has each to do with the other?—one is concerned with things that are extremely small, while the other is concerned with things that are extremely large. Of course, the answer is that they are linked because we live in a dynamical, expanding universe. The fact of universal expansion at the present epoch implies that the universe was much smaller and consequently, much hotter in the distant past.

The hotter things are, crudely speaking, the greater the energy there is available and the more energy one has, the more one becomes sensitive to small distances. So, it seems very likely that at very earler times in the past the structure of the universe was extremely sensitive to its most elementary excitations i.e. particles.

The 'Standard Model' of Cosmology is the Hot Big-Bang(HBB) model which states that the universe began at a definite time in the remote past in a cataclysmic explosion known as the Big-Bang. The temperature was at this time incredibly high, and from this event the universe has been expanding and cooling ever since.

This is shown in table 0.1, listing against time, temperature and corresponding energy the relevant processes which dominated the evolution of the universe.

Mathematically this is modelled in terms of an isotropic, homogeneous, Friedmann–Robertson–Walker fluid model with metric

$$ds^2 = dt^2 - R^2(t)\left(\frac{dr^2}{1-kr^2} + r^2 d\Omega^2\right) \tag{9}$$

written in comoving coordinates. It is thought that our universe is spatially flat, $k = 0$. The functional form of the scale factor, R(t), is found by solving the Einstein equations for a perfect fluid with appropriate source terms; which amount to including pressure and energy density terms for whatever particles happened

to be in thermal equilibrium at that temperature. The scale factor describes how distances between objects are being stretched. Again if one looks at figure.1 one can see what the appropriate degrees of freedom are at each specific instant and temperature. The scale factor varies approximately as $t^{\frac{1}{2}}$ for temperatures less than around 10^3K, and as $t^{\frac{2}{3}}$ for those above it.

The successes of the Hot Big Bang are impressive. The expansion of the universe correctly accounts for the Hubble recession. Galaxy surveys show the universe to be fairly homogeneous and isotropic. The abundances of light elements are correctly predicted, and finally the most convincing evidence is of course the Microwave Background Radiation(MBR), discovered by Penzias and Wilson, which has a black body spectrum and is found to be very homogeneous and isotropic and which is in a sense the faint echo of that initial conflagration.

Galaxy formation in the HBB is assumed to come from small initial perturbations and subsequent gravitational instability.

The HBB is afflicted several serious problems, the solution to which may be some form of 'inflationary' period.

The 'flatness' or 'oldness' problem is this: the universe is thought to be flat and of critical density[5] but this type of solution is an unstable fixed point of the FRW models. This means that if the universe today is of critical density then in the very distant past, it has to be of critical density to an incredibly high accuracy. For example, if the universe contained an infinitesimally small amount more matter then the universe would have re-collapsed, and ended, millions of years ago. To resolve this situation within the HBB results in an ugly fine-tuning problem.

The 'horizon' problem is this: The MBR is homogeneous to an incredible high degree, but in the early universe not all of what we see as homogeneous could have been in causal contact—parts of the sky which could not have any 'knowledge' of each other are incredibly uniform in their structure—this is extremely puzzling.

Other problems are the monopole problem which asks why the universe was

[5]In the FRW models, depending on the initial density the universe may expand forever, recollapse in a 'Big-Crunch'. The value on the density at which the behaviour of the model changes is called the critical density.

not dominated in its early stages by various types of topological defect which must have been produced in copious numbers, and the dark matter problem; we can only see 10% of the matter in the universe which gravitates. Also, where are the inhomogeneities required to seed galaxy formation?

One possible solution to these problems could be *Inflation.* The inflationary hypothesis is this; at some early stage in the history of the universe it underwent a period of exponential expansion, thus flattening out the universe, diluting monopoles and enabling, more of the universe to come into causal contact. The inflationary scenario also gives quite naturally the required spectrum of inhomogeneities for galaxy formation. This inflationary, or de-Sitter, phase is enabled by the presence of a scalar field in the early universe. There is however no favoured candidate for what this 'inflaton' actually is.

Inflation, as one might expect, has problems of its own. This is suggested by the large number of specific models that have been cited. They all more or less result in a tweaking of the scalar potential so that the scalar field has just precisely the right characteristics to reproduce the observational data.

Despite the problems in the fine details of this type of model it is hard to find anything which solves the original sicknesses of the HBB and which is as remotely as compelling.

Time(secs)	Temperature(K)	Energy(GeV)	Event
0	∞	∞	Big Bang
10^{-43}	10^{32}	10^{19}	Planck era; particle creation, quantum gravity, strings?
10^{-31}	10^{27}	10^{14}	Unification time; GUT particles, supersymmetry? GUT phase tansition ? Desert?
10^{-6}	10^{15}	100	Electroweak phase transition
10^{-3}	10^{13}	1	Quark-Hadron phase transition Hadron era; nuclear physics, $p\bar{p}$ annihilation
1	10^{10}	10^{-3}	Lepton era; e^+e^- annihilation
10^2	10^5	10^{-8}	Radiation
10^{13}	10^3	10^{-10}	Matter Decoupling Galaxy formation
10^{18}	2.7	$3\ 10^{-13}$	Now

Table 0.1: History of the Universe.

0.3 Neutron Stars and the Nuclear Equation of State

Since the work in this thesis is primarily concerned with neutron stars it is necessary to provide some more detailed background than has so far been presented in this introductory chapter.

After a historical review the gross feature of neutron stars will be described along with experimental observations and the mechanics of model–building. The most important ingredient of this model building is the equation of state. For this reason the properties of nuclear matter will be reviewed also. This has direct relevance to the models constructed in chapter one.

0.3.1 Historical Review

Two Dutch physicists, Baade and Zwicky first proposed in 1934 that neutron stars could exist, noting that they would be small, extremely dense and highly bound gravitationally. They also pointed out that they could possibly be formed in supernova explosions.

The first models of neutron star structure were constructed five years later by J.R.Oppenheimer and G.M.Volkoff using the equation of state for an ideal gas. Their model predicted that such objects would have a maximum mass of $0.72M_{\odot}$.

At this time the principal motivation for the study of these objects was that they were thought to be a possible source of stellar energy; when this was shown not to be the case, interest waned dramatically, often accompanied by the excuse that such objects were too small to ever be seen anyway.

Interest sparked up again in the early sixties when the first quasi-stellar objects were discovered but again dissolved once it too was realized that quasars were nothing to do with neutron stars. Throughout this period the neutron star was not taken at all seriously, being regarded as little more than a theoretical curiosity.

These views were to change dramatically in 1967, for it was then that the first pulsar was discovered by Jocelyn Bell, then working at Cambridge as a research student in the research group of Anthony Hewish. This provoked a flurry of theoretical interest and it was Gold who first suggested that these periodic signals were being emitted by a rapidly rotating neutron star. This idea was soon accepted as being correct.

In 1968 pulsars were discovered in the Crab and Vela nebulae, strengthening the link, first made by Baade and Zwicky, that neutron star formation was connected with supernovae and stellar deaths.

The next important findings were made by the UHURU satellite in 1971, which found the first compact X-ray souces. These are thought to be binary pulsars accreting gas from their companions.

The most important event of recent times was the observation of the supernova in the lesser Magellanic cloud, SN1987A. This confirmed a great many theoretical predictions about neutron stars, especially the verification of the existence of the 'neutrino burst'.

0.3.2 Gross Features of Neutron stars and Observation

Neutron stars are small; radius approximately 15km, highly dense; central density around nuclear density, objects of approximately stellar mass with significant suface redshift. They are formed in the gravitational collapse of massive stars, $M > 4M_{\odot}$.

The main properties of neutron stars can be calculated by considering cold, non-rotating perfect fluid models. This is done by solving the Tolman-Oppenheimer–Volkoff equation of stellar structure, using a given equation of state. This equation is actually the general relativistic equivalent of the equation of hydrostatic equilibrium.

The 'equation of state' is merely a relationship of the form p=p(ρ) and is the crucial ingredient in this recipe; every aspect of the star's structure is sensitive to it. The models constructed in this manner are parametrised by the central density of the configuration, ρ_c.

Stable configurations are found for all central densities up to that for which the maximum mass is obtained. The maximum mass is very sensitive to the equation of state.

The internal structure of a neutron star consists of a number of distinct layers.

The *surface layer* is a region of density less than about 10^6g cm^{-3} forming a thin outer shell to the star and containing only a very small proportion of its total mass. For this reason the surface is largely ignored by model-builders. It

is quite fortunate that the surface contains so little of the total mass since a proper treatment is difficult—rapid rotation and strong magnetic fields become important factors here.

The *outer crust* is a solid coulomb lattice of heavy nuclei in β–equilibrium with a gas of relativistic electrons.

The *inner crust*, density between $4.3\,10^{11}$g cm^{-3} and nuclear density, $2.4\,10^{14}$g cm^{-3}, is a lattice of neutron rich nuclei.

The *core* will consist of a fluid of neutrons at or above nuclear density. If even higher densitities are available strange particles—'hyperons'—or even quarks and gluons may appear.

Because the maximum mass is so sensitive to the equation of state it is very important to measure the masses of neutron stars found in nature. This data can then be used to provide an astrophysical bound on the properties of nuclear matter. For example, a mass determination of, say, $1.7M_{\odot}$ would invalidate all but the very 'stiffest' equations of state.

Mass determinations of neutron stars are found by applying Kepler's Third Law to observations of binary pulsars.

The experimental limits found are consistent with general relativity and standard theories of hadronic matter, but cannot discriminate between competing theories very well. Observations are also consistent with conventional theories of stellar evolution which suggest that almost all massive stars evolve to a state where they have a cental iron–nickel core of mass $1.4M_{\odot}$.

Pulsar observations are the best 'handle' we have on neutron star properties, but are extremely difficult to model successfully. This is because the treatment of rapid rotation in strong general relativity is so difficult; most existing models assume slow rotation, uniform rotation and/or homogeneity which may not be appropriate. Rotation also invalidates the rather simple stability criterion mentioned previously. It is reckoned, however, that rotation cannot increase the maximum mass by more than 20%.

The most worrying aspect of pulsar physics is that there is no single convincing model which explains how these rapidly rotating neutron stars actually 'pulse'.

The emission mechanism emits radiation in a very narrow beam, with broad

band radiation at radio and optical frequencies and strong linear polarisation at radio frequencies also. No one has yet found an entirely satisfactory explanation of this.

0.3.3 The Nuclear Equation of State

Whenever one seeks to improve a neutron star model, the place to start is with the equation of state; the more accurately one can model the dynamics of nuclear matter the more accurate the derived features of the neutron star model, i.e. mass, radius, surface redshift and keplerian frequency, will be.

The equation of state is, in fact, fairly well known up to a density of approximately $2.4\,10^{11}$g cm^{-3}, but in modelling neutron stars it is the high density region which is of greatest importance. This is a consequence of the fact that, when one integrates the TOV equations one finds that over a major proportion of the star's radius the variation of the density is quite modest. This leads to the 'sensitivity' alluded to previously.

Early approaches to nuclear physics were carried out within the framework of non-relativistic quantum mechanics. The problem is then to find a suitable phenomenological potential which can match the known data and an adequate ansatz for the many-body wavefunction.

Ths non-relativistic nuclear force is conservative and independent of nucleon velocity but does not obey the superposition principle. It depends on the separation and spins of the nucleons and conserves the total spin. Any candidate potential must reasonably fit low energy scattering data and also must satisfy, as closely as possible, the constraints impose by *saturation.*

Saturation is the property that the energy and volume of the nucleus increase in direct proportion to the nucleon number. This is actually a very severe constraint; many apparently satisfactory potentials are ruled out by it. One of the implications of saturation is that the nuclear force must be attractive for small numbers of nucleons but repulsive for larger numbers; it is thought this comes about by a combination of three things, the Pauli Principle, exchange forces and a repulsive core. The saturation constraints boil down to correctly deriving four numbers; saturation density, energy and compressibility of symmetric nuclear matter and the 'volume symmetry coefficient'.

The earliest suggestion for the origin of the nuclear force was due to Yukawa in 1935, who suggested that this force was due to the exchange of a massive virtual boson. The Yukawa potential is of the form $\frac{e^{-\mu r}}{r}$, where μ is the mass of the boson involved. This force is attractive for scalar bosons and repulsive for vector bosons. This picture is known to be too simplistic, but the Yukawa potential is still used in building potential models, except that there would be a sum of such terms with their coefficients fixed to give agreement with experiment. The Reid potential, which reproduces phase shift data very accurately, is of this form.

The other ingredient one needs in this recipe is the assumed form of the many body wave function. There are several names for the various approximations used. The 'Hartree' approximation is to use a product of the one-particle wavefunctions; the 'Hartree–Fock' is a Slater determinant of one particle wavefunctions, which allows one to include the effects of spin. The Hartree–Fock introduces 'exchange' terms into the interaction which add an effective attraction for repulsive forces and an effective repulsion for attractive forces. The next stage in sophistication is to include correlation effects. The wavefunction is now a Slater determinant of one body wavefunctions multiplied by the symmetrised product of 2-body correlations. This is of the type used in the more sophisticated treatments of Pandharipande and, Bethe and Johnson.

The most popular approach, once potential and wavefunction ansatz are chosen is to do a variational calculation, i.e imposing $\delta < \Psi|H|\Psi >= 0$, where H is the Hamiltonian of the system. This technique was first used by Pandharipande. The most highly regarded of the Pandharipande models is the Three-Nucleon-Interaction (TNI) model, which as the name suggests takes into account three body correlations. The TNI equation of state turns out to be very similar to ones constructed by Bethe and Johnson[8]. Since one of the Bethe and Johnson equations of state is used in chapter one it is sensible to review the basis on which it was constructed.

Bethe and Johnson used the constrained variational technique of Pandharipande with a potential consisting of a sum of Yukawa terms, their coefficients tweaked to fit the nucleon-nucleon scattering data below 300MeV. The particle

content of the models was the proton, neutron, ω vector meson[6], and a scalar, σ, to simulate the attractive force from two pion exchange. Models were also construced with the hyperons, Λ, Σ, Δ. Bethe and Johnson used the formalism of a classical field theory since this would be valid for all values of coupling constant and also since the velocities of the particle could be expected to be quite slow which is why the potential was fitted to *low* energy scattering data.

The models constructed by Bethe and Johnson reproduce the phase shifts, neutron matter binding energy and deuteron dipole moment as well as the Reid potential but give rise to a significantly stiffer equation of state. Stiffness is the principal quality of any candidate equation of state used in neutron star model building; a 'stiff' equation of state gives rise to greater pressure for a given density than does a 'soft' equation of state. Stiffer equations of state give rise to increased maximum mass, lower central densities, larger radii and thicker crusts than do softer equations. All the Bethe and Johnson models give maximum masses in the range $1.65M_{\odot}$—$1.85M_{\odot}$. This is phenomenologically acceptable. The Reid equation of state is however, for example, ruled out because the energy loss rate of the pulsar in the Crab nebula is larger than the Reid potential will allow.

The hyperonic models of Bethe and Johnson are very similar to their non-hyperonic models. The main difference is that the equation of state is softened slightly.

The models of Bethe and Johnson can be criticized on several counts; they fail to achieve saturation, the ω coupling is too large, causality is violated at high densities and the hyperons are not really treated adequately. In spite of these faults the models are actually very good and agree surprisingly with the seemingly more rigorous TNI equation of state of Pandharipande.

0.3.4 Uncertainties

At densities much greater than nuclear density very little is known about the properties of matter. This gives one much freedom to speculate and indeed there exist a number of fascinating possibilities which could arise—pion condensates, exotic hyperon production or even a quark gluon plasma.

[6]The ρ and the ϕ were not included since the do not couple as strongly as the ω.

A pionic condensate would lead to a softened equation of state and enhanced cooling by neutrino emission. This possibility is suggested by certain calculations which predict that the negative pion should appear at around twice nuclear density. Since pions are bosons there exists the possibility of a condensate forming at low temperatures.

However, the most obvious omission in neutron star theory there is, is a proper and systematic study of the hyperons. These appear at high densities due to weak interactions.

In this ultra-high density regime a different approach is also required, relativity must fully be taken into account. One formalism which does this is the relativistic mean field theory (RMF) of Walecka and his school. The most complete treatment of the hyperons so far, the paper of Kapusta, Ellis and Olive[9] uses this approach to 'parametrize' the nuclear equation of state. In their paper all the lightest hyperons were included. In this model various condensates arise, giving the baryons 'effective' masses. Charge neutrality and weak chemical equilibrium give an equation of state with only one independent chemical potential plus five other parameters plus the values of the hyperon couplings which are unknown.

A large number of parameter choices were made in their treatment. The main conclusion they reached was that uncertainties in the values of the hyperon couplings lead to an uncertainty by a factor of two in the maximum mass for a neutron star. Other conclusions were that the Ξ could appear at high density, softening the equation of state; a ϕ meson condensate could exist, stiffening the equation of state and that quark-gluon cores were unlikely, though still possible.

More exotic possibilities in neutron star theory include the possible existence of entire 'quark stars' forming a third stable branch of compact objects beyond white dwarfs and neutron stars; and even 'strange stars' [7] with their remarkable properties. These ideas are at present purely speculative and it is difficult to see how they could be tested within the near future. Nevertheless, such possibilites make the study of neutron stars and their properties one of the most interesting

[7]In this idea it is speculated that three quark matter has lower energy per baryon than nuclear matter therefore being the true ground state of bulk matter.

branches of theoretical physics.

References

Of particular help in the preparation of this introduction were the following books, papers and preprints.

1. S.L.Shapiro, S.A.Teukolsky, 'Black Holes, White Dwarfs and Neutron Stars'
2. F.Wilczek, 'Perspectives on Particle Physics and Cosmology' IASSNS-HEP-90/64
3. P.D.B.Collins, A.D.Martin, E.J.Squires, 'Particle Physics and Cosmology'
4. 'Physics of the Early Universe' Proceedings of the 36^{th} Scottish Universities Summer School in Physics, 1989, edited by J.A.Peacock, A.F.Heavens and A.T.Davies
5. 'Particle Physics in the Cosmos' selected writings from Scientific American edited by R.A.Carrigan and W.P.Trower
6. A.A.Tseytlin, 'String Cosmology and the Dilaton' DAMTP-92-36
7. J.Louis, 'Recent Advances in Superstring Phenomenology' CERN-TH-5748
8. H.A.Bethe, M.B.Johnson, Nucl.Phys A230 1 (1974)
9. J.Ellis, J.I.Kapusta, K.A.Olive, UMN-TH-834/90, CERN-TH.5741/90

Chapter One

Neutron Stars and Scalar Fields

In this chapter the object is to consider the possible influence of a weakly coupled scalar particle, mass less than about one electron volt, on the constitution and evolution of neutron stars when the neutrons are sources of the scalar field, and then to find the consequent bounds on the mass and coupling of the scalar, finally comparing these with bounds obtained from other sources.

Considerations of this type have already been made in the paper of Ellis et.al.[3] These considerations shall be somewhat extended and refined in the context of an explicit model which is detailed in §2.1. After that in §2.2 and §2.3 the method of solution is given for the constitution of such a neutron star which is also acting as a source of the scalar field; also discussed is the upper limit on the scalar coupling, g, implied by the fact of neutron star formation. In §2.4 detailed plots of the resulting star configurations are given, followed in §2.5 by the binding energies and maximum rotational frequencies for neutron stars with scalar fields which have masses in the likely pulsar mass range. In §2.6 the corresponding

modification to cooling of the star by neutrino emission are given. In §2.7 the results are discussed, and whether any new limitations can be derived on the strength of the coupling for a given scalar mass.

This investigation of the possible presence of massive scalar fields in stars is closely related to work on the possible effects of massless[4] scalar fields. There are however, two principal qualitative differences between the massive and massless cases, both of which arise from the fact that a massless field has infinite range while a massive field is necessarily of finite range. Firstly, in the massless case, Birkhoff's theorem does not apply and the metric exterior to the star is not Schwarzchild but a different one; secondly in the case of a very large or infinite range field astronomical observations are very much more restrictive on the allowed coupling of the scalar field to matter[5].

This present investigation has also to be distinguished from the cases where there is a conservation law in the number of massive scalars, arising for example from a U(1) charge. Then there can, in principle, be boson stars[6,7,8] which are to be regarded as macroscopic quantum objects with markedly different properties from that of ordinary neutron stars. Boson stars have a conserved number of bosons all in the lowest energy quantum state. These can also exist in association with fermions, making a boson–fermion star[7,8,9,10]. Although related to such other work in this present study the scalar field has the characteristics of a classical field to which it is impossible to ascribe a definite number of quanta. It is worth noting that because of this there can be no limiting procedure through which we may relate both types of study. This is disappointing since one might expect that there should be some analogue of the correspondence principle at work, especially since in certain parameter regimes it is found that the static configuration is dominated by the presence of the scalar field, the normal fermionic component of the neutron star acting only as a 'seed'.

1.1 Construction of the Model

The system to be modelled consists of a neutron star interacting with a field of scalar particles of small mass, μ. It shall be taken to consist of a large number, about 10^{57}, of a single species of fermion, acting as a source for a scalar field, Φ.

Only one species of fermion shall be taken for clarity since emphasizing differences due to the presence of the scalar field is what is required and not those due to the myriad complexities of exotic hyperonic equations of state.

The scalar particles have mass μ and couple via a scalar coupling, coupling constant g, to the fermions; these two constants fix the physical theory sufficiently for the considerations of this chapter. The whole system is localized, and is held together by the mutual gravitational attraction of its constituents. The fermions are cold and degenerate, i.e. their Fermi energy is very much greater than their temperature. One therefore looks for static, spherically symmetric solutions to the coupled Einstein/Klein-Gordon equations with an equation of state for the fermions which is yet to be chosen.

There are a large number of possibilities for the choice [18] of equation of state. A very simple one is that for an ideal gas following the original prescription of Chandrasekhar[12], which was used by Oppenheimer and Volkoff[13] in their original relativistic treatment of the neutron star. Though this has the disadvantage of giving maximum neutron star masses too low in the case $\Phi = 0$, for simplicity of illustration it shall be taken as one of our examples since the greater interest lies in the essential differences between the cases with and without the scalar field. Our other example is one of the more realistic equations of state based on detailed considerations of nucleon–nucleon interactions[14,15]. Two equations of state are used so that by comparing the results from both it will be clearly seen in what respects any novel phenomena are generic, and what are peculiar.

The conventions for the metric and curvature tensors are (– – –) in the terminology of Misner, Thorne and Wheeler[16]. Throughout $\hbar$=c=1, and thus G=$M_{Pl}{}^{-2}$.

1.1.1 Equations

The coordinate system is

$$x^{\mu} = (\tau, r, \theta, \phi) \tag{1}$$

and the metric

$$\mathrm{ds}^2 = B(r)d\tau^2 - A(r)dr^2 - r^2 d\theta^2 - r^2 \sin(\theta)^2 d\phi^2 \tag{2}$$

is of the standard form. One attempts to solve the Einstein equations,

$$R_{\mu\nu} - \frac{1}{2}g_{\mu\nu}R = -8\pi G T_{\mu\nu} \tag{3}$$

with energy momentum tensor given by

$$\begin{aligned} T_{\mu\nu} &= (p+\rho)U_\mu U_\nu - p g_{\mu\nu} + \\ &\partial_\mu\Phi\partial_\nu\Phi - \frac{1}{2}g_{\mu\nu}g^{\alpha\beta}\partial_\alpha\Phi\partial_\beta\Phi + \frac{1}{2}g_{\mu\nu}\mu^2\Phi^2 \\ &-g_{\mu\nu}g\Phi\overline{\Psi}\Psi \end{aligned} \tag{4}$$

where p is the pressure, ρ is the density, and U is the 4-velocity of the fluid. The fluid is in static equilibrium, with the normalisation $U^\mu U_\mu = 1$, so that

$$U = (\sqrt{B(r)}, 0, 0, 0) \tag{5}$$

The Klein-Gordon equation is

$$(\Box + \mu^2)\,\Phi = g\,J \tag{6}$$

where $J = < \overline{\Psi}\Psi >$. Equations (3),(4),(6) may be derived from the Lagrangian density

$$\begin{aligned} \mathcal{L} &= \frac{1}{16\pi G}R + \frac{i}{2}\overline{\Psi}\gamma^\mu\overleftrightarrow{D}_\mu\Psi - m_F\overline{\Psi}\Psi \\ &+\frac{1}{2}\partial^\mu\Phi\partial_\mu\Phi - \frac{1}{2}\mu^2\Phi^2 + g\Phi\overline{\Psi}\Psi \end{aligned} \tag{7}$$

where m and μ are the fermion and scalar masses respectively and g is the scalar–fermion coupling constant. In (4) the exact fermionic stress-energy tensor has been replaced by that of a perfect fluid. The proof that such an approximation is valid for a large number of degenerate fermions has been given by Ruffini and Bonazzola[6]. In (6) $\overline{\Psi}\Psi$ has likewise been replaced by its expectation value over the degenerate fermion gas.

From the $\tau\tau$, rr components of (3), the r-component of the energy conservation equation, $T^{\mu\nu}{}_{;\nu} = 0$, and (6), one may derive the following set of equations

$$\begin{aligned} A' &= \frac{A}{r} - \frac{A^2}{r} + 8\pi G r A^2\rho + 4\pi G r A\Phi'^2 \\ &+4\pi G\mu^2 r A^2\Phi^2 - 8\pi G g r A^2\Phi J \end{aligned} \tag{8}$$

$$B' = \frac{-B}{r} + \frac{AB}{r} + 8\pi GrABp + 4\pi GrB\Phi'^2$$
$$-4\pi G\mu^2 rAB\Phi^2 + 8\pi GgrAB\Phi J \quad (9)$$
$$p' = -\frac{B'}{2B}[\rho + p] - g\Phi J' \quad (10)$$
$$\Phi'' = \Phi'[-\frac{A}{r} - \frac{1}{r} + 4\pi GrA(\rho - p) +$$
$$4\pi Gr\mu^2 A\Phi^2 - 8\pi GgrA\Phi J] + \mu^2 A\Phi - gAJ \quad (11)$$

m is taken to be 939MeV, the neutron mass.

The above equations for A, B, p and Φ contain the additional unknowns ρ and J. However, ρ and p are connected by some equation of state which, typically, expresses ρ and p in terms of one common parametric function of position. Also, in the cases that are dealt with, the source function J can be expressed in terms of the same parametric function. The equations of state used are discussed in §4 below; and these enable the 4 equations (8)—(11) to be re-expressed in terms of just 4 unknown functions, these being A, B, Φ and the equation of state parameter.

1.1.2 Boundary Conditions

To solve the equations (8)—(11) it is necessary to specify boundary conditions which follow from physical considerations. These latter are

1. Regularity at $r = 0$

   Implying $A \to 1$ as $r \to 0$

2. Birkhoff's Theorem

   For the standard metric (2) the exterior solution of Einstein's equations must be of the Schwarzchild form. This implies that A, B must tend to 1 as $r \to \infty$.

3. The solutions describe a compact star, i.e. are localized.

   This may seem like a trivial point to make; it is not. Most solutions of equations (8)—(11) do not describe neutron stars and finding those that do is a nontrivial numerical problem which is discussed in §1.2.2 .

The conditions that are imposed on the solutions are

(a) ρ, p and J become effectively zero for r greater than some value, say R_s. That is the star has an edge.

(b) $\Phi(r) \to 0$ exponentially as $r \to \infty$; the whole system is compact.

4. Spherical symmetry as expressed in standard form (2) for the metric and Einstein equations (8)—(11) leads to the following expansions around $r = 0$

$$A(r) = 1 + \frac{8\pi G}{3}(\rho_o + \frac{\mu^2}{2}{\Phi_o}^2 - g\Phi_o J_o)r^2 + \ldots \quad (12)$$

$$B(r) = b_o + \frac{4\pi G b_o}{3}(\rho_o + 3p_o - \mu^2{\Phi_o}^2)r^2 + \ldots \quad (13)$$

$$\Phi(r) = \Phi_o + \frac{1}{6}(\mu^2\Phi_o - gJ_o)r^2 + \ldots \quad (14)$$

The free parameters in the model are μ, $\rho(r = 0)$ and g

As may be seen from (9)—(11), b_o is an irrelevant parameter for this static solution. The equations are linear in b, so that one can always shift this parameter without making any difference; if necessary b can be shifted at the end of the integration. The remaining task is to calculate the properties of the star, i.e mass, radius and binding energy for as large a range of (μ, ρ_o, g) as possible.

1.2 Method of Solution

1.2.1 Principles and general method

Analytical solution of the field equations is not possible except in very specialized circumstances. The basic method utilized is that used for other star equations[17]. That is, one integrates the equations numerically, outward from the origin, $r = 0$ using an appropriate numerical procedure, which was in this case a fourth order Runge-Kutta method.

Given the physical theory, with a given μ and g, the parameters which fix the initial conditions are those appearing in equations (12)—(14), namely ρ_o, or equivalently p_o or J_o, and Φ_o; b_o is irrelevant as can be seen from equations (9),(10) and (13). In fact, as discussed below, for a given ρ_o the initial value of Φ_o of Φ, is fixed by the condition of compactness. Thus, as in an ordinary neutron

star, only one parameter, the energy density at the origin, is enough to fix the star configuration.

In integrating the equations (8)—(11) out from the origin, to define the star's fermionic edge, R_s, a criterion such as $\rho(r = R_s) < \epsilon$ is used. In the case of no scalar field the criterion is, in principle, $\rho(r = R_s) = 0$ but as it shall be shown there are further complications in the presence of a scalar field.

Integration is continued outwards far past R_s to check that the scalar field Φ has the correct asymptotic behaviour. Once one is convinced that it has, one may stop integrating and attach a Schwarzchild solution to the exterior. This then gives the star's mass M_s, through the equation (R > R_s);

$$M_s = \frac{R}{2}\left(1 - \frac{1}{A(R)}\right) {M_{Pl}}^2 \tag{15}$$

The number of fermions in the star is determined by the fact that in a cold neutron star model, such as this, the degenerate neutrons fill momentum-space up to a radius $p_F(r)$, this being the Fermi-momentum for a volume element at radial coordinate r. The fermion number is then this quantity integrated over the star

$$N_f = \frac{4}{3\pi}\int_0^{R_s} {p_F}^3(r)\sqrt{A}r^2 dr \tag{16}$$

One cannot define a similar expression for the number of scalars in the star, since Φ carries no conserved charge.

An important and useful quantity to know is the binding energy. This is defined as

$$B.E. = N_f m - M_s \tag{17}$$

Since the precursor iron core is a much more extended object, its gravitational binding energy is small relative to the compact remnant; a similar argument holds for the influence of the scalar field on the binding energy. So its total mass–energy is approximately $N_f m$ and thus (17) is the maximum energy available to the burst neutrinos during collapse. The positivity of the binding energy is not sufficient to ensure stability of an envisaged collapsed star configuration.

The difficulty in solving these equations is connected with the fact that the initial value of Φ is undetermined by any condition at $r = 0$; this is not to say

that it is a free parameter—it is not. For instance, if one chose values of Φ_o at random one would find the three types of behaviour seen in figure 1.1, where the solid line represents a curve of Φ falling exponentially outside the fermion edge (at large distances $\Phi \sim \frac{\exp(-\mu r)}{r}$). For the value of Φ_o corresponding to this curve there exists a star with a well–defined mass and a well–defined, though fuzzy, edge, outside which the metric is approximately of Schwarzchild form. This value of Φ_o, unique for a given ρ_o must be found by iteration and defines the lowest energy or ground state of the star.

The iterative procedure used to find the correct value of Φ_o makes this initial value problem very similar to an eigenvalue problem. Indeed a similar procedure is gone through in the case of boson stars or boson–fermion[9] stars, where the eigenvalue is the lowest frequency associated with a quantum state of the scalar field; the configuration of that scalar quantum wave function is analogous to the configuration of our classical scalar field. Similarly to the quantized case, there may exist in our present situation higher energy states of the star in which the classical scalar field Φ has the correct asymptotic behaviour but has nodes.

Checking that Φ has the correct asymptotic behaviour is very computationally expensive since one typically has to do several integrations to find each single configuration. Because of limitations of time this puts an intrinsic error into the final results.

The exact method used to find Φ_o involved choosing an initial guess, then integrating the equations until one of three things happened. If the scalar field became negative, this showed that the guess was too low and so the next guess was taken to be higher. If the scalar field began to increase then a lower guess was taken. If the scalar field went smoothly to zero then this was the correct value required. In this fashion the procedure successively subdivides the interval of investigation so that eventually the computer will 'home-in' on the required value of Φ_o.

The efficiency of this method is itself a function of the scalar field parameters, and indeed breaks down or becomes too expensive in certain cases. The nature of this behaviour and the difficulties caused by the exponential tail of the scalar field are discussed further on.

1.2.2 Limitations and Approximations

1.2.2.1 Scalar mass

The method described above for finding the scalar central density, Φ_o, is sensitive to the scalar mass, μ; for the heavier masses of our range, corresponding to smaller Compton wavelengths, the iteration procedure to find the correct asymptotic behaviour becomes very slow. A serious fine-tuning problem develops. For a neutron star and values of $\mu \geq 10^{-9}$eV it becomes effectively prohibitive to apply.

Fortunately, for a neutron star typically of radius $\gtrsim$ 10km, the scale of significant variation of the scalar field is ≥ 0.1 km. This means, since $\hbar c = 2\,10^{-10}$eV km, that for $\mu \geq 10^{-9}$eV it is a permissible approximation to neglect the Φ derivative terms in (11), compared with the term $\mu^2 A\Phi$. Making the approximation, the scalar field is given in terms of the fermion density by

$$\Phi = \frac{g\,J}{\mu^2} \tag{18}$$

Substitution of this, with J given as in §2.5, into (8) to (11) gives just 3 equations to solve, which is like solving for a star without scalars, but with a modified equation of state for the fermions. There is no difficulty in this.

In the ultralight region of mass, $\mu \leq 10^{-10}$eV the approximation is not valid, and not required anyway.

The method also fails for masses less than 10^{-13}eV. In this case it seems that whatever initial guess for the scalar field one makes, the scalar field and fermion density remain constant for far larger distances than those associated with normal neutron stars. This is largely due to the fact that the range of the scalar field is now much larger than a normal neutron star; in some sense the scalar field hardly notices it is there. None of the solutions of this type can correspond to, or be associated with any known type of star and so are ignored. In any case the numerical procedures used successfully in previous cases, cannot be used here.

1.2.2.2 Coupling strength

It is found that for any given value of μ, there is an approximate limiting value of the coupling, g, in the sense that for greater values the star cannot be constructed

because a proper star boundary does not form; this is similar to the behaviour described previously for very light masses but here it is due to having too large a coupling. Though this is the case for all μ it is only possible to give the following qualitative analysis of this for the regime $\mu \gtrsim 10^{-9}$eV where (18) holds.

In the Einstein equations it is useful to compare the part of the energy–momentum tensor coming from the scalar field and its interactions with that purely from the fermions. That from the scalar field in, for example equation (8) is

$$8\pi Gr\left[\frac{1}{2}\Phi'^2 + A(\frac{1}{2}\mu^2\Phi^2 - \Phi J)\right] \tag{19}$$

making the substitution, and in this regime of μ dropping the derivative term Φ'^2 as small compared to $\mu^2\Phi^2$, the scalar field contribution is

$$8\pi Gr\left(-\frac{1}{2}\left(\frac{g}{\mu}\right)^2 J^2\right) \tag{20}$$

This is to be compared with $8\pi Gr\rho$ or $8\pi Grp$. Forming the ratio

$$\begin{aligned} R &= \frac{8\pi Gr\frac{1}{2}(\frac{g}{\mu}J)^2}{8\pi Gr\rho} \\ &= \frac{1}{2\rho}\left(\frac{gJ}{\mu}\right)^2 \end{aligned} \tag{21}$$

One can illustrate this in terms of the Chandrasekhar equation of state, in §4 below, when ρ, p and J are given in terms of a parameter t. Then

$$R = \left(\frac{g}{\mu}\right)^2 16\pi^2 m^2 \frac{(2\sinh t/2 - t)^2}{(\sinh t - t)} \tag{22}$$

R is greater at regions of high density, t large, towards the centre of the star and less at regions of low density, t small, towards the edge. The condition for the system to resemble, reasonably closely, a normal neutron star should be presumably that R$\leq$1 throughout most of the star. The coupling and the scalar mass occur only in the ratio $\frac{g}{\mu}$, and it is this which is the governing parameter. If $\frac{g}{\mu}$ be too large then this condition will not be fulfilled and one should not be too surprised if the system fails to be a recognisable star.

Though one cannot make a simple quantitative argument like this in the ultralight region one would again expect that a too large source strength for the scalar field, would upset the neutron star–like nature of the system.

One possible explanation is that the coupling is so strong that the neutron star is broken up into a very large dust cloud. It should be noted that this 'strong' coupling regime is still very weak by, say, particle physics standards.

The limitations on g in both scalar mass regimes are discussed further below, as is the associated problem of defining the star's edge for those values of g which are relatively large but still star-forming. In either regime however, one has to be cautious about drawing a definite conclusion that a star could not exist for large coupling. It might be that the equations of state, including the fermions, should be completely revised.

1.3 Equations of State

The principal concerns of this chapter are with quantities such as total mass and radius which are mainly determined by the properties of the cold neutron gas forming the bulk of the star. Many equations of state have been proposed and used in evaluating the properties of neutron stars[11]. Here the questions are what qualitative differences arise from the presence of a very light scalar coupled to the fermions and from these what ranges of scalar coupling and mass (g,μ) are ruled out by existing observations.

In this chapter the object is to look at large corrections to the scalar case. Consequently it seems reasonable for one to take the view that all that is required of an equation of state is that it be not unlikely and fairly representative in a widely interpreted sense.

However, the study shall be started with an equation of state which is distinctly neither. This is the free Fermi gas equation first proposed by Chandrasekhar, used by Oppenheimer and Volkoff in their classic paper, and derived on the basis of relativistic quantum theory by Bonazzola and Ruffini. It is presented for its simplicity and for comparison with those of a more realistic equation of state. Even though the Chandrasekhar–Oppenheimer–Volkoff equation is not correct for a neutron star since it gives a maximum neutron star mass of about $0.72M_{\odot}$, nevertheless it gives most of the qualitative features of neutron stars obtained from sophisticated equations.

1.3.1 Free Fermi Gas Equation

Any volume element of the star at radial coordinate r is supposed to contain a free degenerate Fermi gas with all levels up to a momentum p_F(r) filled, and all others unfilled. The Chandrasekhar parametrisation is given in terms of the parameter t(r) where

$$t = 4\log_e\left[\left(\frac{p_F}{m}\right) + \sqrt{1+\left(\frac{p_F}{m}\right)^2}\right] \tag{23}$$

The pressure and density are given by

$$p = \frac{m^4}{96\pi^2}[\sinh(t) - 8\sinh(t/2) + 3t] \tag{24}$$

$$\rho = \frac{m^4}{32\pi^2}[\sinh(t) - t] \tag{25}$$

From the work of Bonazzola and Ruffini the source term can also be evaluated. This is done by inserting the plane wave expansions for the Dirac fields, and after multiplying out, one is left with an elementary integral, which once expressed in terms of 't' gives for the source $J = <\overline{\Psi}\Psi>$

$$J = \frac{m^3}{3\pi^2}[\sinh(t/2) - t/2] \tag{26}$$

The 4 unknowns in equations (8)—(11) are now taken as A, B , Φ and t, replacing equation (10) for $\frac{dp}{dr}$ by

$$\frac{dt}{dr} = -\left[\frac{dp}{dt} + g\Phi\frac{dJ}{dt}\right]^{-1}\left[\frac{B'}{2B}\{\rho + p\}\right] \tag{27}$$

The above equation of state for a neutron star has low pressure for a given density compared with those stiffer equations of state based on known and surmised properties of nucleon—nucleon interactions. These considerations, referred to in the introduction, are quite detailed and have considerable uncertainties at high density, including the proportion of hyperons and whether a transition to hyperonic matter takes place in the core of neutron stars.

Considering those given by Bethe and Johnson, and Malone et.al[14,15], they are all stiff enough to have the feature that the maximum neutron star mass is greater than about $1.6M_\odot$. Now stellar models for supernovae precursors lead to

an iron core with mass of the order of $1.5M_{\odot}$ all of whose nucleons collapse to form the subsequent neutron star. The few pulsars whose masses have been estimated are in accord with this number of nucleons. Consequently all the equations of state which we have just referred to allow the formation of neutron stars seen as pulsars. Thus any of these equations of state could form an *a priori* realistic basis on which to add the scalar field and estimate its effects, especially as we are looking for relatively large differences due to presence of the scalars.

1.3.2 Bethe and Johnson equation of state VN

Consider the equation of state model VN of [15]. The equation of state is given in terms of the parameter n_B, being the fermion number density expressed in units fm^{-3}. There are three regions of n_B:—

- High density : $n_B > 0.7fm^{-3}$

  In this region the equation of state has the following parametrization

  $p = (\frac{m_N}{10})^4(30.15{n_B}^{2.508})$

  $\rho = (\frac{m_N}{10})^4(91.6n_B + 18.8{n_B}^{2.508})$

- Intermediate density : $0.1fm^{-3} \leq n_B \leq 0.7fm^{-3}$

$n_B(fm^{-3})$	$\mathrm{p}/(\frac{m}{10})^4$	$\rho\ /\ (\frac{m}{10})^4$
0.10	0.073	9.41
0.15	0.180	14.09
0.20	0.369	18.89
0.25	0.671	23.81
0.30	1.126	28.81
0.40	2.517	38.95
0.50	4.682	49.47
0.60	7.752	60.54
0.70	13.16	72.60

Table 1.1: Numerically tabulated equation of state corresponding to Bethe VN model in the intermediate density region.

- Low density : $n_B < 0.1 fm^{-3}$

Model VN of [15] is a high and intermediate density model. For the low density region the free fermi gas equation of §4.1 is used; matching is done by finding the parameter t for a given value of n_B by using the relationship

$$n_B = \frac{{p_F}^3}{3\pi^2} \tag{28}$$

and using the definition of t, (23).

It is also necessary to specify J, the source density of the scalar field. Model VN is an equation of state without the presence of hyperonic matter even at high density. Accordingly it shall be assumed that there is only one species of baryon, the neutrons, and one Fermi-momentum p_F, defined as above in equation (28)

In accord with this assumption the source density J is

$$\begin{aligned} J &= <\overline{\Psi}\Psi> \\ &= \frac{m}{\pi^2}\int_0^{p_F} \frac{p^2 dp}{\sqrt{p^2+m^2}} \end{aligned} \tag{29}$$

Equations (28), (29) give the source density as a function $J(n_B)$ of the baryon number density n_B, and completes the specification of the equation of state in the presence of a scalar field.

1.4 Stellar Configurations

Using both the equations of state described in §4, neutron star properties were calculated for boson masses, μ, of 10^{-5}, 10^{-7}, 10^{-9}, 10^{-11} and 10^{-13} eV. The coupling, g, was varied from zero up to the maximum value with which our procedure could form a star as discussed in §3.2.2 above. In all, over one thousand configurations were calculated, giving an extensive picture of the structure of these objects.

The boson masses investigated are exceedingly small on the scale of known particle masses and so correspond to macroscopic ranges of interaction, given in table 1.2 by their Compton wavelength for future reference. Particularly relevant is their relationship to a typical radius of a neutron star which is of the order of ten kilometres.

μ(eV)	10^{-5}	10^{-7}	10^{-9}	10^{-11}	10^{-13}
λ_B(km)	$2\ 10^{-5}$	0.002	0.2	20	2000

Table 1.2: Correspondence between boson mass and Compton wavelength for various values of μ.

The scalar field produces between two static neutrons, an attractive force with Yukawa potential $\frac{g^2}{4\pi}\frac{exp(-r/\lambda_B)}{r}$. For comparative purposes write

$$g = \gamma\ g_G \tag{30}$$

$$g_G = \frac{m}{\sqrt{4\pi}M_{Pl}} = 2.16\ 10^{-20} \tag{31}$$

So for $\gamma = 1$ and the inter-nucleon distance less than λ_B, the force between the two neutrons is equal to that of the gravitational field.

Recall here the argument given in §3.2. This showed that for $\mu \gtrsim 10^{-9}$eV, the dependence on g and μ is only through the ratio $\frac{g}{\mu}$.

1.4.1 Star Masses

In a simple model of a neutron star, without light scalars, taking account only of the neutrons and with a given equation of state for these, the star mass depends only on one parameter such as the neutron central density, equivalent to ρ_o in the equation of state we have discussed above. The results can be described in a plot of star mass versus the parameter, ρ_o say, and takes the well known form of a curve with a series of turning points of which the first usually gives the maximum possible star mass corresponding to that particular equation of state.

When light scalars are present and for a given μ and g, the situation is the same in this case. However, the primary interest lies in examining the variation with μ and g, and this is more difficult to present. For both equations of state shall be used the parameter $\rho_o = \rho(r = 0)$, the central mass density. In figures 1.2a, 1.2b are given, for fixed $\mu = 10^{-11}$eV, the surface plot of the star mass as a function of $\log_{10}(\rho_o[g\,cm^{-3}])$ and g, figure 1.2a being that for the COV(Chandrasekhar, Oppenheimer—Volkoff) and figure 1.2b being that for the BJ(Bethe, Johnson) equation of state. The diagrams give a good idea of the qualitative changes which can be induced by the scalar field. The result for zero scalar field can be

clearly seen in the bottom front of the plots and note how the maximum mass can be drastically increased, and attained for smaller ρ_o, when the coupling is increased. These effects hold for all μ but are more marked in the ultra–light region. The corresponding plots for $\mu = 10^{-5}$eV is given in figures 1.3a, 1.3b, showing similar though somewhat less prominent effects.

However for $\mu = 10^{-5}$eV one can make a qualitative analysis of the region for the changes with g. In the equations (8)—(11) it is for this mass, as explained in §1.2.2, a very good approximation to put $\Phi' = 0$ and $\Phi = \frac{gJ}{\mu^2}$ from equation (11). Equations (8)—(10) then reduce to

$$\frac{1}{A}\frac{dA}{dr} = \frac{1}{r} - \frac{A}{r} + 8\pi G r A\tilde{\rho} \tag{32}$$

$$\frac{1}{B}\frac{dB}{dr} = -\frac{1}{r} + \frac{A}{r} + 8\pi G r B\tilde{p} \tag{33}$$

$$\frac{d\tilde{p}}{dr} = -\frac{B'}{2B}(\tilde{\rho} + \tilde{p}) \tag{34}$$

where

$$\tilde{\rho} = \rho(r) - \frac{1}{2}\frac{g^2}{\mu^2}J^2(r) \tag{35}$$

$$\tilde{p} = p(r) + \frac{1}{2}\frac{g^2}{\mu^2}J^2(r) \tag{36}$$

Equations (32) to (34) are the normal, scalarless, equations but with the pressure and density modified by equations (39) and (40). The equation of state for ρ and p is stiffer than the original equation of state. The increase of maximum mass with g is just what would be expected for increased stiffness.

One cannot make a similar analysis in the ultra–light region, $\mu < 10^{-9}$eV, but it is interesting that the effect is even more marked. Among others, one reason may be the greater range of the force due to the scalars. At $\mu \simeq 10^{-11}$eV it is comparable, see table 1.2, with the neutron star radius.

For a given g and μ the first turning point of the mass curve at $\rho_o = \rho_m$ say, gives the maximum mass in our models. For a one variable parameter star such as is being considered, it also marks the boundary between stable and unstable configurations; for ρ_o less than ρ_m a star is stable, for ρ_o greater than ρ_m up to the next turning point is unstable.

As noted in §4 the evidence from stellar calculations and from pulsars indicates that neutron stars are formed with a mass of about 1.5 $M_\odot$. For g=0 the COV equation—the original calculation of Oppenheimer and Volkoff—gives a maximum mass of 0.72 $M_\odot$. However, for g large enough the presence of the scalar field converts this into an acceptable model from a purely phenomenological standpoint. But one cannot take the point of view that this could correspond to physical reality as there are too many good arguments for the significant effect of nucleon–nucleon forces of normal provenance.

Thus for the results which will be given in the remainder of this section and in the next section, §2.5, the results from the second equation of state(VN of Bethe and Johnson) are quoted with more weight as corresponding more closely to physical reality.

In figure 1.4 is plotted the contour lines of constant maximum mass in the log(g)/ log(μ) plane.

It has been shown in §3.2 that for μ greater than 10^{-9}eV then the star equations depend on μ and g only through their ratio. Consequently in that region contours of maximum mass, M^{max}(g,μ) must be straight lines on the log/log plane, as is shown. In the ultralight region $\mu < 10^{-9}$eV the plots show that M^{max} becomes less dependent on μ; in this connection one may note that for $\mu < 10^{-11}$eV the range of the scalar interaction encompasses the whole star.

Neutron stars observed as pulsars seem to have masses of the order of $1.5M_\odot$, so for normal neutron star models, the maximum mass attainable is a significant guide to the equation of state. That is one of the reasons why favoured neutron star models have an equation of state significantly stiffer than that in the Oppenheimer–Volkoff calculation, which gives a maximum mass of about $0.72M_\odot$.

1.5 Stellar Properties

1.5.1 Binding Energies

In theories of supernova collapse and subsequent formation of a neutron star, most of the binding energy is released in a few seconds of neutrino pulse. Such a pulse was observed in SN1987A and has been estimated at $(2.5 \pm 1)\,10^{53}$ ergs. For a given equation of state the binding energy usually increases with the neutron

star mass in the stability region of the neutron star, thus reaching its maximum possible value at maximum mass. For a given boson mass and coupling this is the situation in our model and thus for each (g, μ) pair there is a unique maximum binding energy, BE^{max}.

Not surprisingly contours of equal BE^{max} on the $\log(g)/\log(\mu)$ plane follow the trend of the maximum mass contours plotted in figure 1.4. However, a supernova core is unlikely to be of the mass which would collapse to a maximum mass neutron star. So it is more relevant to consider the binding energies, as a function of (g,μ), which would correspond to a typical mass of a neutron star. As an example a mass of $1.4M_{\odot}$. is taken

Mass($M_{\odot}$)	B.E.(10^{54}) ergs	$\frac{g}{\mu}(10^{-9})\text{eV}^{-1}$	$\log \rho_o$	Radius(km)	Angular freq.
1.38	0.286	0.0	15.12	11.07	7261
1.39	0.289	0.5	15.12	11.10	7254
1.40	0.300	1.0	15.12	11.16	7233
1.40	0.315	2.0	15.10	11.44	6900
1.40	0.330	3.0	15.06	12.13	6400
1.40	0.328	4.0	15.00	13.15	5600
1.40	0.288	5.0	14.92	14.60	4800
1.39	0.248	6.0	14.80	16.74	3921
1.41	0.210	7.0	14.63	19.16	3229
1.40	0.190	8.0	14.46	21.80	2660
1.40	0.170	9.0	14.30	24.30	2250
1.40	0.150	12.0	13.92	31.6	1520
1.40	0.130	13.0	13.82	33.9	1370

Table 1.3a: Neutron star binding energies and other parameters for mass $\sim 1.4M_{\odot}$ as a function of the coupling to scalar mass ratio g/μ. Because of the scaling noted in the text these values hold for $\mu > 10^{-9}$eV. ρ_o is in grams per cubic centimetre. Angular frequency is in radians per second. g/μ is in eV^{-1}. The equation of state used was Bethe and Johnson VN.

In table 1.3a is found, for this neutron star mass, $1.4M_{\odot}$, and $\mu > 10^{-9}$eV the binding energy and other properties of the star for a range of values of the coupling

to scalar mass ratio, g/μ. One can see that as g gets larger, for a fixed μ, the radius of the star increases and naturally with this the fermion central density, ρ_o, decreases. Thus for the maximum value of g/μ given, g = 13 $10^{-9}eV^{-1}$, the radius is about 34km and the central density about 10^{14}g cm^{-3}, lower than nuclear density, a picture which is quite unlike the standard model of a neutron star. For values of $g/\mu > 3.0\ 10^{-9}$eV^{-1}radius increases sharply, and $g^2J^2(r)$ decreases with g so that the effective equation of state indicated by equations (35), (36) is becoming less stiff for those larger values of g, but still of course stiffer than for g = 0.

For most of the range of g the binding energy is clearly compatible with the observations from SN1987A and still at $g/\mu = 13\ 10^{-9}$ it has only fallen to about 1.3 10^{53}ergs, a value which cannot be ruled out.

Mass($M_\odot$)	B.E.(10^{54}) ergs	$g(10^{19})$	logρ_o	Radius(km)	Angular freq.
1.40	0.30	0.5	15.11	12.32	6220
1.40	0.28	1.0	15.00	18.0	3500
1.40	0.26	1.4	14.86	25.3	2100
1.40	0.17	1.6	14.61	33.4	1400
1.40	0.146	1.8	14.15	40.0	1100
1.40	0.125	2.0	13.99	45.0	900

Table 1.3b: Star configurations for a fixed scalar mass, $\mu = 10^{-11}$eV calculated as for table 1.1.3a.

In table 1.3b, still for $M_s = 1.4M_\odot$ but now with $\mu = 10^{-11}$eV is given the same quantities for a more limited range of g. As discussed below in §6.2.2 the definition of radius is not so clear–cut for this value of μ, which corresponds to a range of 20km, but the same tendencies in radius, central density and binding energy are observed as in table 1.3a.

1.5.2 Radii and Maximum Rotational Frequencies

There is an upper limit on the rotational frequency, related to the stars mass and radius because of the possibility of centrifugal breakup; rapidly rotating stars tend to shed mass at the equator. In this case the presence of a scalar field

can further complicate the calculation in the ultralight region of the scalar mass where the concept of radius becomes fuzzy.

To find the maximum angular velocity of a star, mass M, in a naive spherically symmetric model one might straightforwardly calculate the angular velocity for which gravitational attraction at the surface is just enough to supply the acceleration towards the centre, Keplerian frequency

$$\Omega_k \;=\; 1.152\,10^4\sqrt{M_s}\Big(\frac{10}{R_s}\Big)^{3/2} s^{-1} \tag{37}$$

where M_s is in $M_\odot$ and R_s is in kilometres.

Taking into account corrections due to non–sphericity and relativity it has been predicted that for a given equation of state the maximum Keplerian frequency is[19,20]

$$\Omega_{max} \;=\; 0.72\,10^4\sqrt{M^s}(\frac{10}{R^s})^{3/2} s^{-1} \tag{38}$$

where M^s and R^s are for the spherically symmetric configurations calculated for that equation of state. It is surmised that this formula is good to better than 10%, but that stars rotating faster than $0.9\,\Omega_{max}$ may develop instabilities.

With scalar fields present further discussion is necessary. If first one considers the model equation of state without a scalar field, the curve of density versus radial distance would fall rapidly to zero near the star edge, and in this ideal model case the curve would be vertical at the star's edge. When the scalar field is introduced then a sharp fermion edge is impossible; for if there were an edge then the scalar field would extend beyond it a distance of the order of $\frac{1}{\mu}$, and then there would be fermions dragged beyond the edge by the scalar field. Analytical and numerical calculations confirm that there is no sharp fermion edge, but rather a tail of interacting bosons and fermions. For $\mu > 10^{-9}$eV, equivalent to a range of 0.2km, there is no practical problem; the fermion density drops sharply enough to enable the definition of an edge to better than 0.2km. It may be noted that near the edge the reasons that one may put $\Phi = gJ/\mu$, for $\mu > 10^{-9}$eV because of the slow variation of Φ' break down. However, this causes only a small error.

For $\mu < 10^{-9}$eV 'tailing' becomes a problem; already at $\mu = 10^{-11}$eV the tail must be of the order of 20km. Firstly, the edge is now seriously fuzzy

(such a star profile is shown in figure 1.5) and the concept of radius becomes likewise fuzzy. Secondly the central density, Φ_o, of the scalar field is determined as that density for which the scalar field for large radial distance, r, drops smoothly to zero without nodes; and for calculation there has to be a criterion of satisfaction of this condition. Associated with any particular criterion is an error $\delta\Phi_o$ on the determination of Φ_o. This is illustrated in figure 1.11. The longer the tail the greater is the difficulty in achieving a reasonably small error $\delta\Phi_o$.

This is the basic physical idea of what is happening. In more practical terms, the problem is to actually do with the fact that tailing behaviour of the scalar field induces a strong dependence of the derived star radius on the arbitrary parameters of the numerical procedures used. For example, when integrating the equations one does not wait until the t parameter becomes negative to define the edge; if one does then the program will crash. Instead a cutoff, usually a small value relative to the initial t value is used. When the effects of the scalar field become large, i.e. very small masses and/or large couplings, the fermion density begins to mimic the behaviour of the scalar field, tailing off very slowly instead of the usual abrupt stop. This leads to the problem of defining where the edge of the star is, and occurs in all boson mass regimes. In the light regime one can simply choose the cutoff to be some suitable value, and this suffices. These results remain insensitive to any other of the arbitrary program parameters. In the ultralight region further, more serious problems arise because there are a further two arbitrary parameters to contend with, i.e. the stopping criterion. This tells the computer that a found configuration has the required behaviour by stopping the integration if and only if the fermion density is less than its cutoff, and the scalar field at a certain multiple of fermion radius is a certain fraction of the starting value of Φ. Now, it turns out that the error introduced by this stopping criterion introduces an enormous error into the definition of the star radius.

In this way the tailing behaviour of the scalar field can also interfere with the convergence of the numerical procedure itself for very small masses.

1.5.2.1 $\mu > 10^{-9}$eV

The first result of the preceding discussion is that for $\mu > 10^{-9}$eV, with a given fermion central density and equation of state and a given (g,μ) yielding a well enough defined radius R_s as well as a mass M_s, one can define a maximum Keplerian frequency Ω_{max}. This is shown in table 1.1.3a calculated using equation (38), where the central density has been chosen to give a neutron star mass M_s=1.4$M_\odot$. Pulsar frequencies have been observed in the range

$$4200 > \Omega_{max} > 10. \tag{39}$$

For the larger values of g given in table 1.3a the maximum attainable frequency is below 4200. Consequently this model implies a limitation on the value of g/μ for $\mu > 10^{-9}$eV:–

$$\frac{g}{\mu} \leq 0.6\,10^{-8}\,eV^{-1} \tag{40}$$

This excludes those values of g which, as noted in §1.5.1 give a star configuration with low central densities very unlike the standard neutron star picture.

1.5.2.2 $\mu \leq 10^{-11}$eV

The conclusions arising in this region are much more complicated and uncertain, and this arises in large part from the definition of radius to be inserted in any formula for the Keplerian frequency, where there is a factor $(M/R^3)^{1/2}$.

A criterion which chooses a smaller R for a given configuration will give a larger Ω_{max} than a criterion choosing a larger R, and thus will allow a larger range of g for a given μ to be in accord with the observation (39). Thus if one chooses a smaller R criterion then one is being more cautious about what range of g can be excluded.

The criterion used in table 1.3a gives the range of g compatible with (39) as

$$\frac{g}{\mu} \leq 1.\dot{0}\,10^{-8}\,eV^{-1},\ \mu = 10^{-11}eV \tag{41}$$

In making the choice of R–criterion one has to bear in mind that if a significant part of the tail breaks away the whole calculated configuration will be invalidated.

Since for $g/\mu = 0.1\ 10^{-9}\ eV^{-1}$ the radius in table 1.3a is given as R=15km and the scalar field range corresponding to $\mu = 10^{-11}$eV is 20km, the criterion used obviously tends to a smaller R rather than for a larger R criterion. Thus the upper limit on plausible g given by equation (40) is, if anything, too big.

1.6 Cooling of Neutron Stars

In the models constructed, there is a scalar field and matter at high density. One can think of the scalar field as producing density dependent fundamental constants. Variation in these constants will affect any astrophysical process in the vicinity of the star. It therefore seems sensible to look at one of the principal phenomena associated with neutron stars; their cooling by neutrino emission.

The end stages of normal stellar evolution tend to result in the existence of an iron-nickel core of around $1.5\,M_{\odot}$. This becomes unstable and collapses until the density is approximately that of nuclear matter. In this process around 10^{53}ergs are released—about 10% of the gravitational energy—mostly in the form of neutrinos. The internal temperature decreases rapidly from around 10^{11}K to 10^{10}K.

For neutron stars starting at a temperature of between 10^{9}K and 10^{10}K further cooling also takes place, this time for a considerably longer period, also by neutrino emission until the temperature drops below 10^{8}K, when photo–emission becomes important.

The equations which describe the structure of hot neutron stars can be found in Glen and Sutherland[21]. Within the star the thermal conductivity of the degenerate relativistic electrons is assumed to be extremely high. This simplifies the analysis greatly since it implies that the structure of the neutron star consists of an approximately isothermal core and a thin envelope. Only in the outer skin of the star is there an appreciable temperature gradient. Energy is lost from the neutron star, in this phase from 10^{10}K downwards to 10^{8}K, primarily in the form of neutrinos which are produced by weak interactions in the core, and, since they have an extremely long mean free path, stream freely from it.

The cooling equation is

$$-\frac{dT'}{dt} = \frac{\int n_F q_\nu B dV + 4\pi R^2 \sigma {T_s}^4 B_c}{\int n_F c_\nu dV} \tag{42}$$

where n_F is the baryon number density, q_ν is the emissivity per baryon, B is g_{00}, and c_ν is the specific heat of baryons. A subscript 'c' denotes the quantity to be evaluated at the core–envelope boundary. This boundary is thought to form when the density falls to approximately 10^{10}g cm^{-3}. T' is the internal temperature multiplied by g_{00}. This equation fully takes into account general relativistic effects.

In the analysis of neutron star cooling there are a number of important ingredients, variations in which can change the ultimate consequences quite considerably. These include, the equation of state, especially at high density, the presence of a pionic condensate, neutron superfluidity, and high magnetic fields. All these considerations tend to make the conclusions, even in the most careful of studies, somewhat qualitative. In this section only a broad comparison is sought between the cases with and without scalar fields. Therefore the possible effects of high magnetic fields and superfluidity will be ignored.

For temperatures around 10^9K, the luminosity is dominated by the modified URCA processes

$$n + n \longrightarrow n + p + e^- + \overline{\nu}_e \tag{43}$$

$$n + p + e^- \longrightarrow n + n + \nu_e \tag{44}$$

The emissivity of the modified URCA process, ϵ_{urca} has been calculated by Friman and Maxwell[22] to be

$$\epsilon_{urca} = 1.8\,10^{21} T_9{}^8 \left(\frac{m_n{}^*}{m_n}\right)^3 \left(\frac{m_p{}^*}{m_p}\right) \left(\frac{\rho}{\rho_{nuc}}\right)^{\frac{2}{3}} ergs\ cm^{-3} s^{-1} \tag{45}$$

where ρ_{nuc} is the density of nuclear matter, which we take to be $2.8\,10^{14}$ grams per cubic centimetre. T_9 stands for $T\ 10^{-9}$K, and $m_{n,p}{}^*$ denote the effective masses of the neutron and the proton respectively. Note the strong dependence of the emissivity on these quantities. These so-called Landau parameters are poorly known from nuclear physics, and are generally taken to be about 0.8 in conventional studies.

The specific heat of the neutrons is given by

$$c_\nu = \frac{\pi^2 m_n{}^* k_B{}^2 T}{p_F{}^2} \tag{46}$$

Here the neutrons are being treated non–relativistically.

It is through the effective masses of the nucleons, we shall assume, that the effects of the scalar field are manifest. By inspection of the Lagrangian density (7) one can set

$$m_{n,p}{}^{*} = m_{n,p} - g\Phi \tag{47}$$

That is, one assumes our model without any extra contribution to the effective masses coming from nucleon forces appropriate to other equations of state.

The effects of general relativity in the cooling of neutron stars are twofold, firstly, they ensure that, even in the infinite conductivity limit there is a temperature gradient. This can be an important effect for very heavy, very compact neutron stars. Secondly, radiation emitted from the surface is redshifted.

Since the effects of scalar fields on neutron stars seem to be to make these objects heavier, but also more extended, it shall be assumed that the core is isothermal. The crust contribution is also neglected. Since there are obviously a great many other factors involved, it is reasonable to simplify the analysis so that the effects of scalar field can be more clearly delineated.

The approximate cooling equation

$$\frac{dT}{dt} = -\frac{\int \epsilon_{urca} B dV}{\int n_F c_\nu dV} \tag{48}$$

will be used. This is written as

$$\frac{dT}{dt} = -\alpha T^7 \tag{49}$$

where

$$\alpha = \frac{1.8\,10^{-51} \int_0^{R_s} (\frac{m_n{}^*}{m_n})^3 (\frac{m_p{}^*}{m_p})(\frac{\rho}{\rho_{nuc}})^{2/3} B\sqrt{A} r^2 dr}{\pi^2 {k_B}^2 10^{-9} \int_0^{R_s} n_F {p_F}^{-2} m_n{}^* \sqrt{A} r^2 dr} \tag{50}$$

The general solution to (49) is

$$\log_{10} T_i = \log_{10} T_o - \frac{1}{6}\log_{10}[1 + 6{T_o}^6 \alpha t] \tag{51}$$

To convert from internal to surface temperatures one may use the approximate relation[21]

$$\log_{10} T_i \approx \frac{5}{2}\log_{10} T_s - 7.5 \tag{52}$$

Temperatures are in Kelvin(K) and the time is in seconds.

Now, one takes stars of approximately equal, and phenomenologically acceptable mass but differing g, and compares the cooling curves of these stars with that of a star without an attached scalar field. This is done for two values of μ, one light and one ultralight and using the Bethe–Johnson equation of state.

1.6.1 Light—μ=10^{-5}eV

STAR	$\log_{10}\rho_o$	g(10^{-14})	Mass($M_\odot$)	Radius(km)	α
0	15.10	0.0	1.38	11.08	$1.09\,10^{-62}$
1	14.92	5.0	1.39	14.61	$7.34\,10^{-63}$
2	14.54	7.5	1.39	20.57	$5.72\,10^{-63}$

Table 1.4a: Cooling factors,(α), for various stellar configurations with boson mass, μ=10^{-5}eV.

1.6.2 Ultralight—μ=10^{-11}eV

STAR	$\log_{10}\rho_o$	g(10^{-19})	Mass($M_\odot$)	Radius(km)	α
3	14.95	1.0	1.39	24.11	$1.26\,10^{-62}$
4	14.68	1.5	1.39	29.72	$7.03\,10^{-63}$

Table 1.4b: Cooling factors for configurations with boson mass of 10^{-11}eV.

The resulting cooling curves are shown in figure 1.12a, and figure 1.12b.

The effect of the scalar field is to alter the cooling rate slightly, but the overall difference is negligible. Initially one might think that because of the fairly strong dependence of the URCA luminosity on the effective masses a noticeable effect could arise. Unfortunately it seems that changes in the integrated luminosity and specific heat largely cancel each other out, to within a factor of a few, and because the overall observational dependence is logarithmic, other physical factors will override any alterations caused by these.

1.7 Conclusions and Discussion

The effect of a very light scalar particle, mass less than 1eV, coupled to nucleons, has been studied on the physics of neutron stars. The nucleons act as a source of the scalar field and Einstein's equations are modified through the change in the energy momentum tensor to include the scalar field and its interaction term; thus the gravitational interaction is modified both by a long range inter-nucleon interaction and by the gravitational effects of the scalar field.

There are two regimes of scalar mass. The light region, $\mu > 10^{-9}$eV and the ultralight region, $\mu \leq 10^{-9}$eV. There are two parameters associated with the scalar field, the coupling constant g and the scalar mass μ. In the light region the effect of the scalar presence on the neutron star only depends on the single parameter $\frac{g}{\mu}$ and the effect of the scalar field can be eliminated from the equations to yield normal neutron star equations with a modified equation of state for the fermion pressure and density. In order for this modification to be not so severe that a neutron star does not form it is necessary that $\frac{g}{\mu}$ is less than or of the order of $2\,10^{-8}\text{eV}^{-1}$.

As μ decreases into the ultralight region, g and μ have an independent effect on at least some of the physical quantities; for example over a large range of g the definition of the radius depends on μ in the ultralight region where the range is of the order or greater than 1km. This effectively put a lower limit of $\mu \geq 10^{-13}$eV on our numerical investigations. It was also found, as in the light region, that the formation of a neutron star required an upper limit on the value of g.

The principal objective was to investigate the effect of a scalar field on the non–detailed features of neutron stars such as mass, binding energy and radius. For example, no evaluation was made of the importance of the fine details of the structure of the surface. The investigation was made using two equations of state, the ideal gas equation plus a stiffer, more realistic equation due to Bethe and Johnson, which is the one that was most fully reported on. In both these cases very similar effects of the scalar field were observed; for example to form a star of a fixed mass an increase in g was accompanied by an increase of radius and a decrease of density.

Of particular interest is whether, from current or potential observation of

neutron stars, limitations not available from other observations can be placed on the parameter pair (g,μ). Currently available observations are pulsar frequencies and the binding energy released by the neutrino burst from probable neutron star formation in one supernova, both being associated with the theory of neutron star formation from the collapse of an iron core of mass about $1.5M_{\odot}$. There is also the observation of the surface temperature of the Crab pulsar, from which cooling rates are deduced.

In the light region comparison of calculations with the observations on rotational frequencies imposes the limit of equation (40), $g/\mu \leq 0.6\ 10^{-8}\ \mathrm{eV}^{-1}$, binding energy and cooling, calculations give a somewhat less stringent limit than this. Though this rotational frequency limit can only be got using actual star configuration calculations as here, it unfortunately does not greatly improve the qualitative limits from other quantities (including binding energy and cooling) made in [3]. Thus over the range $10^{-4}\mathrm{eV} \geq \mu \geq 10^{-9}\mathrm{eV}$ one is left in the situation that Cavendish type experiments and astronomical and satellite observations[5] seem to provide a more stringent bound by a factor of about 10 or more.

For $\mu \geq 10^{-3}\mathrm{eV}$, corresponding to a range $\lambda_B < 210^{-4}\mathrm{m}$, data from Cavendish type experiments does not exist. There is the possibility of other data; for axions whose coupling to mass ratio can be carefully calculated or estimated there are limitations on this mass region from careful calculations on the evolution of red giant stars and the duration of the neutrino burst from SN1987A which would be affected by axion emission in this mass region[2]. In the case of the particles considered here, i.e. with scalar coupling, the coupling to mass ratio of equation (40) is significantly less than the axion coupling to mass ratio and there do not seem to be corresponding careful calculations of cooling by scalar emission in this mass region which might give much better limits than equation (40).

In the part of the ultralight region where we have been able to perform calculations the astronomical and satellite observations[5] give a more stringent bound than equation (41) by a factor of about 10.

Lastly, the importance of crust/surface structure must be mentioned. In this work this aspect of the scalar field/neutron star interaction has been largely ignored, and yet it may be of vital importance to the structure of the star, especially

with respect to the formation of an edge, and how this relates to the existence of the scalar field 'Yukawa tail'. This has an obvious bearing on the question of rotation frequencies and perhaps on the efficiency of cooling also. It bears mentioning that in another type of exotic compact object, the so–called *strange stars*, the crust is radically different from that of normal neutron stars[23]. However, it seems likely that the surface structure would be strongly dependent on the particular type of scalar particle one is interested in.

This section leaves a number of subjects open for further investigation. There is the difficulty posed of finding analytical or computational methods capable of investigating for scalar masses less than 10^{-13}eV. No detailed investigation of light scalar particle emission in radial pulsations or in the gravitational collapse of the supernova, and the possibility of its detection, has been made so far. In the wider context one could consider the influence of a light scalar field on the pattern of gravitational collapse to a black hole, and its influence on much bigger and more massive astronomical objects.

These subjects will be looked at in the following chapters. While using the properties of these static configurations to produce astrophysical bounds on the light scalar parameters has been somewhat unsuccessful, satellite observations typically being better by an order of magnitude, these objects which are more massive, larger and more diffuse than ordinary neutron stars, and with fuzzy edges are quite interesting in themselves. To this end the dynamical phenomena associated with them will be studied further on. It is also possible that these dynamical processes will improve the bounds given by the static properties.

Figure Captions

Figure 1.1: Radial behaviour of the scalar field for arbitrarily chosen values of the central scalar field density, Φ_o. The darker, central curve is the one which could correspond to a neutron star configuration.

Figure 1.2a: Stellar mass as a function of the central density, ρ_o, and the coupling g. The mass of the boson is 10^{-11}eV, and the equation of state is that of Chandrasekhar.

Figure 1.2b: Stellar mass as a function of the central density, ρ_o, and the coupling g. The mass of the boson is 10^{-11}eV, and the equation of state is that of Bethe and Johnson VN[15].

Figure 1.3a: Stellar mass as a function of the central density, ρ_o, and the coupling g. The mass of the boson is 10^{-5}eV and the equation of state is that of Chandrasekhar.

Figure 1.3b: Stellar mass as a function of the central density, ρ_o, and the coupling g. The mass of the boson is 10^{-5}eV and the equation of state is that of Bethe and Johnson VN[15].

Figure 1.4: Contours of equal maximum mass plotted on the log(g), log(μ) plane; the figures indicate the maximum mass of the contour in units of $M_\odot$. The dashed lines are for the COV equation of state and the solid lines for the Bethe and Johnson equation of state. log(g) $\simeq$ -20 corresponds to a coupling approximately equal to that of gravity in the sense of equations (30) and (31) of the text.

Figure 1.5a: Binding energy as a function of the central density and the coupling. Binding energy is in 10^{53}ergs. Boson mass is 10^{-11}eV and the equation of state is that of Chandrasekhar.

Figure 1.5b: Binding energy as a function of the central density and the coupling. Binding energy is in 10^{53}ergs. Boson mass is 10^{-11}eV and the equation of state is Bethe and Johnson.

Figure 1.6a: Binding energy as a function of the central density and the coupling. Binding energy is in 10^{53}ergs. Boson mass is 10^{-5}eV and the equation of state is that of Chandrasekhar.

Figure 1.6b: Binding energy as a function of the central density and the coupling. Binding energy is in 10^{53}ergs. Boson mass is 10^{-5}eV and the equation of state is that of Bethe and Johnson.

Figure 1.7a: Radius, in kilometres, as a function of central density and coupling. Boson mass is 10^{-11}eV. Equation of state is that of Bethe and Johnson.

Figure 1.7b: Radius, in kilometres, as a function of central density and coupling. Boson mass is 10^{-5}eV. Equation of state is that of Bethe and Johnson.

Figure 1.8a: Contour lines of maximum rotational frequency against cen-

tral density and coupling. Boson mass is 10^{-11}eV. Equation of state is that of Chandrasekhar.

Figure 1.8b: Contour lines of maximum rotational frequency against central density and coupling. Boson mass is 10^{-11}eV. Equation of state is that of Bethe and Johnson.

Figure 1.9a: Contour lines of maximum rotational frequency against central density and coupling. Boson mass is 10^{-5}eV. Equation of state is that of Chandrasekhar.

Figure 1.9b: Contour lines of maximum rotational frequency against central density and coupling. Boson mass is 10^{-5}eV. Equation of state is that of Bethe and Johnson.

Figure 1.10: Radial profiles for the fermion density(dark), and the scalar field(light). Note the tailing behaviour of the scalar field.

Figure 1.11: Demonstration of how error arises in the determination of Φ_o. All radial profiles which lie beneath and to the right of the dotted lines are acceptable field configurations. The exact position of where we draw these lines determines our 'stopping criterion'.

Figure 1.12a: Internal temperature of neutron star versus $\log_{10}$[time(secs)] , starting initially from 10^{10}K, for star configurations 0, 1 and 2. 0 is the bottom line, 1 is the middle line and 2 is at the top.

Figure 1.12b: Internal temperature of the neutron star versus $\log_{10}$[time(secs)] , for configurations 0, 3 and 4. 3 is at the bottom, 0 is in the middle and 4 is at the top.

References

1. F.Wilczek, 'Perspectives on Particle Physics and Cosmology' IASSNS–HEP–90/64

2. M.S.Turner, 'Windows on the Axion' Fermilab–Conf 89/104a

3. J.Ellis, S.Kalara, K.A.Olive, C.Wetterich, Phys.Lett B228 264 (1989)

4. A.R.Liddle, R.G.Moorhouse, A.B.Henriques, Class.Quantum Grav. 7 1009 (1990). Here the scalar field arises from a Kaluza–Klein theory.

5. A.de Rujula, Phys.Lett B180 213 (1986)

6. R.Ruffini, S.Bonazzola, Phys.Rev 187 1767 (1969)

7. P.Jetzer, 'Boson Stars' ZU–TH 25/91 (1991)

8. A.R.Liddle, M.S.Madsen, 'The Structure and Formation of Boson Stars' SUSSEX–AST 92/2–1 to be published in the International Journal of Modern Physics A.

9. A.B.Henriques, A.R.Liddle, R.G.Moorhouse, Nucl.Phys B337 737 (1990)

10. A.B.Henriques, A.R.Liddle, R.G.Moorhouse, Phys.Lett B251 511 (1990)

11. J.Ellis, J.I.Kapusta, K.A.Olive, UMN–TH–834/90, CERN–TH.5741/90

12. S.Chandrasekhar, Monthly Notices of the Royal Astronomical Society 95 222 (1935)

13. J.R.Oppenheimer, G.M.Volkoff, Phys.Rev 55 455 (1939)

14. R.C.Malone, M.B.Johnson, H.A.Bethe, Ap.J 99 741 (1975)

15. H.A.Bethe, M.B.Johnson Nucl.Phys A230 1 (1974)

16. C.W.Misner, K.S.Thorne, J.A.Wheeler, 'Gravitation' (1972)

17. S.L.Shapiro, S.A.Teukolsky, 'Black Holes, White Dwarfs and Neutron Stars'

18. see for example L.Lindblom, S.L.Detweiler Ap.J (Supp) 53 73 (1983)

19. S.L.Shapiro, S.A.Teukolsky, I.Wassermann, Ap.J 272 702 (1983)

20. S.L.Friedman, J.R.Ipser, L.Parker, Phys.Rev.Lett 62 3015 (1989)

21. G.Glen, P.Sutherland, Ap.J 239 671 (1980)

22. B.L.Friman, O.V.Maxwell; Ap.J 232 541 (1979)

23. C.Alcock, E.Farhi, A.Olinto, Ap.J 310 261 (1986)

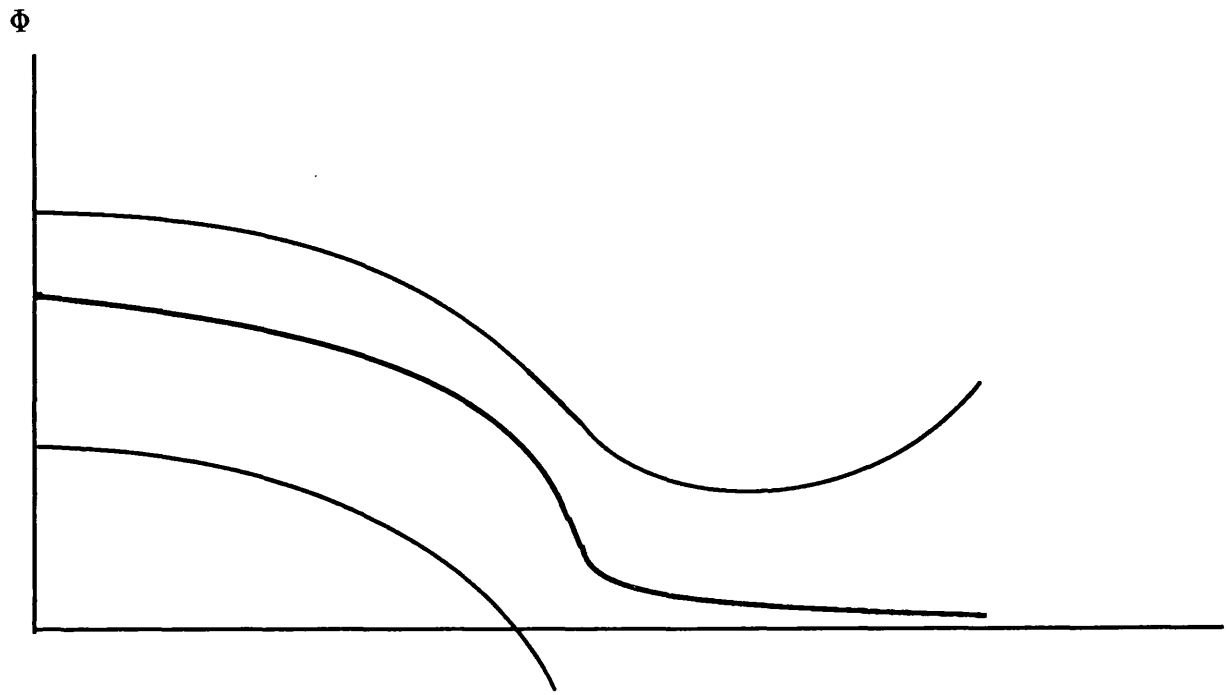

Figure 1.1

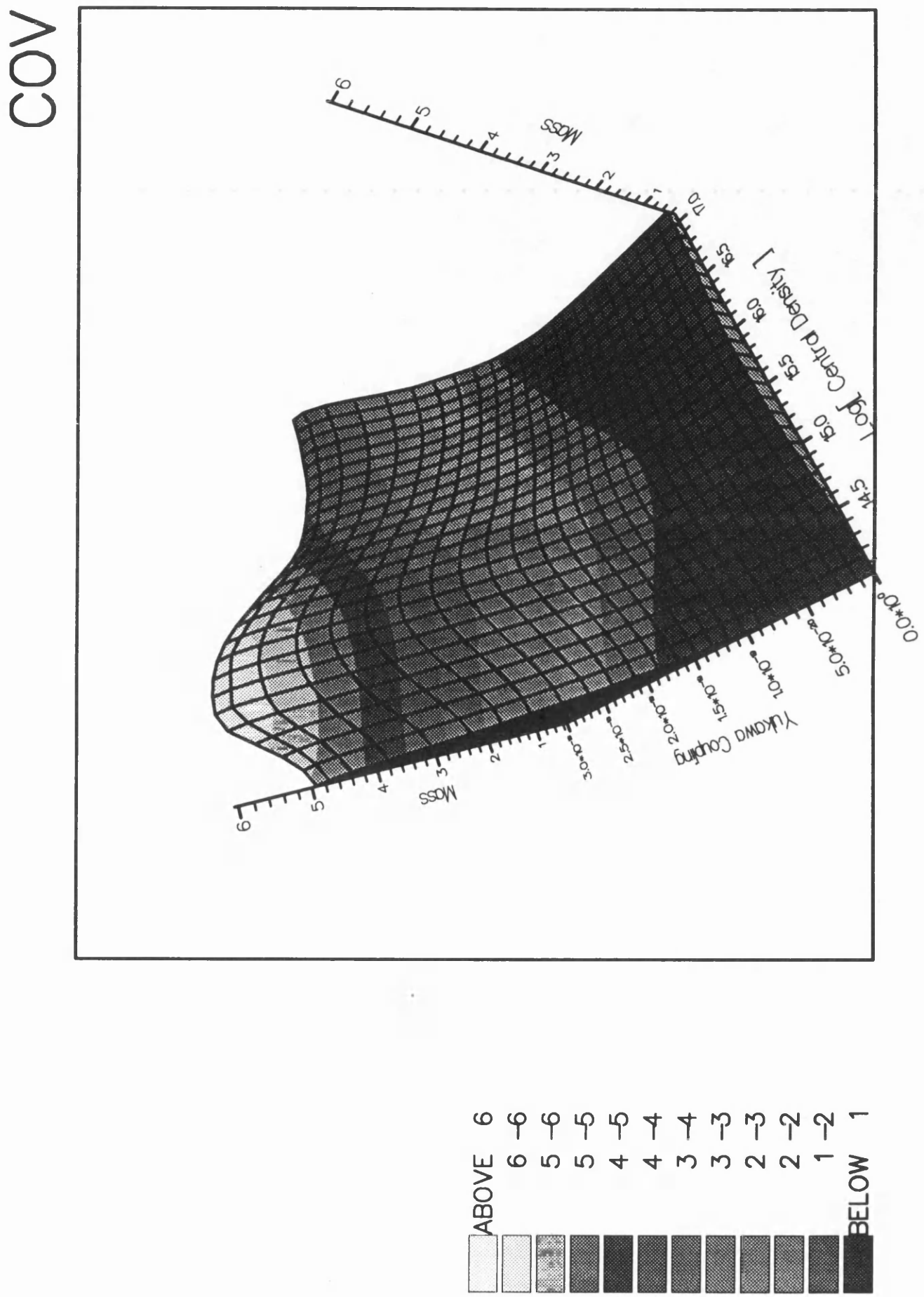
COV
Mass
Mass
Log Centrd Density]
Velocity Coupling
ABOVE 6
6 6
5 6
5 5
4 5
4 4
3 4
3 3
2 3
2 2
1 2
BELOW 1

Figure 1.2a

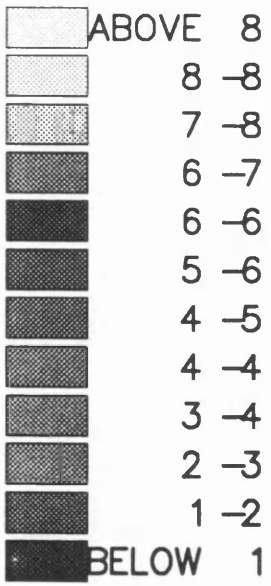
ABOVE 8
8 –8
7 –8
6 –7
6 –6
5 –6
4 –5
4 –4
3 –4
2 –3
1 –2
BELOW 1

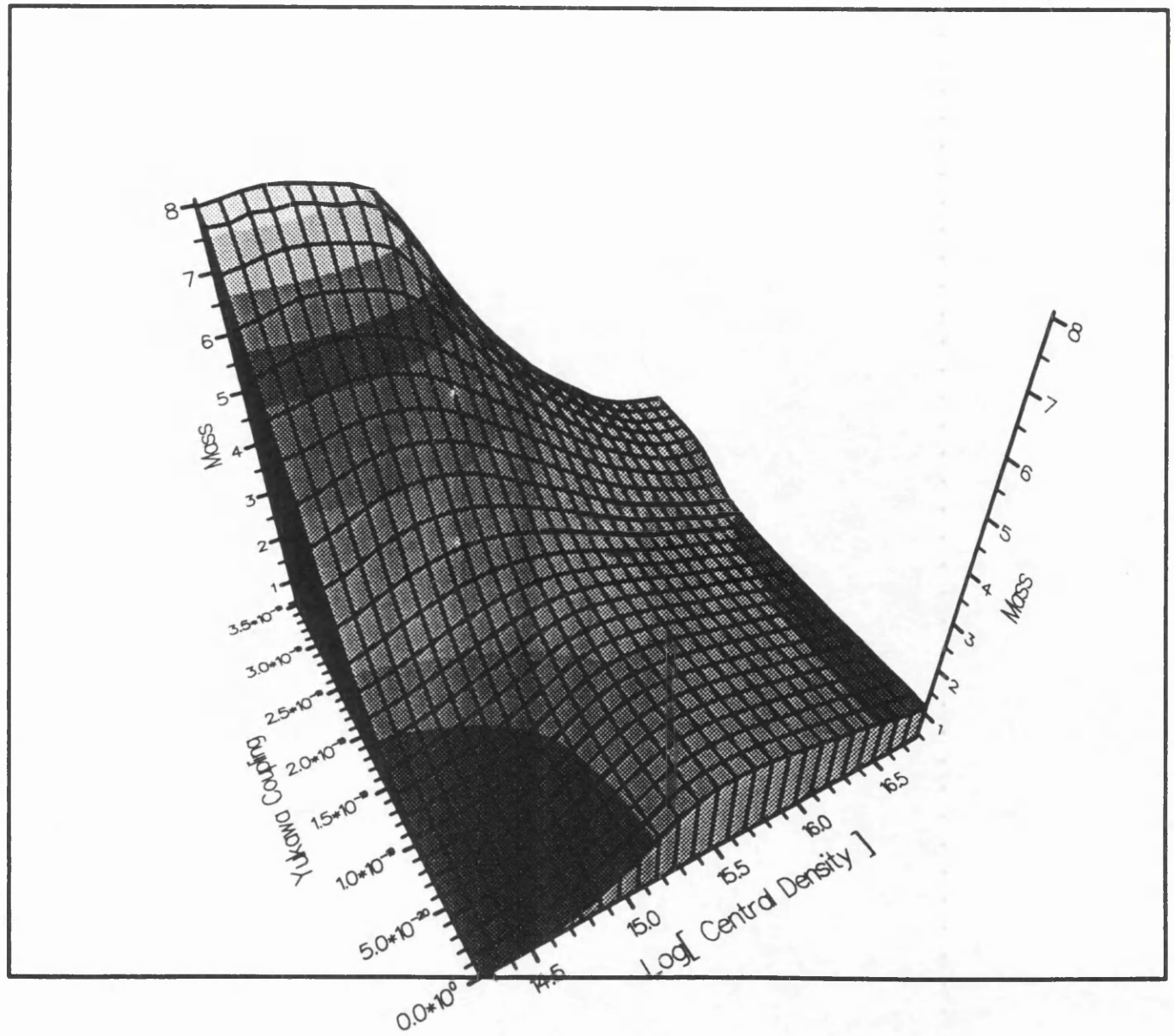
BJ VN
Mass
8
7
6
5
4
3
2
1
Yukawa Coupling
3.5*10⁻⁸
3.0*10⁻⁸
2.5*10⁻⁸
2.0*10⁻⁸
1.5*10⁻⁸
1.0*10⁻⁸
5.0*10⁻⁹
0.0*10⁰
14.5
15.0
15.5
16.0
16.5
Log[Central Density]
Mass
1
2
3
4
5
6
7
8

Figure 1.2b

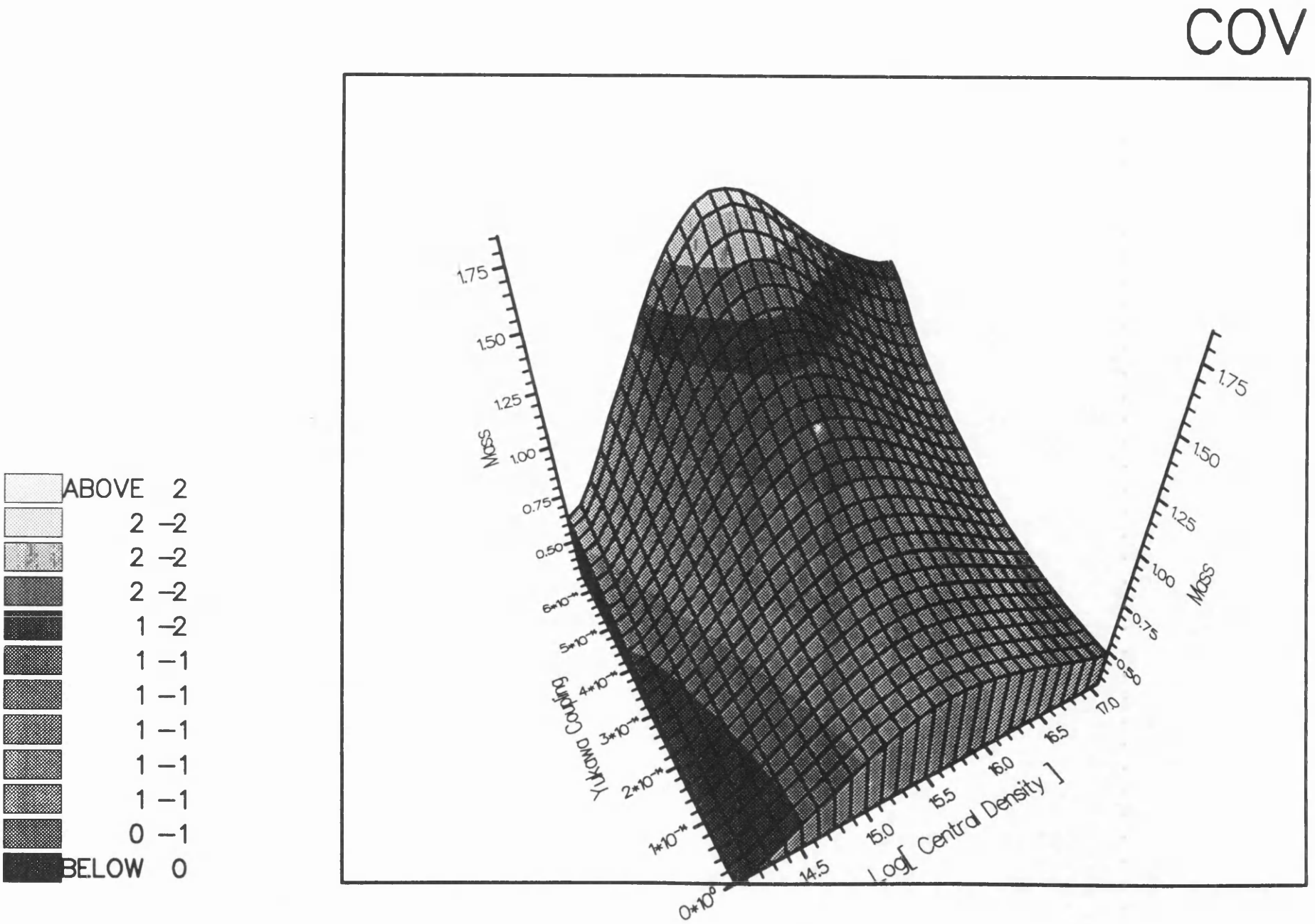

Figure 1.3a
69

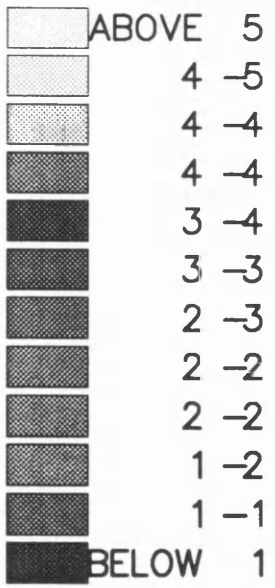

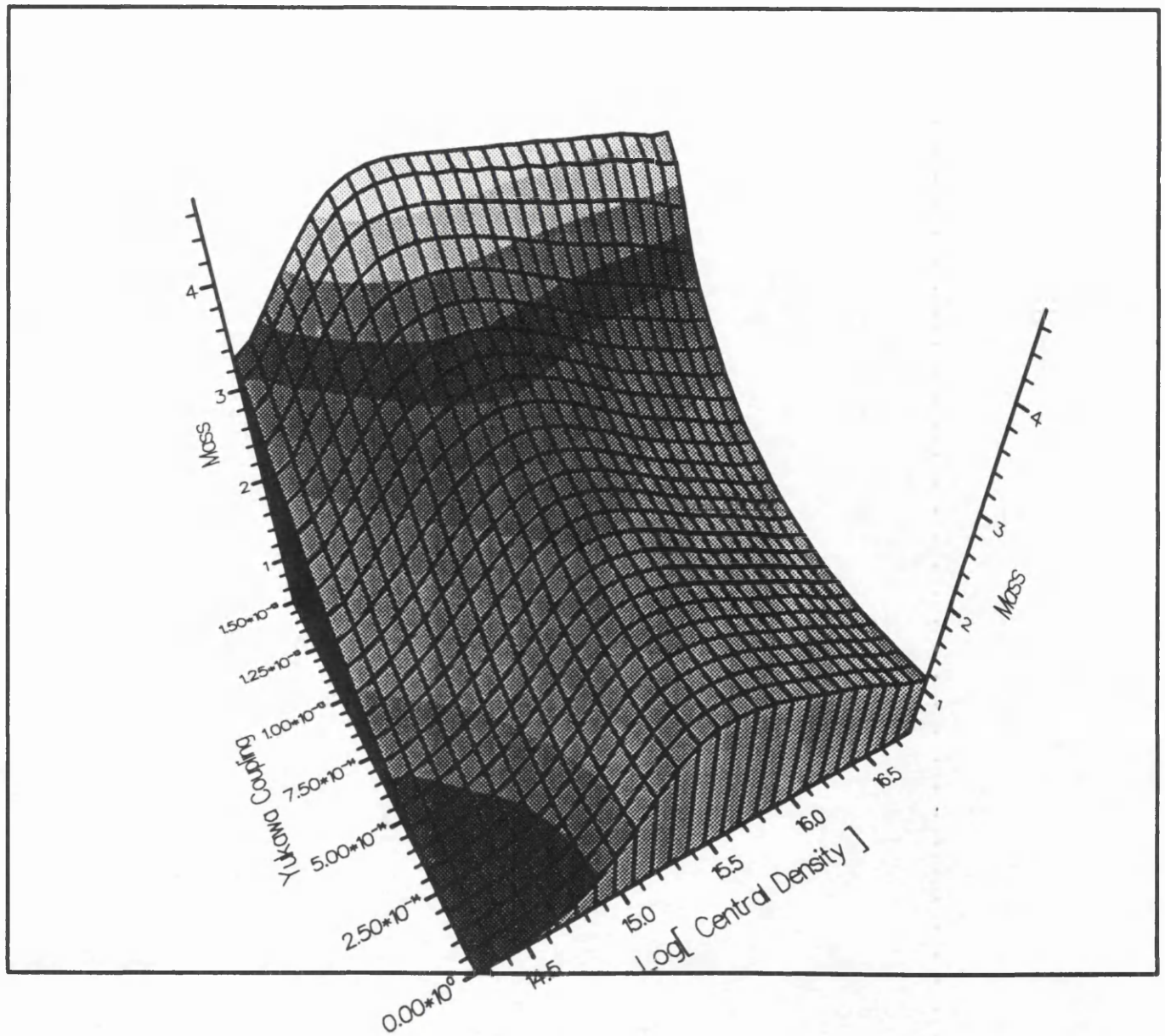

Figure 1.3b
70

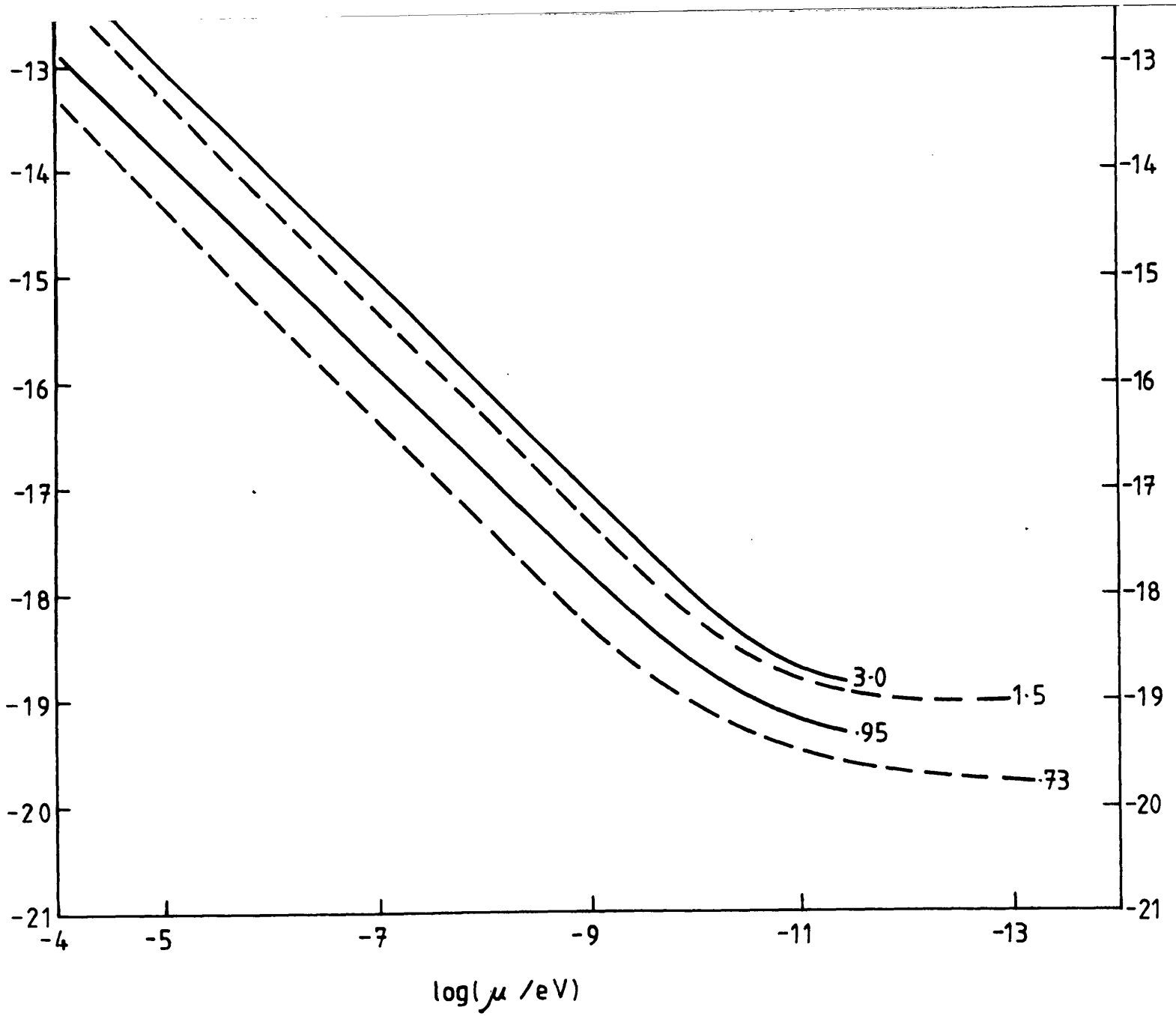

Figure 1.4

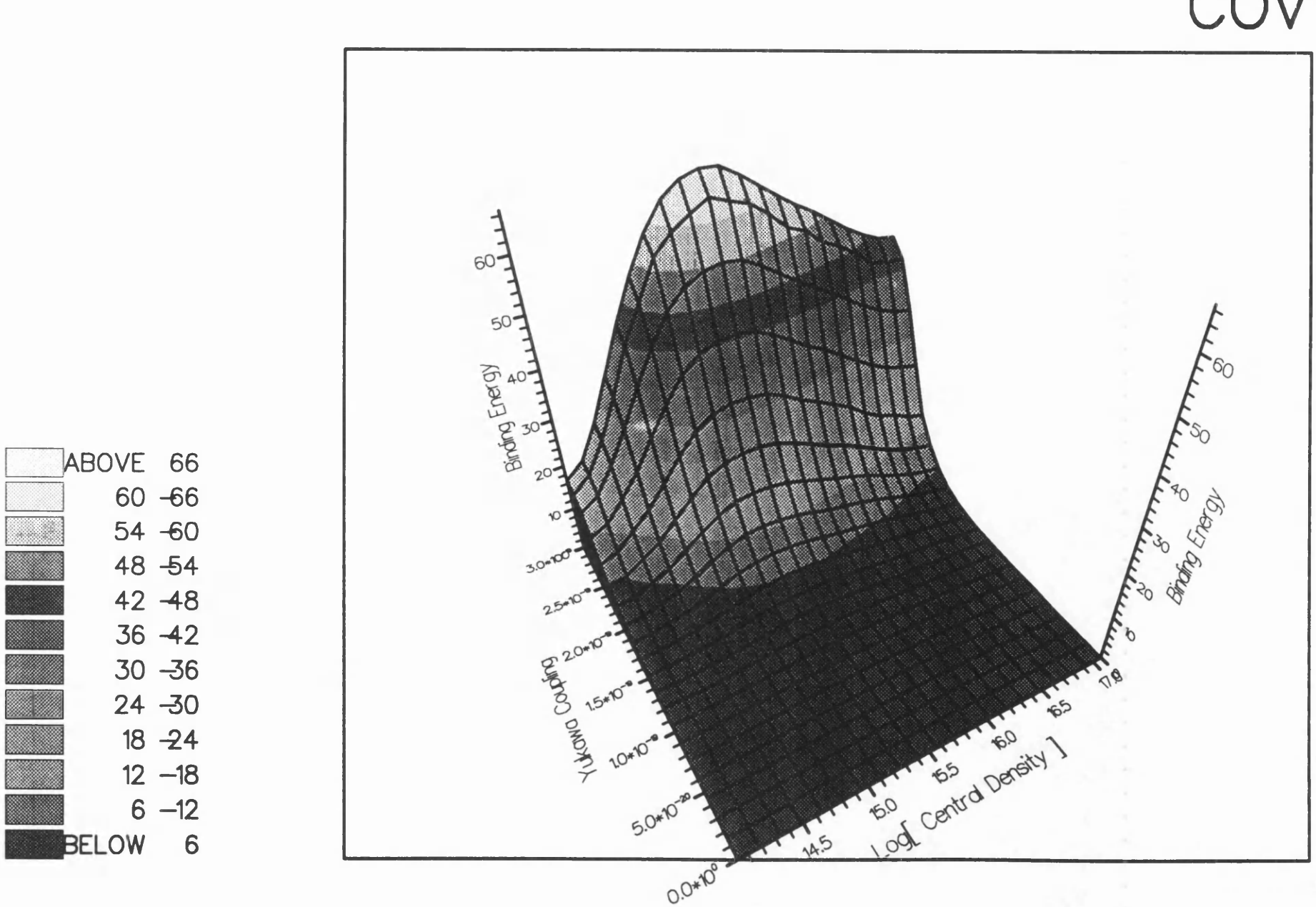
COV
ABOVE 66
60 -66
54 -60
48 -54
42 -48
36 -42
30 -36
24 -30
18 -24
12 -18
6 -12
BELOW 6
Binding Energy
60
50
40
30
20
10
3.0*10^-7
2.5*10^-8
2.0*10^-8
1.5*10^-8
1.0*10^-8
5.0*10^-20
0.0*10^0
Yukawa Coupling
14.5
15.0
15.5
16.0
16.5
17.0
Log[Central Density]
0
20
30
40
50
60
Binding Energy

Figure 1.5a

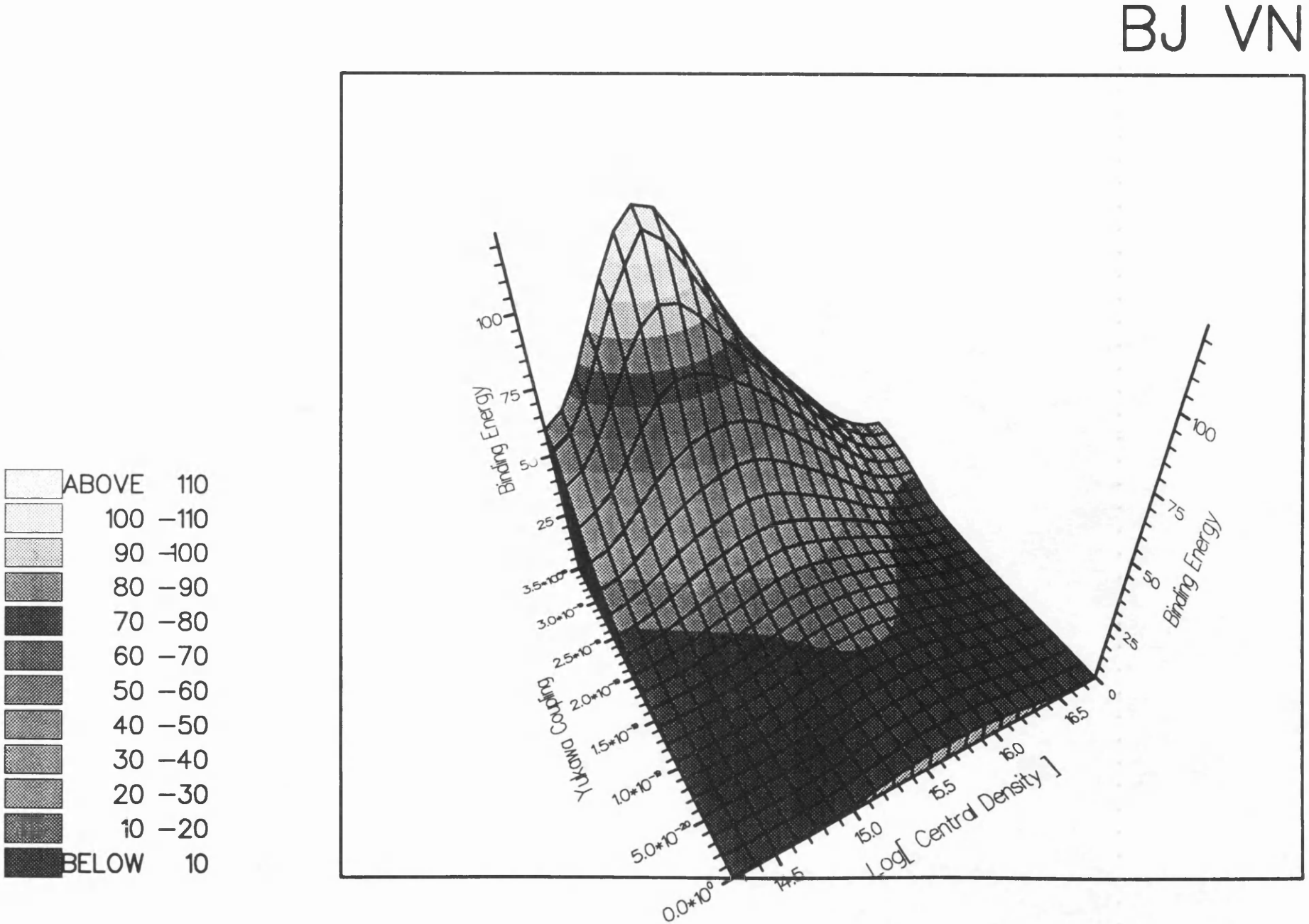
BJ VN
ABOVE 110
100 –110
90 –100
80 –90
70 –80
60 –70
50 –60
40 –50
30 –40
20 –30
10 –20
BELOW 10
Binding Energy
100
75
50
25
Yukawa Coupling
3.5*10⁻⁹
3.0*10⁻⁹
2.5*10⁻⁹
2.0*10⁻⁹
1.5*10⁻⁹
1.0*10⁻⁹
5.0*10⁻¹⁰
0.0*10⁰
14.5
15.0
15.5
16.0
16.5
Log[Central Density]
0
25
50
75
100
Binding Energy

Figure 1.5b

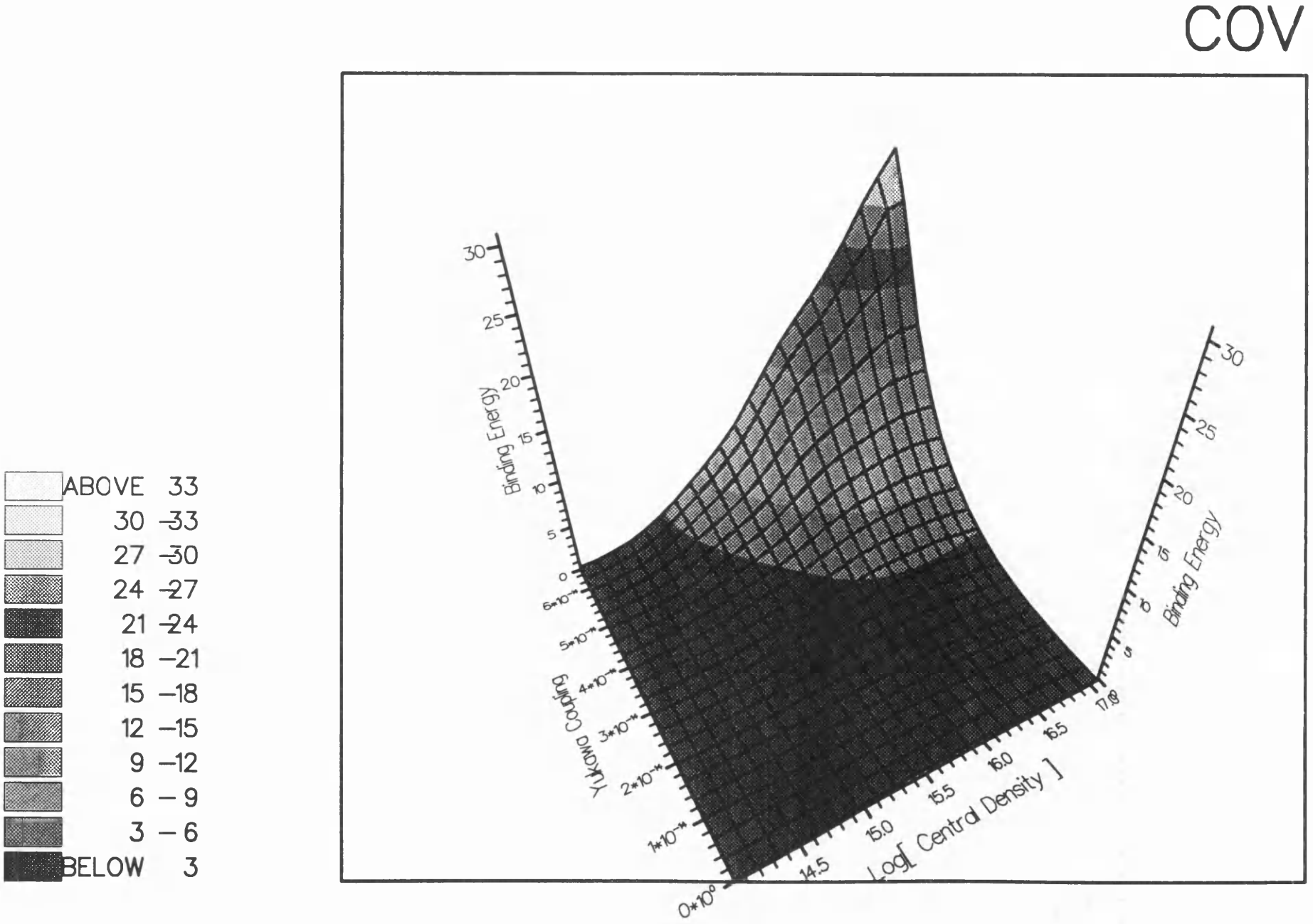
COV
ABOVE 33
30 –33
27 –30
24 –27
21 –24
18 –21
15 –18
12 –15
9 –12
6 – 9
3 – 6
BELOW 3
Binding Energy
Yukawa Coupling
Log[Central Density]
Binding Energy

Figure 1.6a

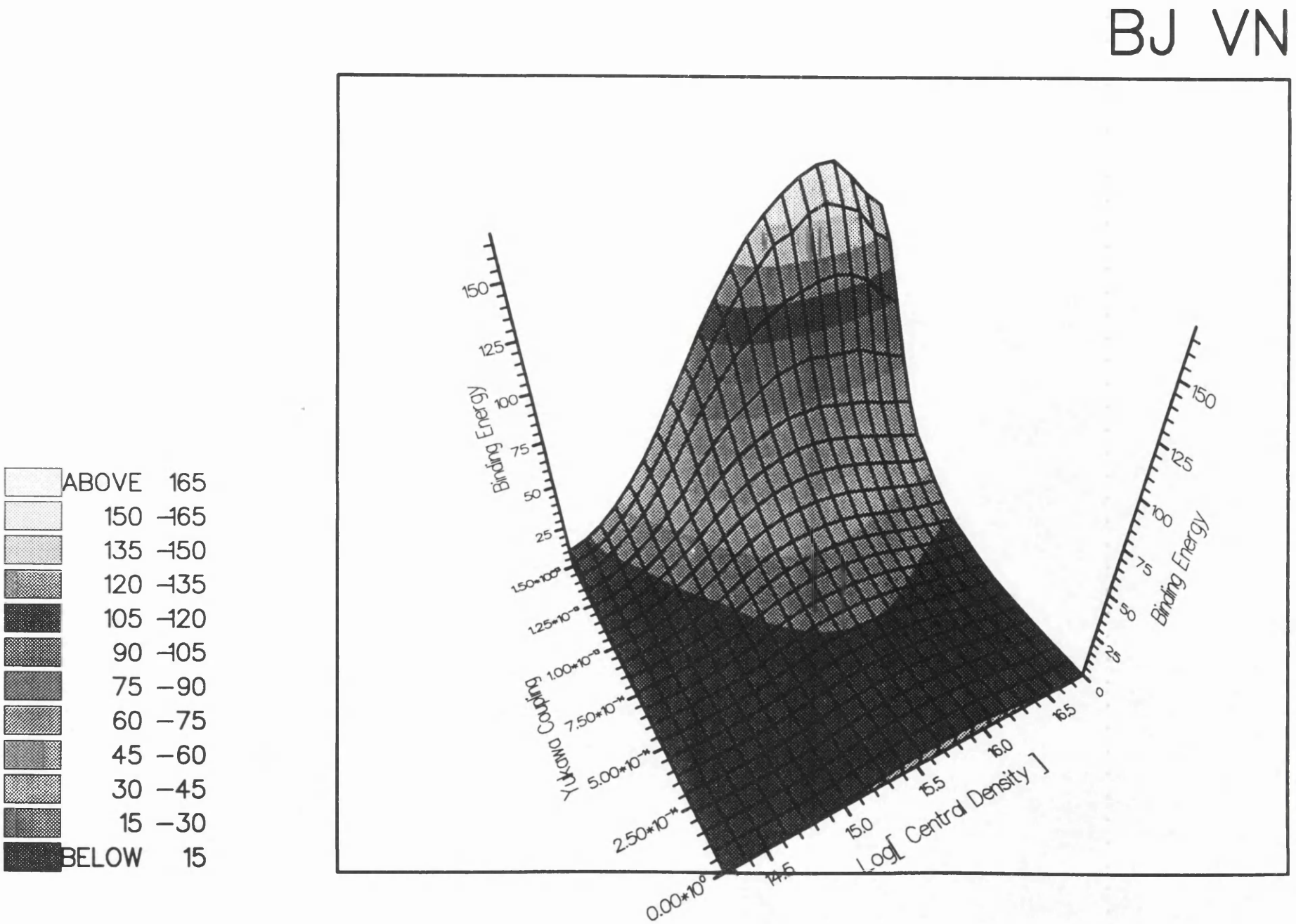

Figure 1.6b
75

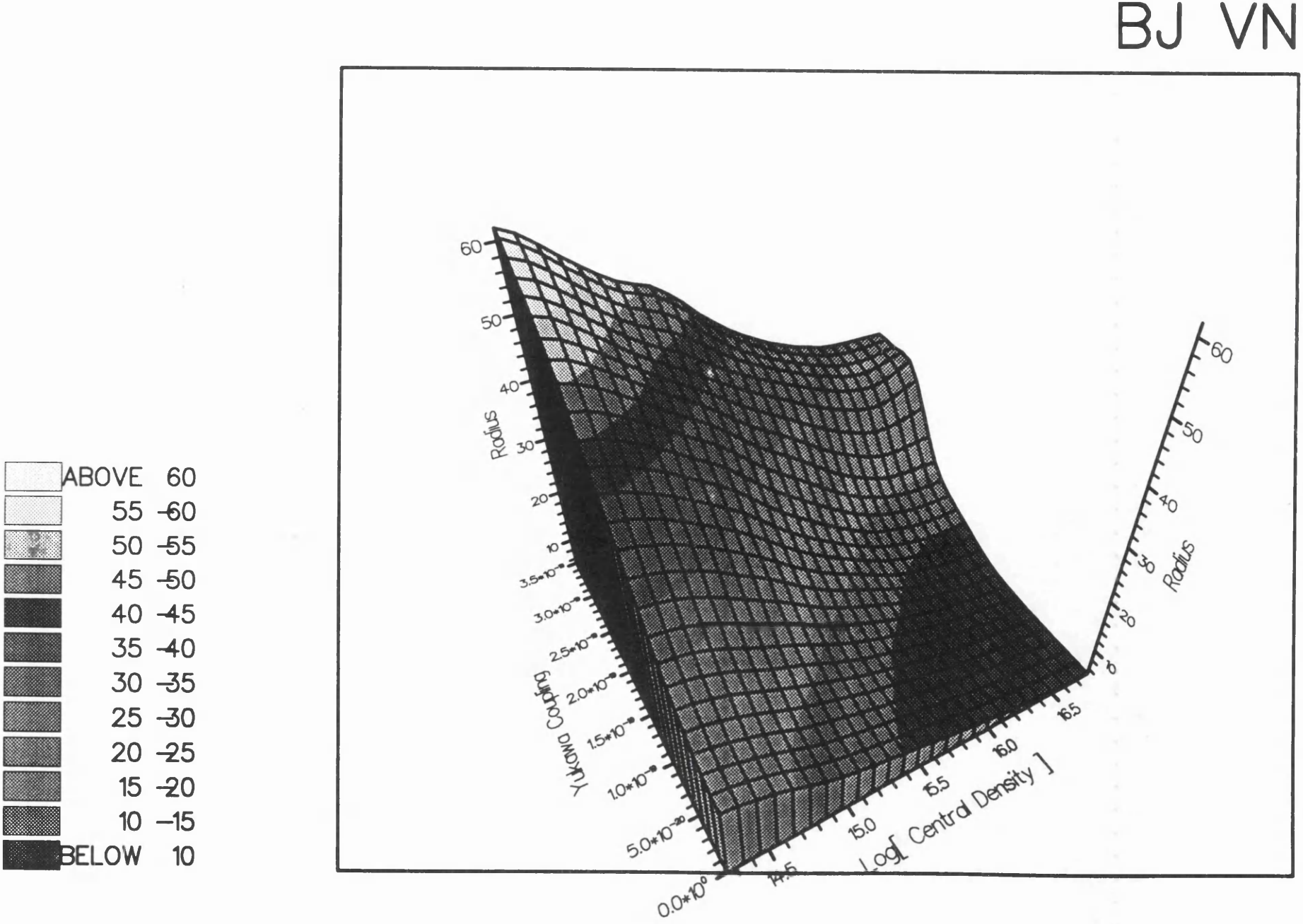
BJ VN
ABOVE 60
55 -60
50 -55
45 -50
40 -45
35 -40
30 -35
25 -30
20 -25
15 -20
10 -15
BELOW 10
Radius
Yukawa Coupling
Log[Central Density]
Radius

Figure 1.7a

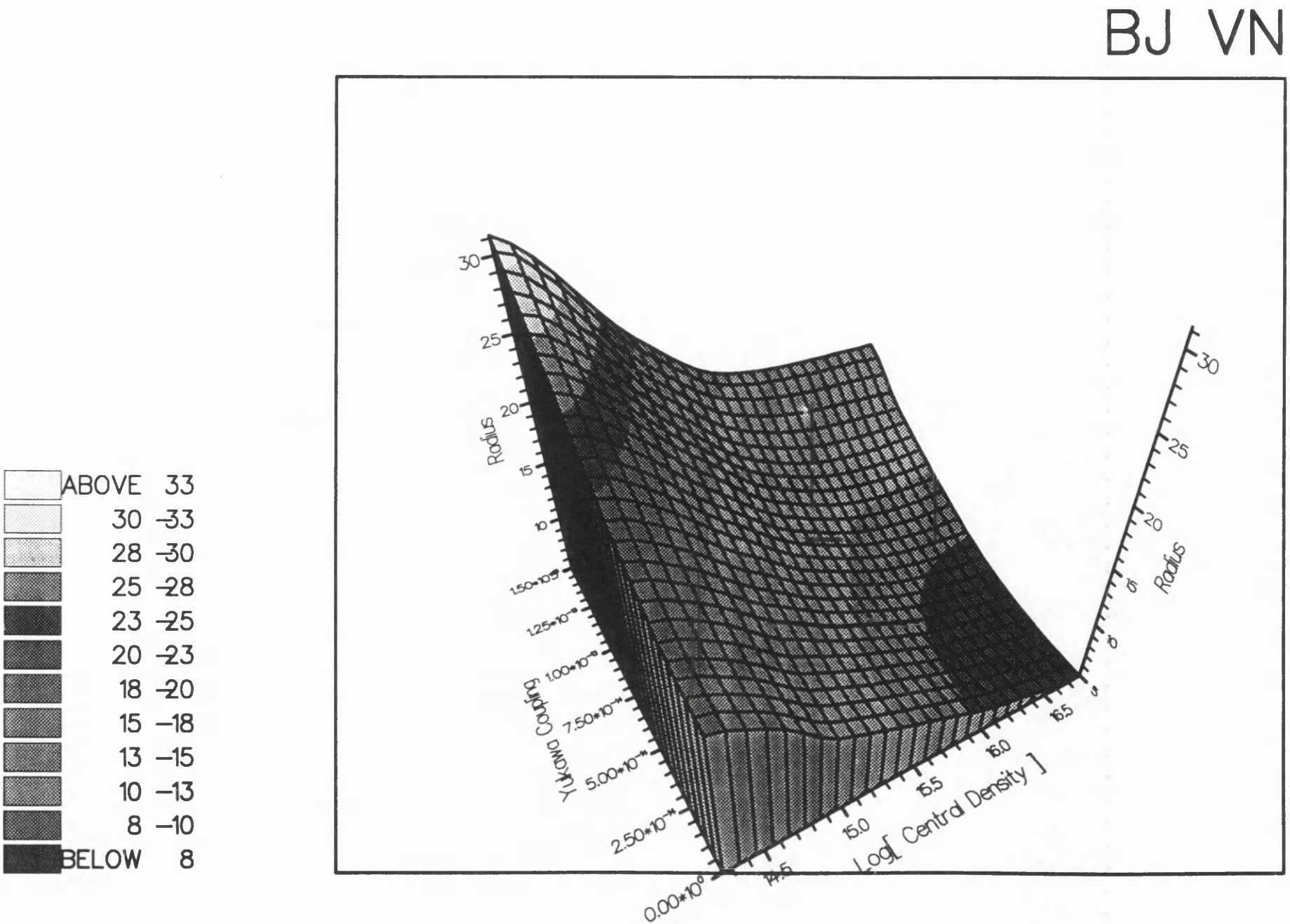
BJ VN
ABOVE 33
30 –33
28 –30
25 –28
23 –25
20 –23
18 –20
15 –18
13 –15
10 –13
8 –10
BELOW 8
Radius
30
25
20
15
10
Yukawa Coupling
1.50*10⁻⁹
1.25*10⁻⁹
1.00*10⁻⁹
7.50*10⁻¹⁰
5.00*10⁻¹⁰
2.50*10⁻¹⁰
0.00*10⁰
14.5
15.0
15.5
16.0
16.5
Log[Central Density]
0
5
10
15
20
25
30
Radius

Figure 1.7b

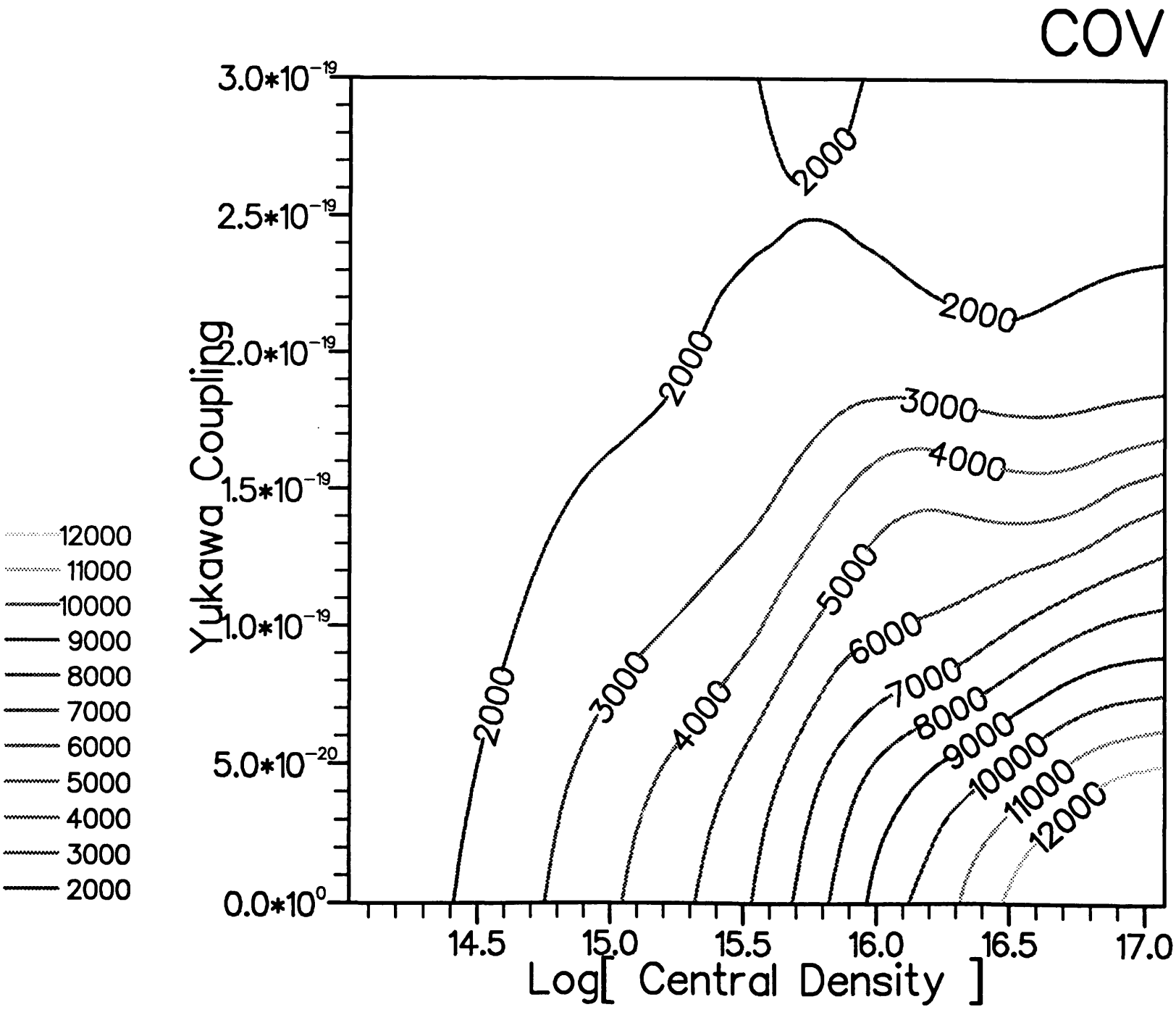

Figure 1.8a
78

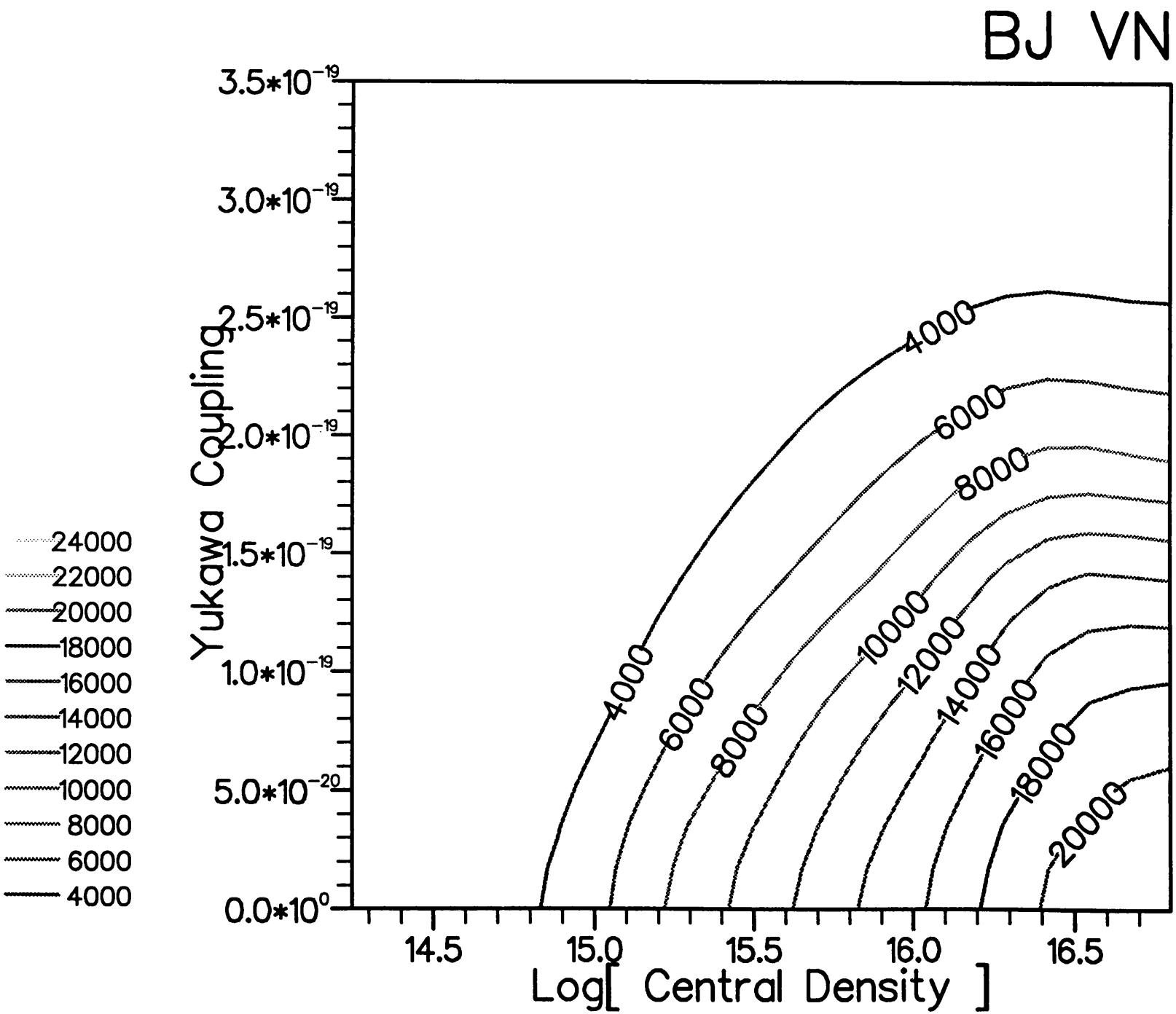
BJ VN
Yukawa Coupling
Log[Central Density]
3.5*10^-19
3.0*10^-19
2.5*10^-19
2.0*10^-19
1.5*10^-19
1.0*10^-19
5.0*10^-20
0.0*10^0
14.5
15.0
15.5
16.0
16.5
4000
6000
8000
10000
12000
14000
16000
18000
20000
24000
22000
20000
18000
16000
14000
12000
10000
8000
6000
4000

Figure 1.8b

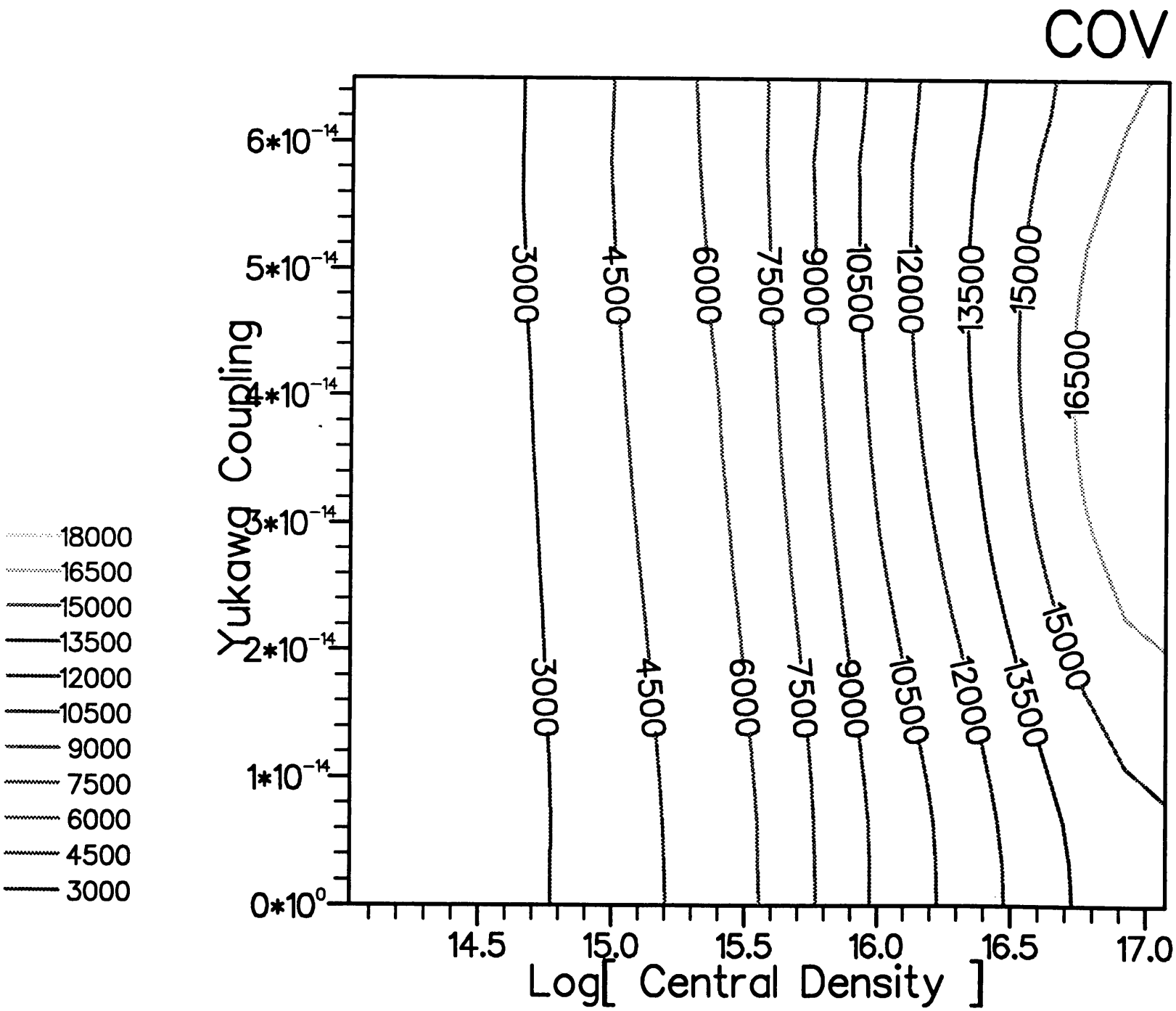
COV
Yukawa Coupling
0*10^0
1*10^-14
2*10^-14
3*10^-14
4*10^-14
5*10^-14
6*10^-14
14.5
15.0
15.5
16.0
16.5
17.0
Log[Central Density]
3000
4500
6000
7500
9000
10500
12000
13500
15000
16500
18000

Figure 1.9a

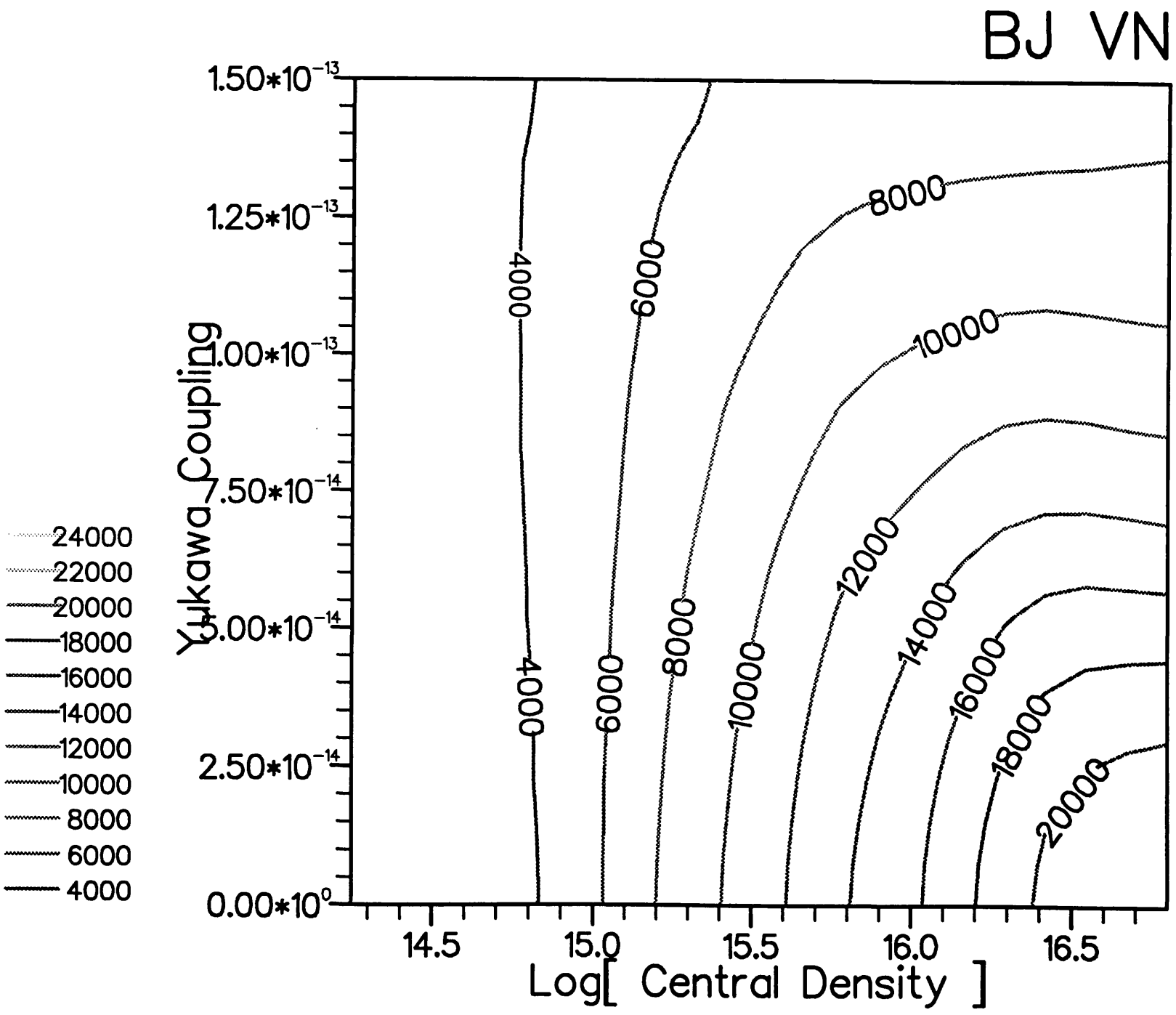
BJ VN
1.50*10^-13
1.25*10^-13
1.00*10^-13
7.50*10^-14
5.00*10^-14
2.50*10^-14
0.00*10^0
Yukawa Coupling
14.5
15.0
15.5
16.0
16.5
Log[Central Density]
4000
6000
8000
10000
12000
14000
16000
18000
20000
24000
22000
20000
18000
16000
14000
12000
10000
8000
6000
4000

Figure 1.9b

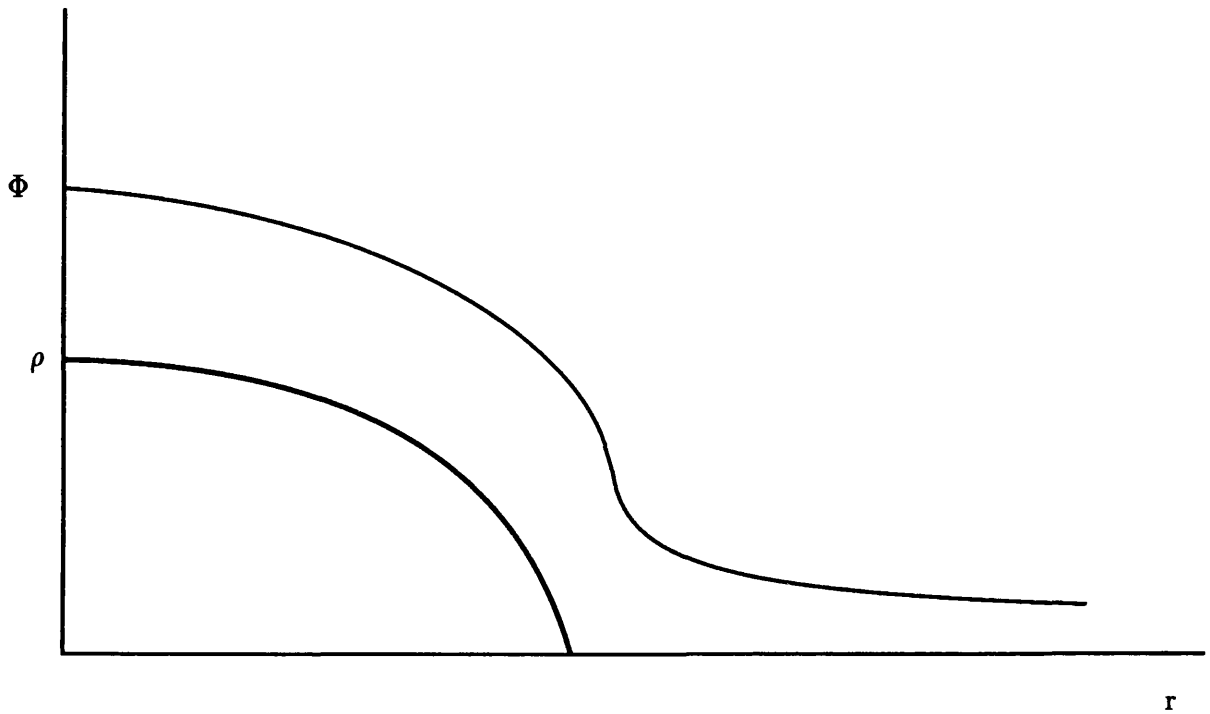

Figure 1.10

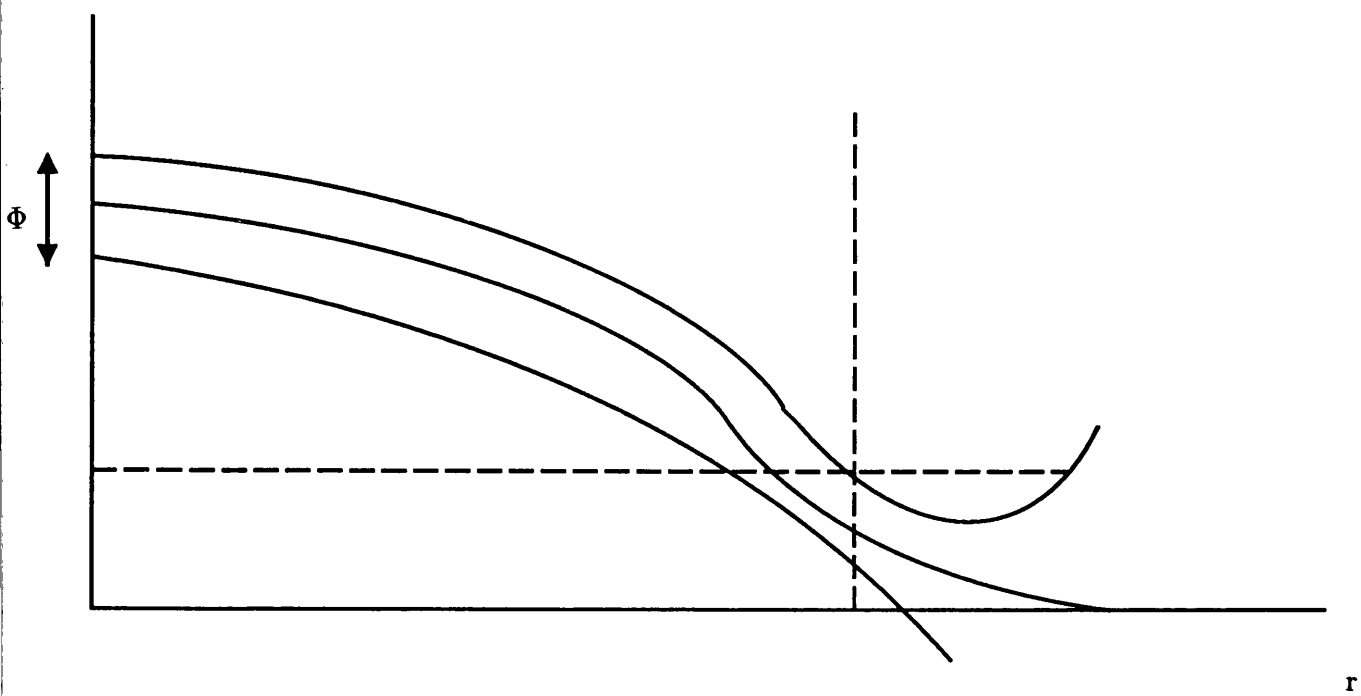

Figure 1.11

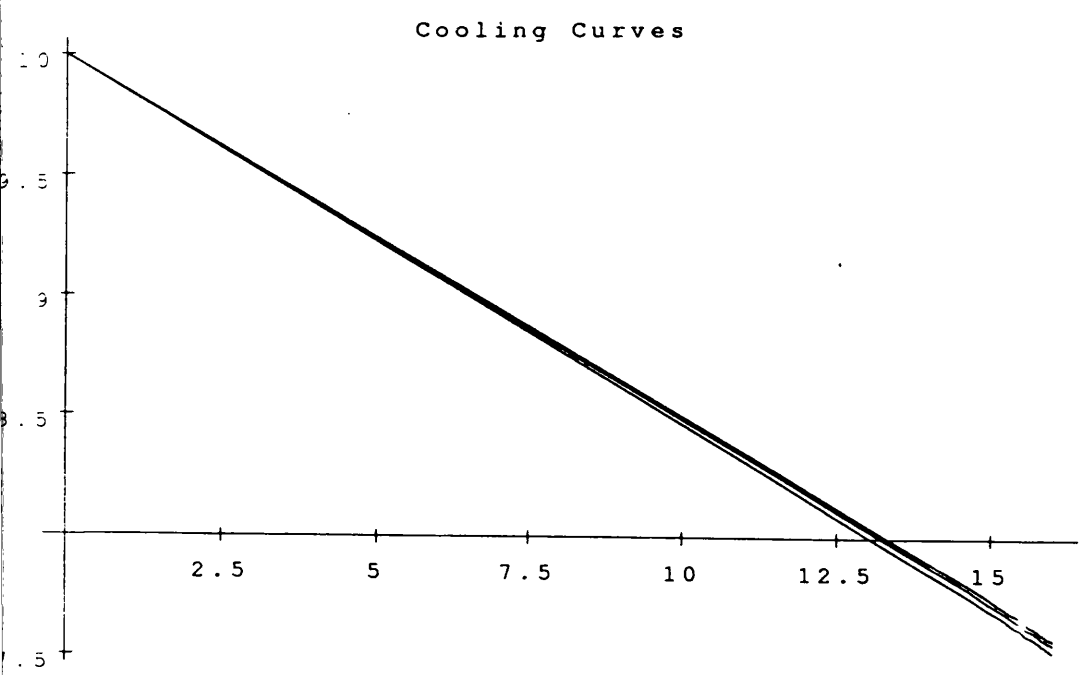

Figure 1.12a

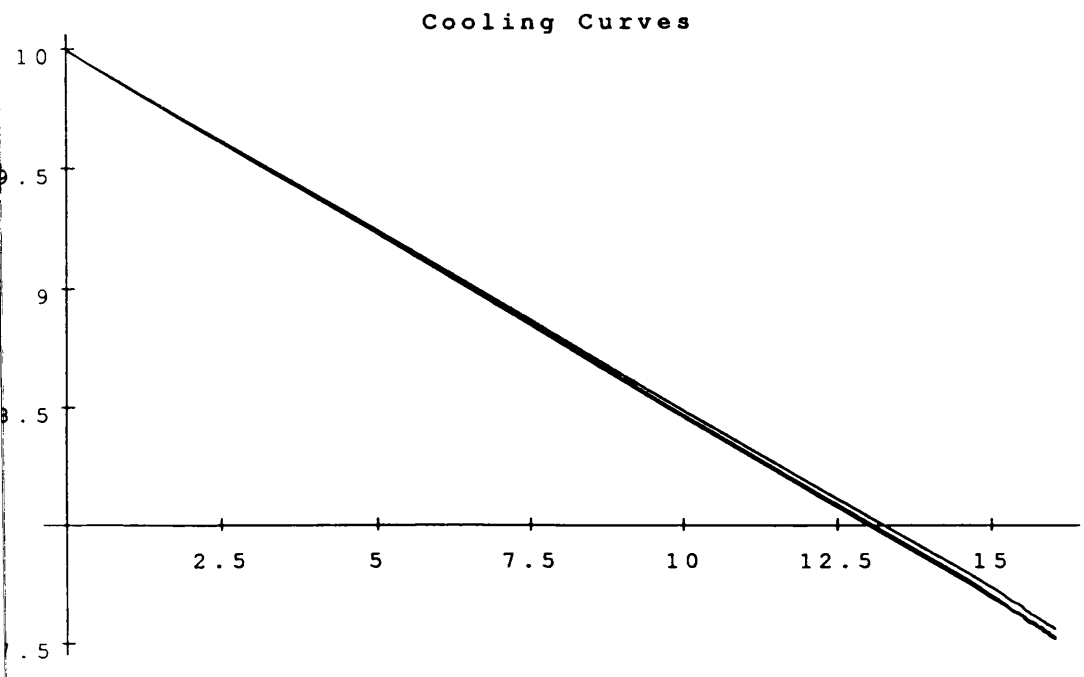

Figure 1.12b

Chapter Two

Neutron Stars: Radial Oscillations, Stability and Scalar Radiation

In the previous chapter static neutron star–scalar field configurations were found and their properties examined. In certain cases, the effects of the scalar field could be quite dramatic. The differences, which arise due to the presence of the scalar field, can be thought of as being due to the fluid's equation of state being significantly stiffened. The next, most natural, question one may ask is, which of these configurations are stable, which are unstable, and, what are the essential differences between the stability criteria for ordinary neutron stars and those for neutron star–scalar field configurations?

To answer these questions one must consider the adiabatic radial pulsations of the stellar configurations. Such considerations were first made for neutron stars by Chandrasekhar[1] in 1964 who derived derived the stability criterion for such objects in terms of an elegant variational formalism. This stability criterion depends crucially on the condition that the oscillating system does not

lose energy. This is obviously true for normal neutron stars because the neutron fluid is localized and because can be no gravitational waves from a monopole source.

For the case of a neutron star with attached scalar field, the situation is more complicated. Monopole scalar waves can exist and so there exists the possibility of scalar radiation escaping to infinity and therefore the oscillations of the star will be damped. These scalar waves will carry away energy making the star lose mass, which will in turn, have a bearing on the stability of the system; will the star release a burst of radiation, then stabilize or will the whole configuration be dispersed?

A general analysis of such phenomena is extremely complicated because of the presence of the radiative backreaction and damping. However, in this chapter it will be shown that a significant simplification occurs depending on which region of scalar mass is being considered; it is found that the stability and the radiation problem can, to an extent, be studied separately. Only in the extreme ultralight region of the scalar mass will there be a strong mixing of these effects. It is worth remembering that in this region even static configurations were extremely difficult to construct, or rather many of the solutions found did not bear any great resemblance to any reasonable neutron star-like configuration.

Before such a discusion may begin one needs the actual pulsation equations for the star. These are derived in the next section.

2.1 Derivation of the Pulsation Equations

Consider a static fluid–scalar configuration, $\mathcal{C}$, labelled by the central density of the fluid and the mass and coupling of the scalar field, (μ, g, ρ_c). Unique for any value of these parameters there exist four functions which describe the configuration, A_o, B_o, ρ_o, Φ_o. So one has

$$\mathcal{C}_{\mu g \rho_c} = (A_o(r), B_o(r), \rho_o(r), \Phi_o(r)) \tag{1}$$

where the four functions satisfy the time-independent Einstein Klein-Gordon equations

$$A_o' = \frac{A_o}{r} - \frac{{A_o}^2}{r} - 8\pi G g r {A_o}^2 J_o \Phi_o + 4\pi G \mu^2 r {A_o}^2 {\Phi_o}^2 + 8\pi G r {A_o}^2 \rho_o + 4\pi G r A_o {\Phi_o}'^2 \quad (2)$$

$$B_o' = -\frac{B_o}{r} + \frac{A_o B_o}{r} + 8\pi G A_o J_o \Phi_o - 4\pi G \mu^2 r {A_o}^2 {\Phi_o}^2 + 8\pi G r A_o p_o + 4\pi G r B_o {\Phi_o}'^2 \quad (3)$$

$$p_o' = -\frac{B'}{2B}(p_o + \rho_o) - g\Phi_o J_o' \quad (4)$$

$$\Phi_o'' = \Phi_o' \left[\frac{A_o'}{2A_o} - \frac{B_o'}{2B_o} - \frac{2}{r}\right] + \mu^2 A_o \Phi_o - g A_o J_o \quad (5)$$

The metric of the static configuration is

$$ds^2 = B_o dt^2 - A_o dr^2 - r^2 d\theta^2 - r^2 \sin^2(\theta) d\phi^2 \quad (6)$$

The strategy employed in this derivation will be to perturb the full time dependent field equations about this static solution keeping only the linear terms in the perturbed quantities. These equations; Einstein, Klein-Gordon plus energy conservation and the equations of thermodynamics will be reduced to only two, the 'pulsation equations'. These are the equations of motion for the fluid and scalar perturbations and depend only on the static quantities.

Consider the time dependent Einstein Klein-Gordon equations

$$ds^2 = B(t,r) dt^2 - A(t,r) dr^2 - r^2 d\theta^2 - r^2 \sin^2(\theta) d\phi^2 \quad (7)$$

now with the pressure, density and scalar field functions of t as well.

The displacement of the fluid is denoted ξ, and the fluid 4-velocity is now

$$U_\mu = \left(\sqrt{B_o}, -\frac{A_o \dot{\xi}}{\sqrt{B_o}}, 0, 0\right) \quad (8)$$

This last relationship follows from the definition $U^r/U^t = \dot{\xi}$, and the normalization condition of the fluid 4-velocity $U_\mu U^\mu = 1$.

The time dependent equation are

$$-\frac{B}{r^2} + \frac{B}{Ar^2} - 8\pi G B J \Phi + 8\pi G \mu^2 B \Phi^2 + 8\pi G B \rho - \frac{BA'}{rA^2} + 4\pi G \frac{B \Phi'^2}{A} + 4\pi G \dot{\Phi}^2 = 0 \quad (9)$$

$$-\frac{\delta\dot{A}}{rA} - 8\pi G A_o (p+\rho)\frac{\sqrt{B}}{\sqrt{B_o}}\dot{\xi} + 8\pi G\Phi'\dot{\Phi} = 0 \quad (10)$$

$$-\frac{1}{r^2} + \frac{A}{r^2} + 8\pi GAp + 8\pi GgAJ\Phi - 4\pi G\mu^2 - \frac{B'}{rB} + 4\pi G\Phi'^2 + 4\pi G\frac{A\dot{\Phi}^2}{B} = 0 \quad (11)$$

$$8\pi GABp + 8\pi GgJ\Phi AB - 4\pi G\mu^2\Phi^2 AB - 4\pi GB\Phi'^2 + \frac{A'B}{2r} + \frac{A'B'}{4A} + B'^2 - \frac{B''}{2} + \frac{\ddot{A}}{2} = 0 \quad (12)$$

$$\frac{\ddot{\Phi}}{B} + \dot{\Phi}\left[\frac{\dot{A}}{2AB} - \frac{\dot{B}}{2B^2}\right] - \frac{\Phi''}{A} + \Phi'\left[\frac{A'}{2A^2} - \frac{B'}{2AB} - \frac{2}{Ar}\right] + \mu^2\Phi - gJ = 0 \quad (13)$$

The energy conservations are omitted for the sake of brevity.

It is necessary to define here *Eulerian* and *Lagrangian* perturbations. Eulerian perturbations, denoted δX, are measured by observers who remain fixed in the coordinate system while Lagrangian perturbations, denoted ΔX, are those measured by observers who move with the fluid. These types of perturbation are related by the following

$$\Delta X = \delta X + X_o'\xi \quad (14)$$

Making the following substitutions

$$A(t,r) = A_o(r) + \delta A(t,r) \quad (15)$$

$$B(t,r) = B_o(r) + \delta B(t,r) \quad (16)$$

$$p(t,r) = p_o(r) + \delta p(t,r) \quad (17)$$

$$\rho(t,r) = \rho_o(t,r) + \delta\rho(t,r) \quad (18)$$

$$J(t,r) = J_o(r) + \delta J(t,r) \quad (19)$$

$$\Phi(t,r) = \Phi_o(r) + \delta\Phi(t,r) \quad (20)$$

and inserting these expressions into the time dependent equations, after which expanding and linearizing, gives the following set

$$\delta A\left[-\frac{B_o}{r^2} - 8\pi GgB_oJ_o\Phi_o + 4\pi G\mu^2 B_o{\Phi_o}^2 + 8\pi GB_o\rho_o + \frac{B_oA_o'}{{A_o}^2 r}\right] - \delta A'\left[\frac{B_o}{A_o r}\right] + \delta\Phi\left[-8\pi GgA_oB_oJ_o + 8\pi G\mu^2 A_oB_o\Phi_o\right] + \delta\Phi'\left[8\pi G\Phi_o'B_o\right] + \delta J\left[-8\pi GgA_oB_o\Phi_o\right] + \delta\rho\left[8\pi GA_oB_o\right] = 0 \quad (21)$$

$$-\frac{\delta\dot{A}}{rA_o} - 8\pi GA_o(p_o+\rho_o)\dot{\xi} + 8\pi G\Phi_o{}'\delta\dot{\Phi} \;=\; 0 \qquad (22)$$

$$\delta A\left[\frac{1}{r^2} + 8\pi Gp_o + 8\pi GgJ_o\Phi_o - 4\pi G\mu^2{\Phi_o}^2\right] + \delta p\,[8\pi GA_o]$$
$$+\delta\Phi\left[8\pi GgA_oJ_o - 8\pi G\mu^2A_o\Phi_o\right] + \delta\Phi'\,[8\pi G\Phi_o{}'] +$$
$$\delta J\,[8\pi GgA_o\Phi_o]\,\delta B\left[\frac{B_o{}'}{{B_o}^2r}\right] - \frac{\delta B'}{B_or} \;=\; 0 \qquad (23)$$

$$8\pi GJ_o\Phi_o - 4\pi G\mu^2{\Phi_o}^2 + 8\pi Gp_o + \frac{A_o{}'}{2{A_o}^2r} - \frac{B_o{}'}{2r^2A_oB_o}$$
$$\frac{A_o{}'B_o{}'}{4{A_o}^2B_o} + \frac{{B_o{}'}^2}{4A_o{B_o}^2} - 4\pi G\frac{\Phi_o{}'}{A_o} - \frac{B_o{}''}{2A_oB_o} + \delta A\left[-\frac{A_o{}'}{{A_o}^3r}\right.$$
$$+\frac{B_o{}'}{2r^2{A_o}^2B_o} - \frac{A_o{}'B_o{}'}{2{A_o}^3B_o} - \frac{{B_o{}'}^2}{4{A_o}^2{B_o}^2} + 8\pi G\frac{{\Phi'_o}^2}{2{A_o}^2} + \frac{B_o{}''}{2{A_o}^2B_o}$$
$$+\delta B\left[\frac{B_o{}'}{2r^2A_o{B_o}^2} - \frac{{B_o{}'}^2}{2A_o{B_o}^3} + \frac{B_o{}'}{2A_o{B_o}^2} + \frac{B_o{}''}{2A_o{B_o}^2}\right] + 8\pi Gg\Phi_o\delta J$$
$$+8\pi G\delta p + 8\pi GJ_o\delta\Phi - 8\pi G\mu^2\Phi_o\delta\Phi + \frac{\delta A'}{2{A_o}^2r} - \frac{\delta B'}{2r^2A_oB_o}$$
$$-\frac{\delta B'A_o{}'B_o{}'}{4{A_o}^2{B_o}^2} + \frac{A_o{}'\delta B'}{4{A_o}^2B_o} + \frac{B_o{}'\delta A'}{4{A_o}^2B_o} -$$
$$\frac{8\pi G\Phi_o{}'\delta\Phi'}{A_o} - \frac{\delta B''}{2A_oB_o} + \frac{\delta A''}{4A_oB_o} \;=\; 0 \qquad (24)$$

$$(p_o+\rho_o)\left[\frac{\delta A}{2A_o} + \frac{2\xi}{r} + \frac{B_o{}'\xi}{2B_o} + \xi'\right] + (p_o{}'+\rho_o{}')\xi - g\Phi_o\delta J + \delta\rho = 0 \qquad (25)$$

$$(p_o+\rho_o)\frac{A_o}{B_o}\ddot{\xi} + \delta p' + (p_o+\rho_o)\frac{\delta B'}{2B_o} - (p_o+\rho_o)\frac{B_o{}'\delta B}{2{B_o}^2}$$
$$+\frac{B_o{}'}{2B_o}(\delta p+\delta\rho) + g\Phi_o\delta J' + gJ_o{}'\delta\Phi \;=\; 0 \qquad (26)$$

$$\frac{\delta\ddot{\Phi}}{B_o} - \frac{\delta\Phi''}{A_o} + \delta\Phi'\left[\frac{A_o{}'}{2{A_o}^2.} - \frac{B_o{}'}{2A_oB_o} - \frac{2}{A_or}\right] + \mu^2\delta\Phi - g\delta J$$
$$+\delta B\left[\frac{B_o{}'\Phi_o{}'}{2A_o{B_o}^2}\right] - \delta B'\left[\frac{\Phi_o{}'}{2A_oB_o}\right] + \delta A'\left[\frac{\Phi_o{}'}{2{A_o}^2}\right]$$
$$+\frac{\delta A}{A_o}\left[\mu^2\Phi_o - gJ_o - \frac{A_o{}'\Phi_o{}'}{2{A_o}^2}\right] \;=\; 0 \qquad (27)$$

To these are added the equations of baryon number conservation and the adiabaticity relation.

Baryon conservation is expressed as

$$\nabla \cdot n = 0 \tag{28}$$

which becomes explicitly

$$\begin{aligned} u^\alpha \partial_\alpha (\Delta n) + \frac{n}{\sqrt{-g}} \partial_\beta \left(\sqrt{-g} u^\beta \right) &= 0 \\ \frac{n_o \delta \dot{A}}{2A_o} + \delta \dot{n} + \frac{n_o A_o{}' \dot{\xi}}{A_o} + \frac{2n_o \dot{\xi}}{r} + n_o{}' \dot{\xi} + n_o \dot{\xi}' &= 0 \end{aligned} \tag{29}$$

Adiabaticity, i.e negligible heat flow in the system, is expressed by the relation

$$\Gamma_1 = \frac{n}{p} \frac{\Delta p}{\Delta n} \tag{30}$$

The pulsation equations are equations (26) and (27) of the set. (26) describes the fluid oscillations and (27) describes the scalar oscillations. The derivation is however not complete. The pulsation equations are not in the required form. The remaining equations must be used to eliminate the unknown auxiliary functions, $\delta A, \delta B, \delta p, \delta \rho, \delta J$ from the pulsation equations.

From (22) after one integration, setting the constant equal to zero one finds that

$$\delta A = -8\pi G r A_o{}^2 (p_o + \rho_o) \xi + 8\pi G r A_o \Phi_o{}' \delta \Phi \tag{31}$$

and from the baryon conservation equation one also gets

$$\delta n = -\left(\frac{2n_o \xi}{r} + \frac{n_o A_o{}' \xi}{2A_o} + \frac{n_o \delta A}{2A_o} + n_o \xi' + n_o{}' \xi \right) \tag{32}$$

The adiabatic relation gives

$$\begin{aligned} \delta p &= \left(\frac{p_o \Gamma_1}{n_o} \right) \delta n + \left(\frac{p_o n_o{}' \Gamma_1}{n_o} - p_o{}' \right) \xi \\ &\quad - \Gamma_1 p_o \left(\frac{2\xi}{r} + \frac{A_o{}' \xi}{2A_o} + \frac{\delta A}{2A_o} + \xi' \right) - p_o{}' \xi \end{aligned} \tag{33}$$

and the tt-component of the linearized Einstein equations gives

$$\delta \rho = (p_o + \rho_o) \left(\frac{2\xi}{r} + \frac{A_o{}' \xi}{2A_o} + \frac{\delta A}{2A_o} + \xi' \right) - \rho_o{}' \xi + g \Phi_o \delta J + g \Phi_o J_o{}' \xi \tag{34}$$

There is no equation for δB, but instead one for $\delta B'$. This does however completely eradicate δB from the pulsation equations since δB and $\delta B'$ always appear in the specific combination which allows the cancellation to take place.

$$\begin{aligned}\delta B' &= \frac{B_o'\delta B}{B_o} + 8\pi G A_o B_o \Phi_o r \delta J + [8\pi G B_o \Phi_o' r]\,\delta\Phi' \\ &+\delta\Phi\left[8\pi G g r A_o B_o J_o - 8\pi G\mu^2 r A_o B_o \Phi_o\right] + \delta p\,[8\pi G r A_o B_o] \\ &+\delta A\left[\frac{B_o}{r} + 8\pi G B_o p_o r + 8\pi G g B_o J_o \Phi_o r - 4\pi G\mu^2 B_o {\Phi_o}^2 r\right] \end{aligned} \quad (35)$$

There is no analogous initial value equation for δJ; in practice one would need to use the equation of state.

With these relations for the auxiliary functions one can then do a series of recursive substitions into the pulsation equations, which subsequently become extremely lengthy. In view of this it is convenient to define the pulsation equations as

$$a_1\ddot{\delta\Phi} + a_2\delta\Phi'' + a_3\delta\Phi' + a_4\delta\Phi + a_5\xi' + a_6\xi = 0 \quad (36)$$

$$b_1\ddot{\xi} + b_2\xi'' + b_3\xi' + b_4\xi + b_5\delta\Phi' + b_6\delta\Phi = 0 \quad (37)$$

The coefficients are then

$$a_1 = \frac{1}{B_o} \quad (38)$$

$$a_2 = -\frac{1}{A_o} \quad (39)$$

$$a_3 = \frac{{A_o}'}{2{A_o}^2} - \frac{{B_o}'}{2A_oB_o} - \frac{2}{A_o r} \quad (40)$$

$$\begin{aligned} a_4 &= \mu^2 - 16\pi G g r J_o \Phi_o' + 16\pi G\mu^2 r \Phi_o \Phi_o' \\ &-4\pi G {\Phi_o'}^2 + 4\pi G\frac{{\Phi_o'}^2}{A_o} - 32\pi^2 G^2 g r^2 J_o \Phi_o \Phi'^2 \\ &+16\pi^2 G^2\mu^2 r^2 {\Phi_o}^2 {\Phi_o'}^2 - 16\pi^2 r^2 p_o {\Phi_o'}^2 + 16\pi^2 G^2 r^2 \Gamma_1 p_o {\Phi_o'}^2 \\ &+\frac{2\pi G r {A_o}' {\Phi_o'}^2}{{A_o}^2} - \frac{2\pi G r {B_o}' {\Phi_o'}^2}{A_o B_o} \end{aligned} \quad (41)$$

$$a_5 = 4\pi G r \Phi_o' (\Gamma_1 p_o - p_o - \rho_o) \quad (42)$$

$$\begin{aligned} a_6 &= 8\pi G g r A_o J_o p_o - 8\pi G\mu^2 r A_o \Phi_o p_o + 8\pi G g r A_o J_o \rho_o \\ &-8\pi G\mu^2 r A_o \Phi_o \rho_o - 4\pi G p_o \Phi_o' 4\pi G A_o p_o \Phi_o' + \\ &8\pi G\Gamma_1 p_o \Phi_o' + 32\pi^2 G^2 g r^2 A_o J_o \Phi_o p_o \Phi_o' - 16\pi^2 G^2\mu^2 r^2 A_o {\Phi_o}^2 p_o \Phi_o' \\ &+32\pi^2 G^2 r^2 A_o {p_o}^2 \Phi_o' - 16\pi^2 G^2 r^2 A_o \Gamma_1 {p_o}^2 \Phi_o' - 4\pi G\rho_o \Phi_o' + 4\pi G A_o \rho_o \Phi_o' \end{aligned}$$

$$+32\pi^2G^2gr^2A_oJ_o\Phi_o\rho_o\Phi_o{}' - 16\pi^2G^2\mu^2r^2A_o\Phi_o{}^2\rho_o\Phi_o{}' +$$
$$32\pi^2G^2r^2A_op_o\rho_o\Phi_o{}' - 16\pi^2G^2r^2A_o\Gamma_1p_o\rho_o\Phi_o{}' - 4\pi Grp_o\frac{A_o{}'\Phi_o{}'}{A_o}$$
$$+2\pi Gr\Gamma_1p_o\frac{A_o{}'\Phi_o{}'}{A_o} - 4\pi Gr\rho_o\frac{A_o{}'\Phi_o{}'}{A_o} - 4\pi Gr\Phi_o{}'\rho_o{}' \tag{43}$$

$$b_1 = \frac{A_o}{B_o}(p_o+\rho_o) \tag{44}$$

$$b_2 = -\Gamma_1p_o \tag{45}$$

$$b_3 = -\frac{2\Gamma_1p_o}{r} - \frac{\Gamma_1p_oA_o{}'}{2A_o} - \frac{p_oB_o{}'}{2B_o} - \frac{\Gamma_1p_oB_o{}'}{2B_o}$$
$$\frac{\rho_oB_o{}'}{2B_o} - p_o\Gamma_1' - p_o{}' - \Gamma_1p_o{}' \tag{46}$$

$$b_4 = \frac{2\Gamma_1p_o}{r^2} - 4\pi GA_o{}^2p_o{}^2 - 4\pi GA_o\Gamma_1p_o{}^2$$
$$-32\pi^2G^2gr^2A_o{}^2J_o\Phi_op_o{}^2 + 16\pi^2G^2\mu^2r^2A_o{}^2\Phi_o{}^2p_o{}^2 - 32\pi^2G^2r^2A_o{}^2p_o{}^3$$
$$+16\pi^2G^2r^2A_o{}^2\Gamma_1p_o{}^3 - 8\pi GA_o{}^2p_o\rho_o - 4\pi GA_o\Gamma_1p_o\rho_o$$
$$-64\pi^2G^2gr^2A_o{}^2J_o\Phi_op_o\rho_o + 32\pi^2G^2\mu^2r^2A_o{}^2\Phi_o{}^2p_o\rho_o$$
$$-64\pi^2G^2r^2A_o{}^2p_o{}^2\rho_o + 32\pi^2r^2A_o{}^2\Gamma_1p_o{}^2\rho_o$$
$$-4\pi GA_o{}^2\rho_o{}^2 - 32\pi^2G^2gr^2A_o{}^2J_o\Phi_o\rho_o{}^2 + 32\pi^2G^2\mu^2r^2A_o{}^2\Phi_o{}^2\rho_o{}^2$$
$$-32\pi^2G^2r^2A_o{}^2p_o\rho_o{}^2 + 16\pi^2G^2r^2A_o{}^2\Gamma_1p_o\rho_o{}^2$$
$$+2\pi Gr\Gamma_1p_o{}^2A_o{}' + 2\pi Gr\Gamma_1p_o\rho_oA_o{}' + \frac{\Gamma_1p_oA_o{}'^2}{2A_o{}^2} - \frac{p_oB_o{}'}{B_or}$$
$$-\frac{\Gamma_1p_oB_o{}'}{B_or} + \frac{2\pi GrA_op_o{}^2B_o{}'}{B_o} + \frac{2\pi GrA_o\Gamma_1p_o{}^2B_o{}'}{B_o}$$
$$-\frac{\rho_oB_o{}'}{B_or} + 4\pi GrA_op_o\rho_o\frac{B_o{}'}{B_o} + 2\pi GrA_o\Gamma_1p_o\rho_o\frac{B_o{}'}{B_o}$$
$$+2\pi GrA_o\rho_o{}^2\frac{B_o{}'}{B_o} - \frac{p_oA_o{}'B_o{}'}{4A_oB_o} - \frac{\Gamma_1p_oA_o{}'B_o{}'}{4A_oB_o}$$
$$-\frac{\rho_oA_o{}'B_o{}'}{4A_oB_o} - \frac{p_oB_o{}'^2}{4B_o{}^2} - \frac{\rho_oB_o{}'^2}{4B_o{}^2}$$
$$-\frac{2p_o\Gamma_1{}'}{r} + 4\pi GrA_op_o{}^2\Gamma_1{}' + 4\pi GrA_op_o\rho_o\Gamma_1{}'$$
$$-\frac{p_oA_o{}'\Gamma_1{}'}{2A_o} - \frac{2\Gamma_1p_o{}'}{r} - 4\pi GrA_op_o\rho_o{}'$$
$$+8\pi GrA_o\Gamma_1p_op_o{}' - 4\pi GrA_o\rho_op_o{}' + 4\pi GrA_o\Gamma_1\rho_op_o{}'$$
$$-\frac{\Gamma_1A_o{}'p_o{}'}{2A_o} - \frac{B_o{}'p_o{}'}{B_o} + 4\pi GrA_o\Gamma_1p_o\rho'$$
$$-\frac{B_o{}'\rho_o{}'}{2B_o} - \frac{\Gamma_1p_oA_o{}''}{2A_o} - p_o{}'' \tag{47}$$

$$b_5 = 4\pi G r \Phi_o' (p_o + \rho_o - \Gamma_1 p_o) \tag{48}$$

$$\begin{aligned} b_6 = {} & 4\pi G g r A_o J_o p_o + 4\pi G g r A_o \Gamma_1 J_o p_o - 4\pi G \mu^2 r A_o \Phi_o p_o \\ & -4\pi G \mu^2 r A_o \Gamma_1 \Phi_o p_o + 4\pi G g r A_o J_o \rho_o - 4\pi G \mu^2 r A_o \Phi_o \rho_o \\ & + g J_o' + 4\pi G A_o p_o \Phi_o' + 4\pi G \Gamma_1 p_o \Phi_o' \\ & + 32\pi^2 G g r^2 A_o J_o \Phi_o p_o \Phi_o' - 16\pi^2 G^2 \mu^2 r^2 A_o p_o {\Phi_o}^2 \Phi_o' \\ & + 32\pi^2 G^2 r^2 {A_o}^2 {p_o}^2 \Phi_o' - 16\pi^2 G^2 r^2 A_o \Gamma_1 {p_o}^2 \Phi_o' + 4\pi G A_o \rho_o \Phi_o' \\ & + 32\pi^2 G^2 g r^2 A_o J_o \Phi_o \rho_o \Phi_o' - 16\pi^2 G^2 \mu^2 r^2 A_o {\Phi_o}^2 \rho_o \Phi_o' \\ & + 32\pi^2 G^2 r^2 A_o p_o \rho_o \Phi_o' - 16\pi^2 G^2 r^2 A_o \Gamma_1 p_o \rho_o \Phi_o' - \frac{2\pi G r \Gamma_1 p_o A_o' \Phi_o'}{A_o} \\ & - \frac{2\pi G r p_o B_o' \Phi_o'}{B_o} - \frac{2\pi G r \rho_o B_o' \Phi_o'}{B_o} - 4\pi G r p_o \Gamma_1' \Phi_o' - \\ & 4\pi G r \Gamma_1 \Phi_o' p_o' \end{aligned} \tag{49}$$

These can be 'reduced' to an even greater extent by repeated application of the time independent field equations, but this is not necessary since any practical usage of these equations must depend on a numerical treatment, and in this case there would be no need to express the derivatives of the time dependent quantities in terms of the time dependent quantities themselves.

The pulsation equations are a pair of coupled linear second order partial differential equations which describe the motions of the fluid and scalar pertrubations. They are parametrized by a complicated set of coefficient functions (a_i, b_i) which depend on the static configurational functions in a non-trivial way. This makes an analysis of the properties of the scalar and fluid perturbations very difficult since such complicated equations of motion are, obviously, hard to solve. Also, since the static configurations are labelled by the triple (g, μ, ρ_c) one has twelve coefficients for each triple, and one would like to see how the properties of the pulsation equations change as one changes (g, μ, ρ_c), it would seem to be a quite hopeless task to make a general study of the system.

Again, the motivation for this work is in finding out which configurations are stable, the nature and bearing on stability of any scalar radiation emitted, and how this picture changes as one varies the parameters of the static configurations. The equations as they stand would seem to shed little light upon this, luckily an exhaustive analysis of the pulsation equations is not required. Earlier on it was

found that the most important parameter for the static case seemed to be the scalar mass, μ, it does not take too much intuition to see that this should be for the case of radial pulsations also. That this is indeed the case will become clear in the §2.3. Firstly, the more general properties which the pulsation equations may have or may not have should be discussed.

If one assumes a harmonic time dependence for the pulsation equations and then separating variables in the usual manner, the pulsation equations become an eigenvalue problem. To progress further one would need to know the number, distribution, nature and, eventually, the values of these eigenvalues. The 'nicest' property that such a system of equations may have for the answering of such questions is that of self-adjointness. If the system has this property then one knows immediately that the eigenvalues are real, discrete and form an infinite denumerable set(as well as other things). Knowing this information makes their subsequent calculation a whole lot easier, for example, one may then use a variational technique to estimate them. From there one may calculate the eigenfunctions and proceed to analyse the dynamics of the system in terms of a complete set of normal modes. Self-adjointness of the equations also guarantees completeness of the eigenfunctions, and so the problem becomes essentially solved once this process has been completed. This happens in the case of ordinary fluid neutron stars and is detailed in the next section.

So, one may ask: are the pulsation equations for the fluid-scalar perturbations self-adjoint? Without doing any hard work one may conclude immediately that they are almost certainly not, for one excellent physical reason: the system can radiate scalar particles. That the system can radiate must of course depend on the values of the defining parameters, and so far one has no explicit knowledge of this dependence; all the same, if the scalar coupling is strong enough and the scalar mass is light enough there must be some radiation.

To study this radiation one could integrate the full equations of motion and in certain parameter regions this is almost certainly required, however, the interest here lies in studying configurations which are, initially at least, 'close-to' the static configurations of chapter one. To this end it would seem natural to regard the background configuration as static and then study the propagation of

scalar particles on this background, i.e. ignoring the backreaction problem for the moment.

The equation for the scalar perturbations in the static background is elliptic, non self-adjoint, and has to be studied over a non-compact domain [0, ∞). This makes it difficult to analyse, and again one doesn't know have any *a priori* information about the eigenvalues except the naive expectation that for any configurations remotely resembling neutron stars the eigenvalues should be discrete and form an infinite set, perhaps having small imaginary parts to account for the damping of the fluid oscillations.

If one wanted to find the response of the scalar field for some initial perturbation the best one could hope for is that some analogue of the normal Green function and normal mode expansions may be used, i.e. a quasi-normal mode expansion[4]. That is

$$\delta\Phi(t,r) = \int\int G(t\, r|t'\, r')Q(t'\, r')dt'dr' \tag{50}$$

where G is expressed as a sum over the quasi-normal modes of the system

$$G = \sum_n \frac{\Phi_n{}^*\Phi_n}{\lambda_n} \tag{51}$$

If successful, this method would enable one to find very accurately how much mass was being radiated by the star, as well as giving the precise scalar 'footprint' for the radiation. The method seems quite straightforward, get $\delta\Phi$ from (50), get G from (51), then get the eigenfunctions by numerical integration of the scalar equation once the quasi-normal modes are known. This apparent simplicity founders on the fact that the evaluation of the quasi-normal modes is very difficult indeed. There are special methods for finding the quasi-normal modes of black holes[4] but these are not applicable for neutron star-scalar field systems. Instead, direct numerical integration is required, and lots of it, even for a single configuration never mind a representative sample of parameter space. So although this procedure seems possible in principle it appears to be prohibitive in practice.

Supposing one managed to do it, what would one find? Well, if the modes were lightly damped then mass loss could be significant whereas if the modes

were highly damped then little mass could be radiated away. Considering the backreaction problem to be 'quasi-static' one might then assume that the configuration would move to a less massive configuration on a curve of constant scalar coupling in the mass/coupling/density diagram. Since one would expect higher central density configurations to be less stable than the lower ones this reasoning leads one to expect that, similar to the ordinary case, the stable configurations lie to the left of the maximum mass ridge. This conclusion is borne out by the simpler methods detailed in the next section, where the stability criterion are given more fully.

2.2 Stability

When there is no scalar field present there is only one pulsation equation. By making the following manipulations, and assuming a harmonic time dependence of the form $\xi(t,r) = \xi(r)e^{i\omega t}$, the pulsation equation can be written in the manifestly self-adjoint form

$$(P\xi')' + Q\xi + \omega^2 W\xi = 0 \tag{52}$$

Where, in the notation of the previous section

$$P = e^{\int \frac{b_3}{b_2}} \tag{53}$$

$$Q = \frac{b_4}{b_2} P \tag{54}$$

$$W = \frac{b_1}{b_2} P \tag{55}$$

and g, Φ_o and J_o have been set equal to zero in the b-coefficients.

From the theory of Sturm-Liouville systems it follows that such a system has an infinite series of discrete real eigenvalues, and the eigenfunctions of the system ξ_n are orthonormal over [0,R) with respect to the weight function W.

It is this important property that gives one an elegant and practical way of determining whether or not a given configuration, $\mathcal{C}$ is unstable.

It can be shown that the eigenvalues of the system satisfy the following relationship[8]

$$\omega_n{}^2 = \frac{\int_0^R \left(P\xi_n{}^2 - Q\xi_n{}^2\right) dr}{\int_0^R W\xi_n{}^2 dr} \tag{56}$$

Of course, one does not know the eigenfunctions ξ_n, but an estimate of the eigenvalue can be obtained by replacing the unknown ξ_n by a suitable trial eigenfunction. By 'suitable', meaning one which satisfies the relevant boundary conditions. These boundary conditions are that the Lagrangian perturbation of the pressure vanishes at the star surface and the the fluid displacement is zero at the star centre

$$\nabla p \rightarrow 0 \; as \; r \rightarrow R \tag{57}$$

$$\xi = 0 \; at \; r = 0 \tag{58}$$

A consequence of this is that the n^{th} eigenfunction has (n–1) nodes in the interval [0,R).

The evaluation of such an integral will always overestimate the value of the eigenvalue but it is this property which gives the stability criterion that is required, that is, a given configuration is unstable if for any suitable trial eigenfunction the right hand side of equation (56) becomes zero or negative.

Furthermore, if the fundamental mode of the star is stable, all other radial modes will be stable also, and correspondingly if any of the radial modes are unstable, then the fundamental mode will have the fastest growing instability.

For Newtonian stars several other results may be established, the importance of these being that while derived from the Newtonian theory, some tend to be general results applicable even in the case of General relativity. For example, a homogeneous star will be stable or unstable depending on whether the adiabatic index, Γ_1 is greater than or less than $\frac{4}{3}$. The general result for Newtonian stars corresponding to this, is that stars are stable or unstable depending on whether the pressure-averaged adiabatic index, $\overline{\Gamma}_1$ is greater than or less than $\frac{4}{3}$. General relativity modifies this result further, for instance for weak general relativistic effects one has stability if

$$\overline{\Gamma}_1 - \frac{4}{3} > c\frac{GM}{R} \tag{59}$$

where c is some number of order one. General relativity tends to make stellar configurations more unstable.

Further results enable one to study stability by looking at the plots of mass against central density(though mass against radius can also be used). Stable

configurations on the mass/density plot are found between critical points and have positive gradient. The critical points show where there is a changeover from stable to unstable and vice versa.

Another approach to the stability of neutron stars which has been used in recent years is that of catastrophe theory[7]. This method is completely general as opposed to the merely linear and extremely tedious analysis presented previously; it also tends to make the study rather easy. In this approach one studies how a 'potential function' varies as a 'control parameter' is altered. The graph of this is known as the 'bifurcation' diagram. When there is only a small number of control parameters it is found that the qualitative nature of the bifurcation diagram must be one of a small number of generic types; these are known as catastrophes.

For the case of neutron star stability, the potential function is the mass of the configuration while the control parameter may be taken to be the fermion number. Consider the mass–density curves for white dwarfs and neutron stars given in figure 2.1 and the corresponding bifurcation diagram, figure 2.2. The branches AB and CD are known to be stable corresponding to white dwarfs and neutron stars repectively. Notice how the changeover from stability to instability is shown as a cusp in the bifurcation diagram.

This analysis is more general than the usual linear perturbation treatment and is very simple. The simplicity of this case is due to the fact that neutron stars are only one parameter systems, the only catastrophe for which is the simple fold. Multiple parameter systems are much harder to analyse in this fashion. A classification theorem, Whitney's theorem, exists for two parameter systems, which allows, for example, a catastrophe theory analysis of boson stars to be done [6]. It has not been possible to perform an analogous study of boson-fermion star stability because there is no generalization of Whitney's theorem which applies to this case which has more than two integrals of motion.

Despite seeming more complicated than that of ordinary neutron stars, it is still possible to use these methods for the case of neutron star–scalar field configurations since this is still a one parameter system. If one considers the mass/density plots for constant coupling one sees similar behaviour to that of figures 2.1, 2.2. An immediate consequence of this is that when there is no scalar

radiation the stable neutron star–scalar field configurations lie to the left of the maximum mass ridge on the scalar coupling, central density plane.

2.3 Relaxation time of Scalar Waves

As stated previously, the general case of resolving the Einstein Klein-Gordon equations in which the star pulsates radially sending scalar radiation off to infinity, is extremely complicated, requiring the full intensive apparatus of numerical General Relativity. It is possible though to gain significant insight into this problem by much simpler considerations.

By making an approximate calculation of how the scalar waves tend to damp the radial pulsations it is possible to see how the coupled stability-radiation problem separates into different classes of behaviour depending upon the value of the scalar particle mass as well as providing another useful bound on the scalar coupling. For a certain region of scalar mass the treatment of the stability problem is similar to that of the pure neutron star case, though the equations are lengthier; in other regions one is required to construct the scalar propagator in the curved background and find the quasi-normal modes of the system, finally, only in a region so far unconsidered will the full numerical treatment of general relativity be required.

In this section the treatment is analogous to that given by Chiu and Morganstern[5] for the case of a zero mass Jordan–Brans–Dicke scalar particle.

One starts by considering the equations of energy conservation for the system

$$T^{\mu\nu}{}_{;\nu} = 0 \tag{60}$$

Making the substitutions of (15)—(20) , allows one to decompose the energy momentum tensor into the separate contributions from the different components of the system

$$T^{\mu\nu} = T_{star}{}^{\mu\nu} + T_{scalar}{}^{\mu\nu} + T_{grav}{}^{\mu\nu} \tag{61}$$

The first term contains the static, time independent quantities corresponding to a static configuration of chapter one. The second contains the scalar perturbations which give rise to scalar radiation, and the third contains the perturbations of the metric tensor. These do not give rise to gravitational radiation since this is not possible from purely radial motions of the star.

The covariant conservation equation (60), is not in the most suitable form required since it is not possible to use certain theorems of calculus which only hold for ordinary partial derivatives. To this end it is necessary to use instead of the energy momentum tensor, the Landau-Lifshitz pseudotensor denoted $\tau^{\mu\nu}$. The point of using this object is that instead of (60) holding one has

$$\tau^{\mu\nu}{}_{,\nu} = 0 \tag{62}$$

where the comma now denotes the partial, rather than covariant derivative.

The pseudotensor splits up in a similar fashion to the energy momentum tensor; now one can do several useful manipulations.

Ignoring the gravitational perturbations one has

$$-\tau_{star}{}^{\mu\nu}{}_{,\nu} = \tau_{scalar}{}^{\mu\nu}{}_{,\nu} \tag{63}$$

Taking $\mu = 0$, splitting $\nu = (0, a)$ where a =1,2,3 and integrating gives

$$-\int \left(\tau_{star}{}^{00}{}_{,0} + \tau_{star}{}^{0a}{}_{,a}\right) dV = \int \left(\tau_{scalar}{}^{00}{}_{,0} + \tau_{scalar}{}^{0a}{}_{,a}\right) dV \tag{64}$$

By Gauss's divergence Theorem

$$-\int \tau_{star}{}^{0a}{}_{,a} dV = -\int \tau_{star}{}^{0a} n_a dS \tag{65}$$

holds, and this vanishes for large spatial distances. Also the first term on the right hand side of(64)ill average to zero over a complete cycle, so that one is left with

$$-\int \tau_{star}{}^{00}{}_{,0} dV = \int \tau_{scalar}{}^{0a} n_a dS \tag{66}$$

again using Gauss's theorem.

This equation simply states that the energy loss of the is due to the flux of scalar radiation escaping to infinity.

Furthermore

$$-\frac{\partial}{\partial x^0}\int \tau_{star}{}^{00} dV = \int \tau_{scalar}{}^{0a} n_a dS \tag{67}$$

$$\frac{d\epsilon}{dt} = \lim_{R\to\infty} \int \tau_{scalar}{}^{0a} n_a dS \tag{68}$$

$$\frac{d\epsilon}{dt} = \lim_{R\to\infty} 4\pi R^2 \tau_{scalar}{}^{or} \tag{69}$$

Since the right hand side is approximately $4\pi R^2 \delta\dot{\Phi}\delta\Phi'$ this gives the energy loss rate of the star as

$$\frac{d\epsilon}{dt} \simeq 4\pi R^2 \delta\dot{\Phi}\delta\Phi' \tag{70}$$

evaluated in the limit of infinite radius.

To proceed further one needs to find the far field waveform of the scalar field. The Klein-Gordon equation is

$$\frac{\delta\ddot{\Phi}}{B_o} - \frac{\delta\Phi''}{A_o} + \delta\Phi'\left[\frac{A_o'}{2A_o^2} - \frac{B_o'}{2A_oB_o} - \frac{2}{A_or}\right] + \mu^2\delta\Phi \;=\; Q \tag{71}$$

Here the source term is now $-(a_5\xi' + a_6\xi)$. At large radial distance $A_o, B_o \to 1$ and $A_o', B_o' \to 0^-$. Putting $\delta\Phi(t,r) = \sigma(r)e^{i\omega t}$ gives the simplified equation

$$\sigma'' + \frac{2}{r}\sigma' + (\omega^2 - \mu^2)\sigma = Q \tag{72}$$

An approximate solution to this is

$$\delta\Phi(t,r) = \left[\int Qr^2dr\right]\frac{\sin(kr - \omega t)}{r} \tag{73}$$

This consists of damped, outgoing wave multiplied by the 'strength of the source' (in square brackets).

The condition that one actually has wave propagation is that $k^2 > 0$, where $k^2 = \omega^2 - \mu^2$. This puts a very strong constraint on which class of configurations can actually radiate. For example, most oscillation frequencies of neutron stars will be of the order of a millisecond and it seems likely that the oscillation frequencies of the neutron star–scalar field configuration must remain within no more than a few orders of magnitude of this. This is not unreasonable.

This implies that unless the boson mass, μ is less than, or approximately equal to 10^{-11}eV there can be no emission of scalar radiation. Without the emission of scalar radiation the pulsation operator will revert to being self-adjoint and so the treatment of stability can proceed in a qualitatively similar manner to that of normal neutron stars. This is exactly the information that is required to facilitate the decoupling of the various theoretical aspects of this problem.

Substituting the large radius solution for $\delta\Phi$ into the energy loss equation one obtains

$$\left\langle\frac{d\epsilon}{dt}\right\rangle_{ave} = -\frac{1}{2}\left[\int Qr^2dr\right]^2\omega k \tag{74}$$

The average energy of each oscillation is

$$\langle \epsilon \rangle_{ave} = \frac{1}{2} \int \rho \left\langle v^2 \right\rangle_{ave} dV = \pi\omega \int_0^R \rho \xi^2 r^2 dr \tag{75}$$

Combining these gives $< \epsilon >_{ave} \simeq e^{-\frac{t}{\tau_R}}$. Where τ_R, the relaxation time is defined as

$$\tau_R = \frac{2\pi\omega}{k} \frac{\int_0^R \rho \xi^2 r^2 dr}{\left(\int_0^R Q r^2 dr\right)^2} \tag{76}$$

A rough estimate of this quantity may be obtained by assuming the following

$$Q \simeq 8\pi G g r A_o J_o \rho_o \tag{77}$$

and $A_o \simeq 1$, $J_o \simeq \frac{\rho_o}{m}$. Taking $\xi \simeq r^\alpha$ gives for the relaxation time

$$\tau_R = \left(\frac{\omega}{k}\right) \frac{(\alpha+4)^2}{(2\alpha+3)} \frac{1}{32\pi} \frac{m^2}{g^2 {\rho_o}^3 R^5} \tag{78}$$

After substituting reasonable neutron star values this gives

$$\tau_R = 2.5\ 10^{-41} \frac{\omega}{k} \frac{1}{g^2} \tag{79}$$

An immediate consequence of this result is that any observation of a pulsating neutron star would put severe constraints on the coupling of the scalar field, thus providing a dynamical bound that provides a link with the bounds that were derived from static quantities in chapter one.

2.4 Discussion

As well as providing a strong bound on the scalar coupling, should ever a neutron star be seen to pulsate, the relaxation time calculation provides the information that the stability/radiation problem for neutron stars with massive scalar fields breaks down into three types of behaviour depending on the value of the scalar boson mass, μ, based on the not outrageous assumption that the pulsation frequncies for these combined scalar fluid systems must stay within an order of magnitude, or so, of their normal counterparts.

For $\mu \gtrsim 10^{-11}$eV no radiation can take place. In this region the treatment of stability is qualitatively similar to that for ordinary neutron stars. The stable configurations lie to the left of the maximum mass ridge in the g/ρ plane.

In the region $10^{-13}\text{eV} \lesssim \mu \lesssim 10^{-11}\text{eV}$ some scalar radiation is likely. If the mass loss is not too rapid one may do an accurate 'quasi-static' calculation by assuming the background metric to be static and then calculating the scalar propagator in this background. This is done by expressing the Green function as a mode sum over the quasi-normal modes of the system. The quasi-normal modes of the system have to be found by numerical integration of the pulsation equations. In this way the far field form of the scalar field may be evaluated accurately allowing an exact calculation of the energy loss of the system. The difficulty of calculating the quasi-normal modes of the system prohibits this more extended study.

For the extreme ultralight region the quasi-static approximation will probably break down and integration of the full time dependent Einstein–Klein-Gordon equations would be required. Again it should be emphasized that even finding static neutron star-like configurations in this region was extremely difficult.

Figure Captions

Figure 2.1: Star mass against density for Harrison, Wakano, Wheeler(HWW) equation of state. The branches AB and CD represent stable configurations corresponding to white dwarfs and neutron stars respectively.

Figure 2.2: Bifurcation diagram for HWW stellar configurations. Note the correspondence between the cusps and a change of stability.

Figure 2.3a: Mass contours against central density and coupling for boson mass 10^{-11}eV and Chandrasekhar equation of state. The dark line separates the stable and unstable configurations.

Figure 2.3b: Mass contours against central density and coupling for boson mass 10^{-11}eV and Bethe and Johnson equation of state. The dark line separates the stable and unstable configurations.

Figure 2.4a: Mass contours against central density and coupling for boson mass 10^{-5}eV and Chandrasekhar equation of state. The dark line separates the stable and unstable configurations.

Figure 2.4b: Mass contours against central density and coupling for boson mass 10^{-5}eV and Bethe and Johnson equation of state. The dark line separates the stable and unstable configurations.

References

1. S.Chandrasekhar, Ap.J 140 (1964) 417

2. P.Jetzer, 'Boson Stars' ZU-TH 25/91

3. M.Gleiser, Phys.Rev D38 (1988) 2376

4. E.Leaver, Phys.Rev D34 (1986) 384

5. R.E.Morganstern, H.Y.Chiu, Phys.Rev 157 (1967) 157

6. F.V.Kusmartsev, E.W.Mielke, F.E.Schunk, Phys.Rev D43 (1991) 3895

7. J.M.T.Thompson, 'Instabilities and Catastrophes in Science and Engineering' Wiley 1982

8. Hans Sagan, 'Boundary and Eigenvalue Problems in Mathematical Physics'

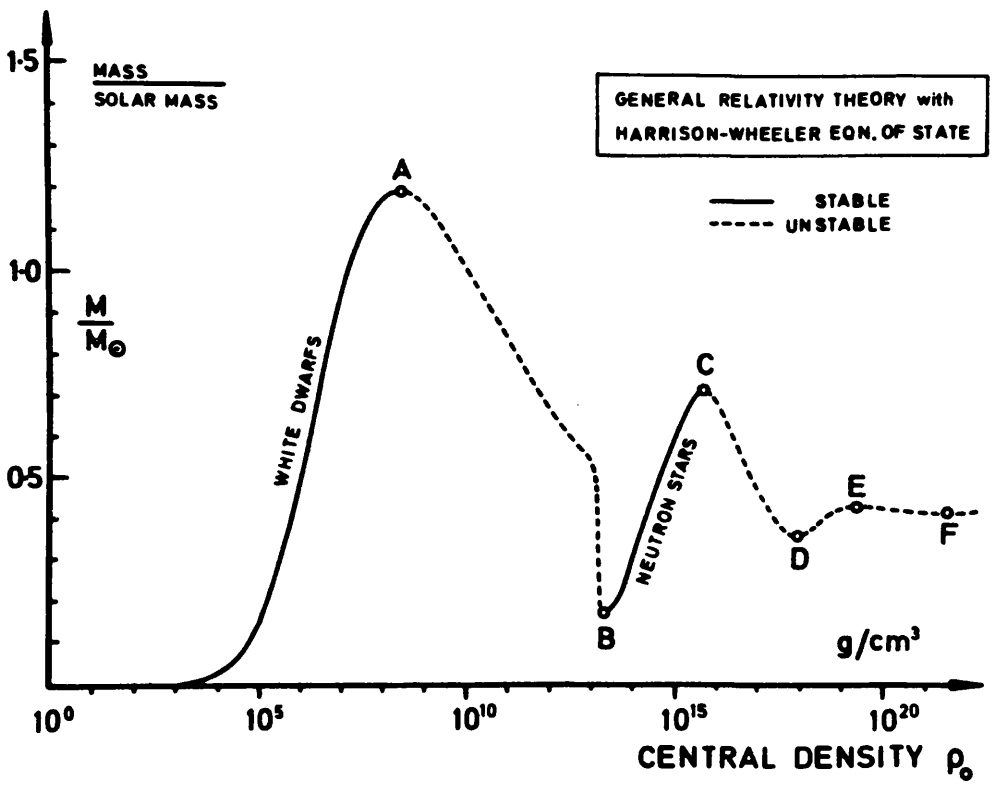
1·5
MASS
SOLAR MASS
GENERAL RELATIVITY THEORY with
HARRISON-WHEELER EQN. OF STATE
STABLE
UNSTABLE
1·0
M
M⊙
0·5
A
B
C
D
E
F
WHITE DWARFS
NEUTRON STARS
g/cm³
10⁰
10⁵
10¹⁰
10¹⁵
10²⁰
CENTRAL DENSITY ρ₀

Figure 2.1

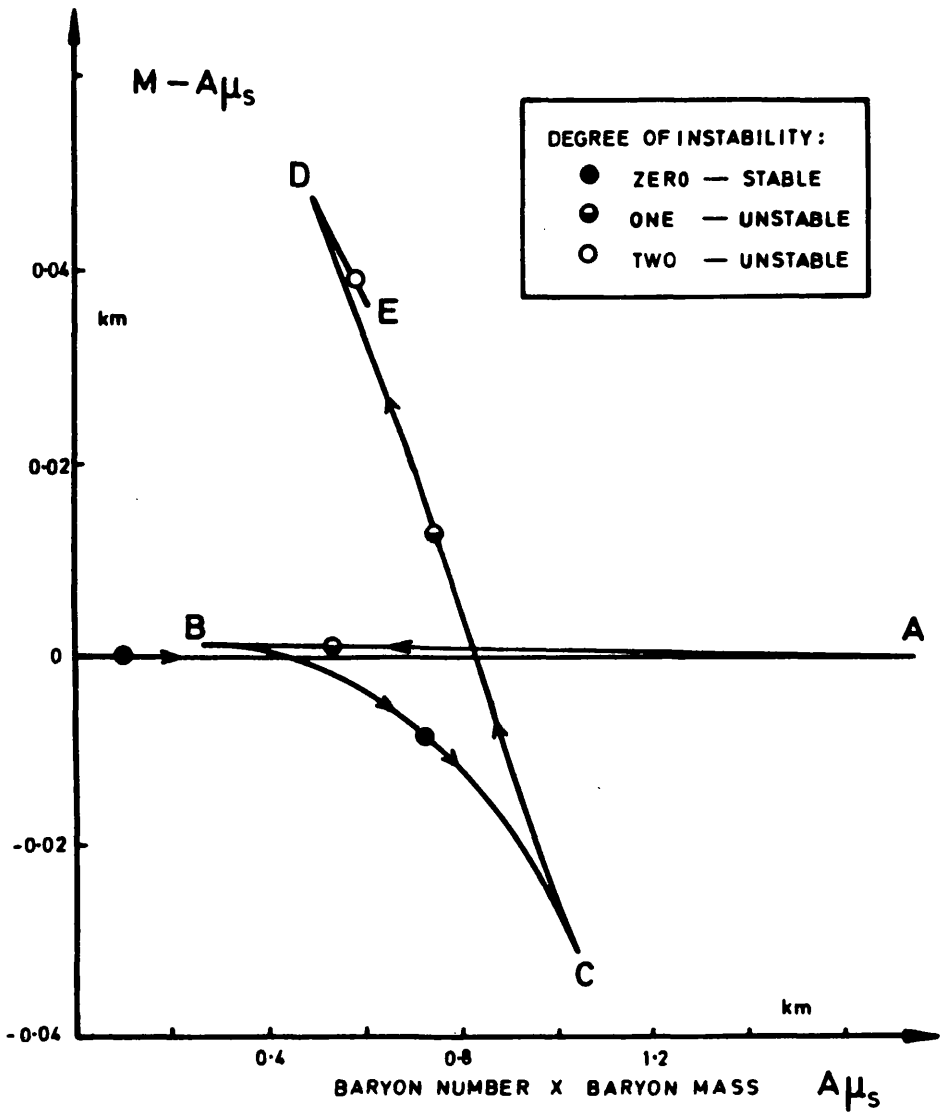
M − Aμs
DEGREE OF INSTABILITY:
ZERO — STABLE
ONE — UNSTABLE
TWO — UNSTABLE
D
E
B
A
C
0·04
km
0·02
0
-0·02
-0·04
km
0·4
0·8
1·2
BARYON NUMBER X BARYON MASS
Aμs

Figure 2.2

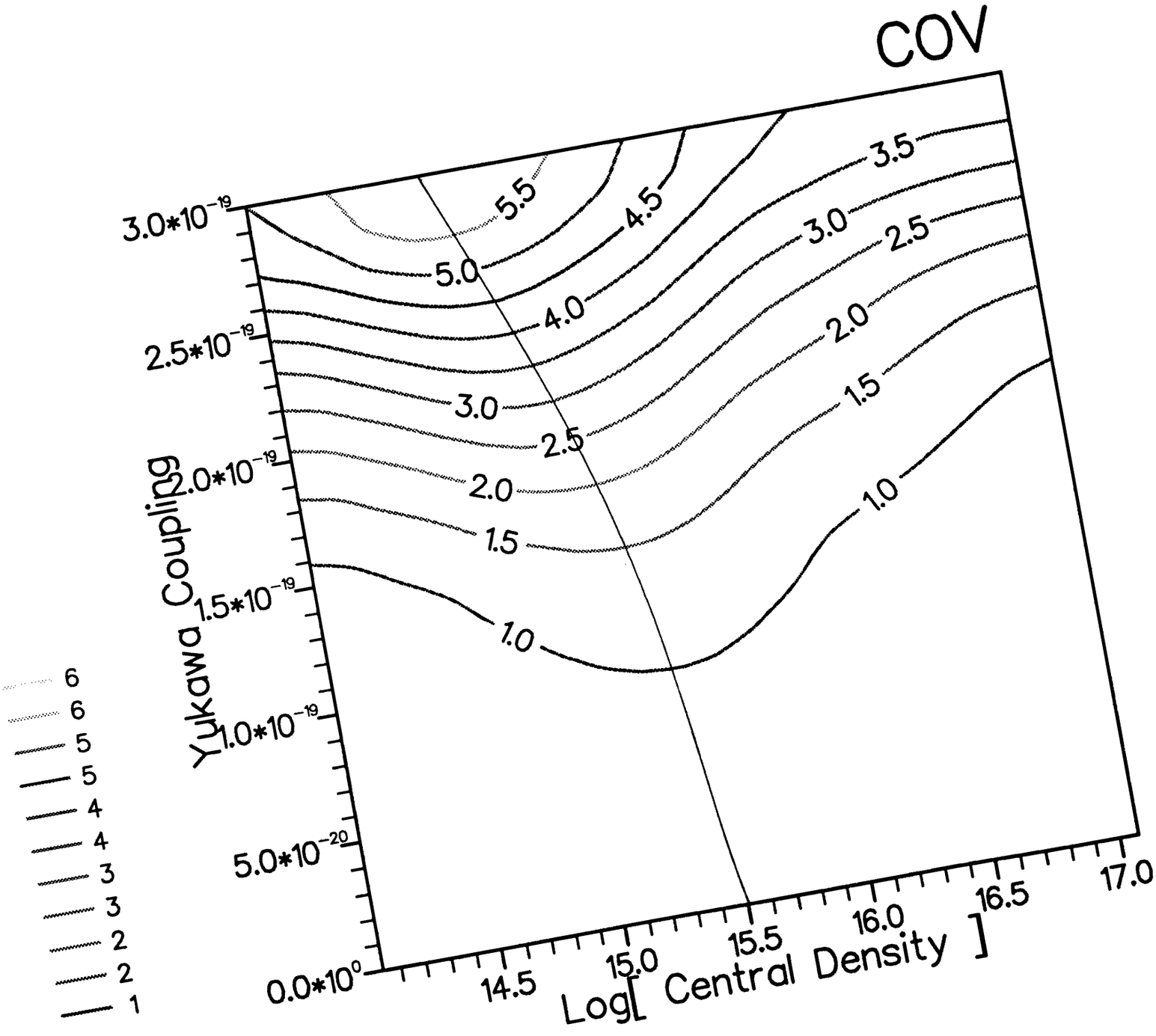
COV
Yukawa Coupling
3.0*10^-19
2.5*10^-19
2.0*10^-19
1.5*10^-19
1.0*10^-19
5.0*10^-20
0.0*10^0
14.5
15.0
15.5
16.0
16.5
17.0
Log[Central Density]
5.5
5.0
4.5
4.0
3.5
3.0
2.5
2.0
1.5
1.0
6
6
5
5
4
4
3
3
2
2
1

Figure 2.3

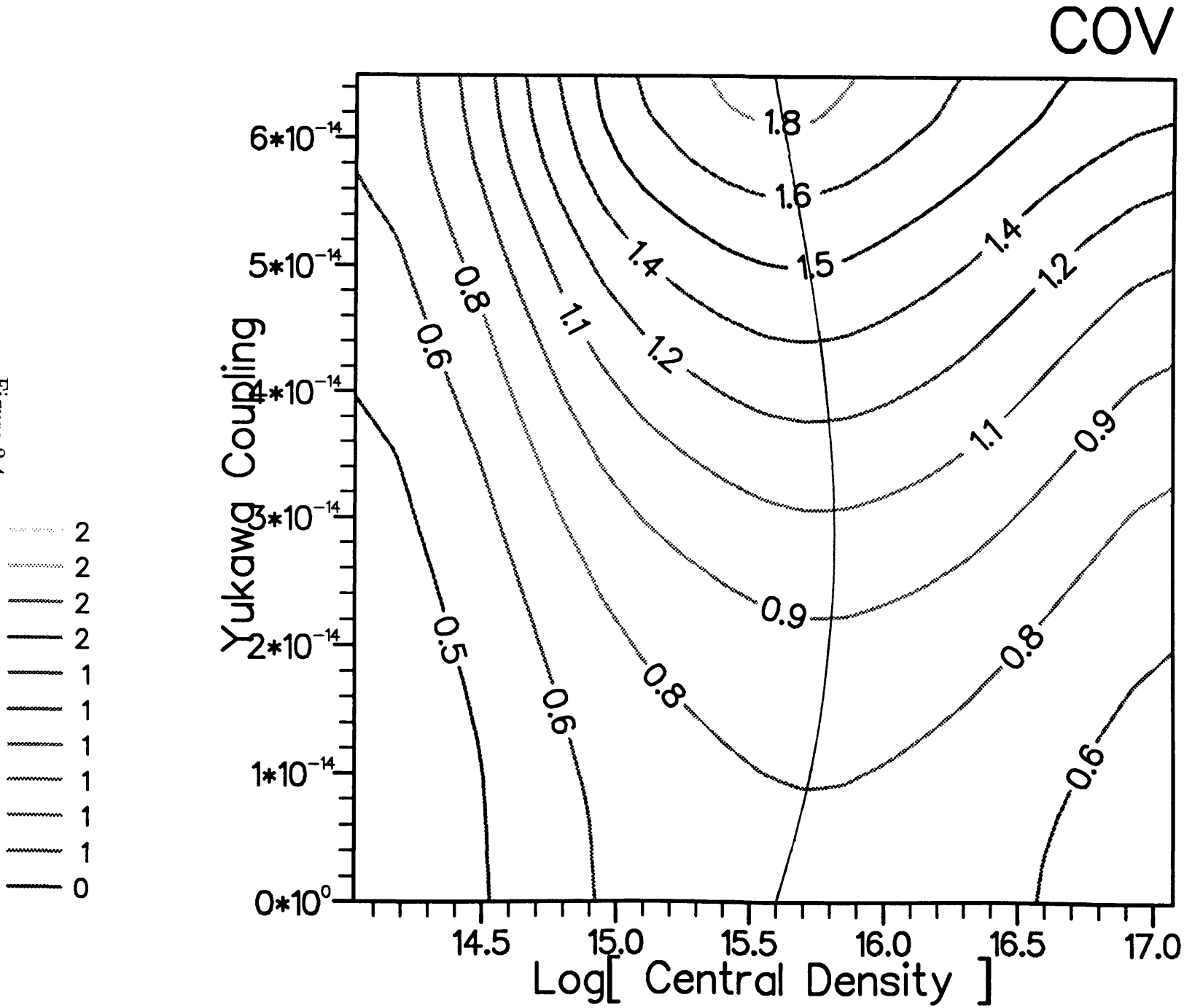
COV
Yukawa Coupling
6*10^-14
5*10^-14
4*10^-14
3*10^-14
2*10^-14
1*10^-14
0*10^0
14.5
15.0
15.5
16.0
16.5
17.0
Log[Central Density]
1.8
1.6
1.5
1.4
1.4
1.2
1.2
1.1
1.1
0.9
0.9
0.8
0.8
0.8
0.6
0.6
0.6
0.5
2
2
2
2
1
1
1
1
1
1
0

Figure 2.4

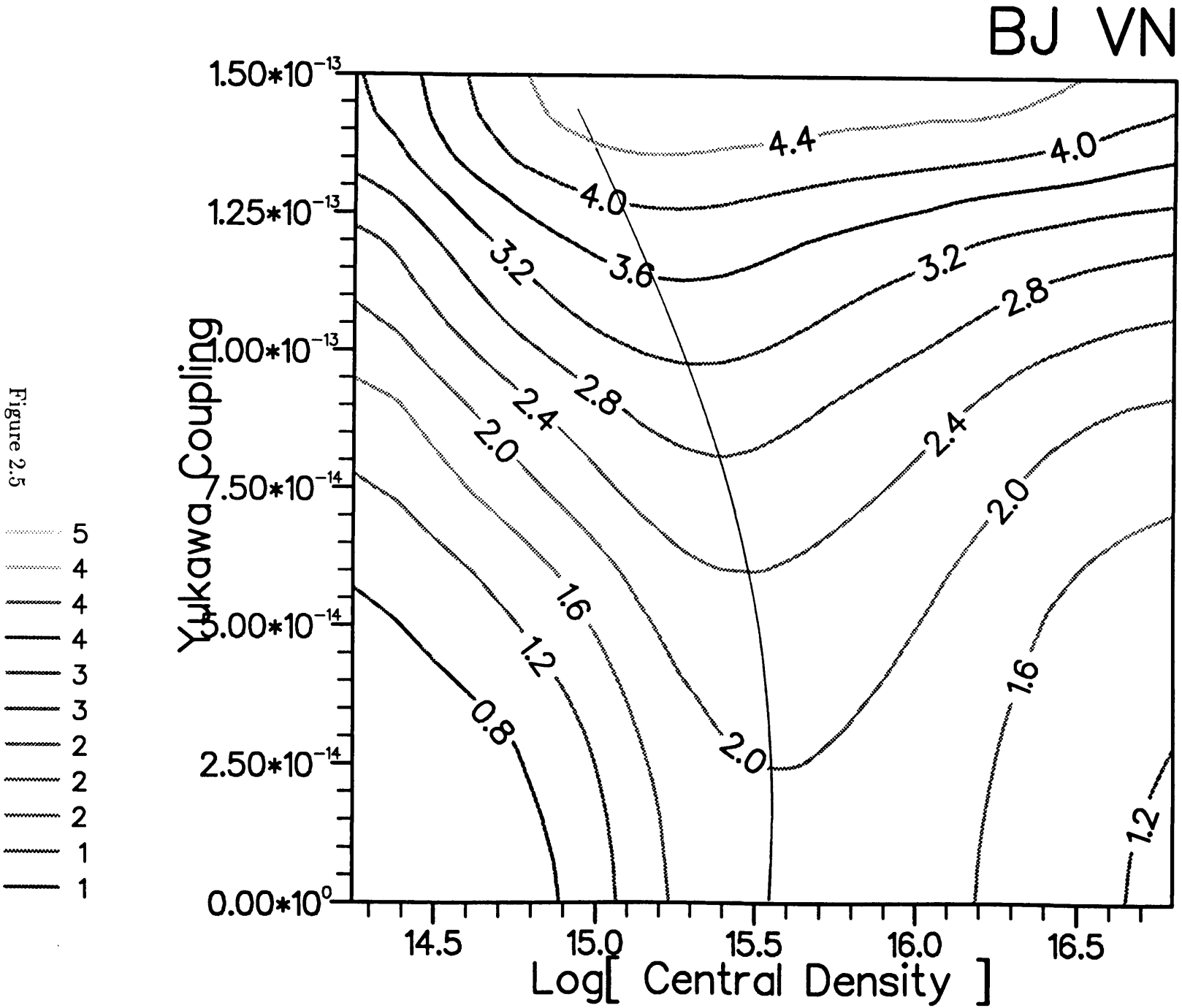
BJ VN
1.50*10^-13
1.25*10^-13
1.00*10^-13
7.50*10^-14
5.00*10^-14
2.50*10^-14
0.00*10^0
Yukawa Coupling
14.5
15.0
15.5
16.0
16.5
Log[Central Density]
4.4
4.0
4.0
3.6
3.2
3.2
2.8
2.8
2.4
2.4
2.0
2.0
2.0
1.6
1.6
1.2
1.2
0.8
5
4
4
4
3
3
2
2
2
1
1

Figure 2.5

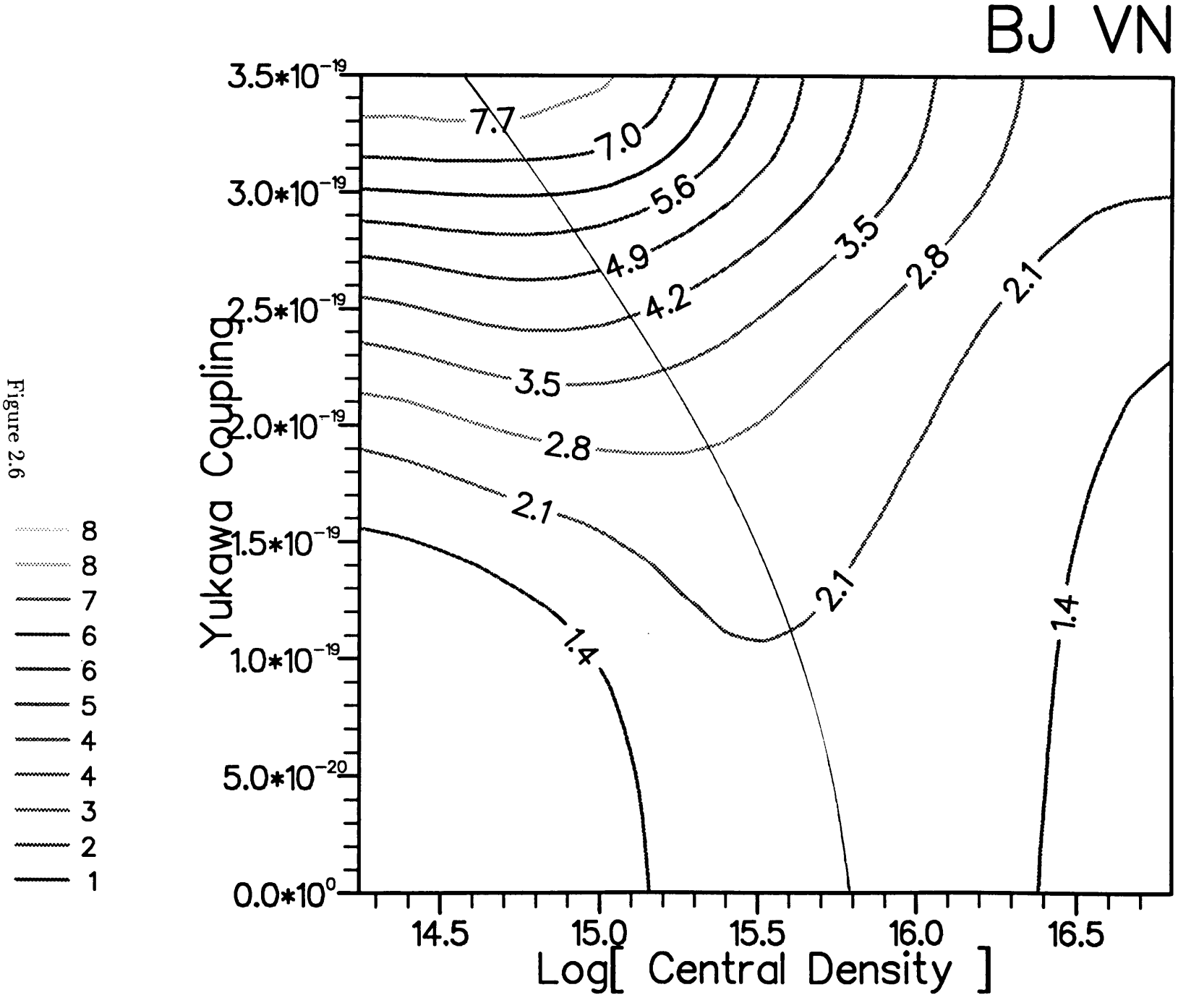
BJ VN
3.5*10^-19
3.0*10^-19
2.5*10^-19
2.0*10^-19
1.5*10^-19
1.0*10^-19
5.0*10^-20
0.0*10^0
Yukawa Coupling
7.7
7.0
5.6
4.9
4.2
3.5
2.8
2.1
1.4
14.5
15.0
15.5
16.0
16.5
Log[Central Density]
8
8
7
6
6
5
4
4
3
2
1

Figure 2.6

Chapter Three

Gravitational Collapse of Scalar Fields

In this chapter the gravitational collapse of a scalar field coupled to a pressureless dust is analysed and discussed, extending the considerations of earlier chapters, which centred on static and pulsating solutions of the Einstein–Klein-Gordon equations, to the more general, time-dependent case.

The treatment applied here is however, a very simple one, being the natural extension of the original model of Oppenheimer and Snyder[3] to include scalar fields. This is not to say that the inherent simplicity of the model precludes it being informative or interesting, after all, it is well known that the main qualitative predictions of the Oppenheimer–Snyder model are not significantly altered when more complex models are considered. It is in this spirit which this chapter is written; the object is to identify and study any major qualitative alterations to the Oppenheimer–Snyder model which could be caused by the presence of a scalar field, and to attempt to interpret these differences so that information about the scalar field parameters could be gathered by a hypothetical observer.

In the first two sections will be presented the derivation of the equations of motion and their solutions. The significance of these will then be discussed with respect to the possibilities of particle production, phase transitions and certain quantum mechanical phenomena.

Of particular interest to the study of collapse are the celebrated Hawking-Penrose theorems which predict the inevitability of singularity formation under most physically reasonable conditions. These conditions can in certain circumstances be violated by the presence of a scalar field and so there exists the possibility of singularity avoidance. Although this is *not* found to be the case, the solutions found do differ from the Oppenheimer-Snyder model, perhaps indicating that when treated 'properly' more exotic phenomena, i.e. quantum effects, phase transitions, could greatly alter the gravitational collapse process resulting in singularity avoiding 'bounce' behaviour.

In section §3.3 the problem of finding the spacetime exterior to the collapsing region is considered. This is of vital importance if one wishes to make a proper interpretation of the interior solutions, that is, describe what a distant observer would observe; this primarily involves predicting how the redshift of the collapsing object would behave. It is found that difficulties exist in carrying out this process. These difficulties are discussed and clarified.

3.1 Equations of Motion

In this derivation of the collapse equations the treatment of Weinberg[1] will be followed closely. The assumptions of the model are that the collapse is spherically symmetric, spatially homogeneous and isotropic; since it is the qualitative aspects of the situation which are of primary interest this should be perfectly adequate. The matter present in the model is a 'dust' having the equation of state p=0.

The coordinate system is

$$x^{\mu} = (\tau, r, \theta, \phi) \tag{1}$$

where it is to be understood that these coordinates are co-moving.

The metric is

$$\mathrm{ds}^2 = dt^2 - A(t,r)dr^2 - B(t,r)(d\theta^2 + \sin^2\theta d\phi^2) \tag{2}$$

This is the most general line element required for spherically symmetric, isotropic collapse.

The matter content of the model is described by the energy-momentum tensor, $T_{\mu\nu}$

$$\begin{aligned} T_{\mu\nu} &= T_{\mu\nu}{}^{dust} + T_{\mu\nu}{}^{scalar} + T_{\mu\nu}{}^{interaction} \\ &= \rho U_\mu U_\nu \\ &\quad +\partial_\mu\Phi\partial_\nu\Phi - \frac{1}{2}g_{\mu\nu}g^{\alpha\beta}\partial_\alpha\Phi\partial_\beta\Phi + \frac{1}{2}g_{\mu\nu}\mu^2\Phi^2 \\ &\quad -g_{\mu\nu}V(\Phi,\rho) \end{aligned} \tag{3}$$

where U is the 4-velocity of the dust, ρ is the energy density of the dust, Φ is the scalar field density, μ is the mass of the scalar boson, and $V(\Phi,\rho)$ is an unspecified potential representing the interaction between the scalar field and the dust.

Typical types of potential for a scalar field include a yukawa coupling to fermions, $g\Phi\overline{\Psi}\Psi$, or a self-coupling of the form $\lambda\Phi^4$. These are the common particle-physics type interactions present in quantum field theories. Throughout this paper the scalar field will be treated classically, but some of the possibilities of using a quantum description for the scalar field will be discussed. This potential can also be temperature dependent but this will not be considered here.

When one have a yukawa coupling present between the scalar particle and the fermionic 'dust' matter particles, one can approximate the $\overline{\Psi}\Psi$ term by the following

$$\begin{aligned} < \overline{\Psi}\Psi > &\simeq < \overline{\Psi}\gamma^0\Psi > \\ &= n_F \\ &\simeq \frac{\rho}{m} \end{aligned} \tag{4}$$

where g is the coupling constant and m is the mass of the dust particle.

The evolution of the system is determined by the coupled Einstein/Klein-Gordon equations

$$R_{\mu\nu} - \frac{1}{2}g_{\mu\nu}R = -8\pi G T_{\mu\nu} \tag{5}$$

$$\left(\Box + \mu^2\right)\Phi = \frac{\delta V}{\delta\Phi} \tag{6}$$

Explicitly, these are[1]

$$\frac{1}{B}+\frac{A'B'}{2A^2B}+\frac{B'^2}{4AB^2}-\frac{B''}{AB}+\frac{\dot{A}\dot{B}}{2AB}+\frac{\dot{B}^2}{4B^2}= 8\pi G\left(\rho+\frac{\mu^2\Phi^2}{2}+\frac{\Phi'^2}{2A}+\frac{\dot{\Phi}^2}{2}-\frac{g\rho\Phi}{m}\right) \quad (7)$$

$$\frac{\dot{A}B'}{2AB}-\frac{\dot{B}'}{B}+\frac{\dot{B}B'}{2B^2} = 8\pi G\dot{\Phi}\Phi' \quad (8)$$

$$\frac{B'^2}{4B^2}+\frac{A\dot{B}^2}{4B^2}-\frac{A}{B}-\frac{A\ddot{B}}{B} = 8\pi GA\left(\frac{\dot{\Phi}^2}{2}+\frac{\Phi'^2}{2A}-\frac{\mu^2\Phi^2}{2}+\frac{g\rho\Phi}{m}\right) \quad (9)$$

$$\frac{-A'B'}{4A}-\frac{B'^2}{4AB}+\frac{B''}{2A}+\frac{B\dot{A}^2}{4A^2}-\frac{\dot{A}\dot{B}}{4A}+\frac{\dot{B}^2}{4B}-\frac{B\ddot{A}}{2A}-\frac{\ddot{B}}{2}= 8\pi GB\left(\frac{\dot{\Phi}^2}{2}-\frac{\Phi'^2}{2A}-\frac{\mu^2\Phi^2}{2}+\frac{g\rho\Phi}{m}\right) \quad (10)$$

$$\ddot{\Phi}+\dot{\Phi}\left(\frac{\dot{B}}{B}+\frac{\dot{A}}{2A^2}\right)-\frac{\Phi''}{A}+\Phi'\left(\frac{A'}{2A^2}-\frac{B'}{AB}\right)+\mu^2\Phi = \frac{g\rho}{m} \quad (11)$$

In the above $'$ represents $\frac{d}{dt}$, and $\cdot$ represents $\frac{d}{dr}$.

These equations are obviously very complicated. To make them tractable one can make the further simplifying assumption that Φ and ρ are spatially homogeneous. This allows one to look for separable solutions.

$$A(t,r) = R(t)^2 f(r) \quad (12)$$

$$B(t,r) = S(t)^2 g(r) \quad (13)$$

Equation (8) now implies that S is equal to R times a constant. This can be taken to be one by suitably normalising f and g. Also it is useful to re–define the radial coordinate as $\bar{r} = \sqrt{g(r)}$. Inserting this into the equations, and immediately dropping the bar over the r to avoid any visual messiness, one has, since now $A = R^2 f$, and $B = R^2 r^2$, the following set

$$3\dot{R}^2 - 8\pi GR^2\left(\rho+\frac{\mu^2\Phi^2}{2}+\frac{\dot{\Phi}^2}{2}-\frac{g\rho\Phi}{m}\right)+\left\{\frac{1}{r^2}-\frac{1}{r^2 f}+\frac{f'}{rf^2}\right\} = 0 \quad (14)$$

[1]The equations shown are specifically for the case of a Yukawa potential. Other potentials are dealt with similarly.

$$2R\ddot{R} + \dot{R}^2 + 8\pi G R^2 \left(\frac{\dot{\Phi}^2}{2} - \frac{\mu^2 \Phi^2}{2} + \frac{g\rho\Phi}{m} \right) + \left\{ -\frac{1}{fr^2} + \frac{1}{r^2} \right\} = 0 \quad (15)$$

$$\ddot{\Phi} + \frac{3\dot{R}\dot{\Phi}}{R} + \mu^2 \Phi = \frac{g\rho}{m} \quad (16)$$

Immediately one may see the benefits of these manipulations, the bracketed terms in equation (15) must be equal to a constant, which is taken to be κ. This implies

$$f(r) = (1 - \kappa r^2)^{-1} \quad (17)$$

Furthermore the radial coordinate, r, is re-scaled so that $R(0) = 1$ and the boundary condition $\dot{\Phi}_o = 0$ is imposed. Equation (14) then determines the separation constant, κ.

$$\kappa = \frac{8\pi G}{3} \left(\rho_o + \frac{\mu^2 {\Phi_o}^2}{2} - \frac{g\rho_o \Phi_o}{m} \right) \quad (18)$$

The final set of equations to be solved is

$$\ddot{R} + \frac{\dot{R}^2}{2R} + 4\pi G R \left(\frac{\dot{\Phi}^2}{2} - \frac{\mu^2 \Phi^2}{2} + \frac{g\rho\Phi}{m} \right) + \frac{4\pi G}{3R} \left(\rho_o + \frac{\mu^2 {\Phi_o}^2}{2} - \frac{g\rho_o \Phi_o}{m} \right) = 0 \quad (19)$$

$$\ddot{\Phi} + \frac{3\dot{R}\dot{\Phi}}{R} + \mu^2 \Phi = \frac{g\rho}{m} \quad (20)$$

$$\dot{\rho} + \frac{3\dot{R}\rho}{R(1 - \frac{g\Phi}{m})} = 0 \quad (21)$$

The last equation comes from the τ–component of the energy conservation equation ${T^{\mu\nu}}_{;\nu} = 0$, and using (20) to cancel certain terms.

It should be noted that the interior collapse metric we have just specified is of Robertson—Walker type, and can have positive, negative or zero spatial curvature depending on the initial conditions. In many cases it is more usual to redefine the radial coordinate so that the curvature constant is +1 or –1, then the absolute value of the scale factor, R(t), is of physical relevance. Whenever the constant is zero, so that the metric is spatially flat, only the relative magnitude of the scale factor is physically relevant.

Finally, the interior metric of the collapsing star is given by

$$ds^2 = dt^2 - R^2(t) \left(\frac{dr^2}{1 - \kappa r^2} + r^2 d\theta^2 + r^2 \sin^2(\theta) d\phi^2 \right) \quad (22)$$

where $R(t)$, ρ and Φ are to be determined by solving (19), (20) and (21).

3.2 Results

The first figure shows the form of the scale factor, R(t), for the pure dust collapse model of Oppenheimer and Snyder. Note the characteristic cycloidal shape. The three curves correspond to initial expansion, contraction and stationarity. For the star initially at rest, collapse to singularity occurs in a time $\frac{\pi}{2}\left(\frac{8\pi G\rho_o}{3}\right)^{-1/2}$.

Figure 3.2 shows the scale factor for the collapse of a pure scalar configuration, and figure 3.3 shows the evolution of the scalar field itself. Particularly interesting is the 'bump' in the scale factor, which seems to be a general feature of scalar collapse.

In figure 3.4 can be seen the effect of varying the mass of the scalar boson upon the scale factor. Notice how the maximum value of the scale factor is not affected by any variation of the scalar mass; it depends only on the initial value of the scalar field. The time taken for the collapse to proceed to singularity is inversely proportional to the scalar mass, as would be expected on dimensional grounds.

Figure 3.5 shows the effect of variation in the initial value of the scalar field. As the initial value is increased the extent of the expansion caused by the scalar field increases markedly. Figure 3.6 shows the evolution of the scalar field corresponding to the largest curve in figure 3.5. In contrast to figure 3.3 the scalar field oscillates several times before diverging. If one examines closely the graph of the scale factor in figure 3.5 one can just see slight undulations in the scale factor which correspond with the scalar field oscillations.

Figures 3.7 and 3.8 show the evolution of the scale factor and the scalar field for a peculiar value of initial scalar field. Choosing such an initial value has produced a very strange pattern of behaviour of the scale factor. This is caused by the oscillation of the scalar field occurring near the time when the expansion has just reached its maximum.

So far, the overwhelming conclusion one may derive from these results is that the scalar field may, under certain conditions, tend to make the star expand, but does not prevent the eventual formation of singularities.

For these results, a non-zero initial value of the scalar field has been assumed—it sort of appears from 'nowhere'. This can happen under somewhat more exotic

circumstances than have been considered here, but perhaps it is more natural to expect that the scalar field must initially be of extremely small value. The question then arises as to what effect it can have, if, starting from zero, the scalar field is driven by the collapse itself, perhaps from the motion of the dust particles through a yukawa coupling. Figure 3.9 shows a comparison of two collapses, both starting with zero scalar field but one having no yukawa coupling, and the other having such a coupling. Here there is no expansion, no scalar 'bump' but the coupling term has in fact accelerated the collapse; notice how the scale factor is significantly steepened in its late stages. Such a treatment of scalar particle production would seem to have little observational effect, the steepening would be very difficult to detect, but later on will be discussed how a more rigorous treatment of particle production could result in more significant alterations to the Oppenheimer–Snyder model.

Lastly is shown the scale factors for scalar collapse, but this time including a quartic self interaction for the scalar field. The effect of the coupling term is to increase the collapse time.

The basic conclusion one may draw is that in the early stages of collapse a large scalar density may halt contraction and cause expansion before finally collapsing to a singularity; in late stages, in this classical model, the scalar field may only hasten singularity formation.

While it may seem that this instantaneous 'dumping' of the scalar field is a somewhat unphysical process, it turns out that such a thing is entirely possible. This is precisely what happens when a spontaneously broken gauge theory undergoes a symmetry-restoring phase transition.

It has long been known that a spontaneously broken gauge symmetry can be restored at very high temperatures[15]. The scalar field originally in the asymmetric vacuum evolves into the symmetric vacuum liberating the energy stored there. In the cosmological context this scenario has been used to create the exponential expansion period which is invoked in the inflationary theories. This expansion comes about because the scalar field gives rise to a negative effective pressure in the Einstein equations. It is interesting to imagine the effects of such a high temperature phase transition on a hot collapsing star. Qualitative consid-

erations of this type have been made in the paper of Sinha and Prasanna[16]. The phase transition considered by these authors is that of the electroweak theory, which has a critical temperature of around 100GeV, whereas the phase transition considered in the inflation theories is that of the GUT phase transition, critical temperature 10^{14}GeV.

By the standard of stellar interiors, temperature around 10^{-3}GeV, the electroweak critical temperature is very high and possibly quite inaccessible in the course of normal stellar evolution. The whole scenario therefore requires quite unusual physical conditions to become possible. Several ideas have been proposed to suggest how such high temperatures could be obtained but these are very speculative.

Assuming that such a high temperature can be obtained once the scalar field makes the transition to the symmetric vacuum, the energy release gives a negative pressure which tends to act against the collapse, perhaps causing an expansion. This expansion, if acting for long enough results in cooling, and a subsequent decay back into the symmetric vacuum; this results in a large amount of latent heat being released(assuming the transition is first order) which could result in a catastrophic explosion, with the heat being transported away. Eventually this cycle could repeat itself. Alternatively, the negative pressure could be just enough to halt the collapse, resulting in a new type of star, one with a core of symmetric vacuum. Simple arguments using the Tolman-Oppenheimer-Volkoff equations and Oppenheimer-Snyder equations show that such behaviour is possible.

Such a scenario demands that certain constraints be satisfied; firstly, by whatever means the high temperature must be attained, secondly the star must be in quasi-equilibrium, i.e. contracting very slowly, this lets one evade the entropy constraint pointed out by Sher[14] who used it to show that a cosmological bounce would, in fact, violate the second law of thermodynamics.

So far the scalar field has been treated classically, and this is the extent to which it is possible to study the system with present technology, all the same it is worthwhile to speculate further; what are the possible consequences when a proper quantum tretament is applied?

In a realistic collapse scenario one would envisage, say, a $1.5M_{\odot}$ core of degenerate nucleons contracting inwards, reaching tremendous densities and tem-

peratures in the process. If a light scalar as we have been considering exists, one would expect that at high densities a large amount of scalar particle production would take place, the particles produced either being radiated away, trapped inside the collapsing matter or both. To understand these phenomena one must treat the scalar field using the methods of quantum field theory. Because of the distinctive character of the scalar field one may surmise that the backreaction effects produced in this process could be particularly interesting.

Scalar production during collapse can take place due to two mechanisms, the first from the usual yukawa vertex, the second from mixing of positive and negative modes[6]. The second method is a curved space effect and results in particle production even for free fields. The two mechanisms also mix so that production can also take place to first order in the coupling constant, whereas this could not happen in flat space due to momentum conservation constraints.

This leads one naturally on to a consideration of the discipline of quantum field theory in curved spacetime which can be regarded as a first approximation to a theory of quantum gravity, akin to the phenomenologically successful semi-classical electrodynamics of the 1930s. Here the matter fields are treated field-theoretically and the gravitational field is to be regarded as a classical background field. Presumably this approach should give one the first quantum corrections to the classical collapse equations. This is done by replacing Einstein's equation by their quantum, 'renormalized' counterparts

$$G_{\mu\nu} = 8\pi G T_{\mu\nu} \rightarrow G_{\mu\nu} = 8\pi G < T_{\mu\nu} > \tag{23}$$

The bracket round the energy momentum tensor indicates that one is taking an expectation value with respect to some specific state.

The calculations of renormalised stress-energy tensors has been something of an industry for two decades now. In the early days much attention was spent on calculations for free massless scalar fields. Indeed the renormalised stress tensor has been calculated for free massless fields in a Robertson–Walker background in closed form in terms of the Ricci tensor[7].

$$\begin{aligned} < T_{\mu\nu} > &= \alpha \left[\frac{1}{3} g_{\mu\nu} \Box R - \frac{1}{3} R_{;\mu\nu} - \frac{1}{3} R R_{\mu\nu} + \frac{1}{12} g_{\mu\nu} R^2 \right] \\ &+ \beta \left[-\frac{2}{3} R R_{\mu\nu} + R_{\mu}{}^{\lambda} R_{\nu\lambda} - \frac{1}{2} g_{\mu\nu} R_{\lambda\sigma} R^{\lambda\sigma} + \frac{1}{4} g_{\mu\nu} R^2 \right] \end{aligned} \tag{24}$$

The coefficients α, β depend on the method of regularization used.

This results in a third order field equation[2]

$$R^{(3)} = \frac{\ddot{R}^2}{2\dot{R}} + \frac{\dot{R}^3}{R^2}\left[\frac{3}{2} - \frac{\beta}{2\alpha}\right] + \frac{\dot{R}}{16\pi G\alpha} - \frac{\dot{R}\ddot{R}}{R} - \frac{\rho_o}{6\alpha R\dot{R}} \tag{25}$$

Equation (25) has been investigated in cosmological scenarios[9] primarily because it was expected that quantum effects may alter or eradicate the initial singularity[8], this being thought possible since quantum effects can lead to negative energies and pressures; the Hawking–Penrose singularity theorems predict the ubiquity of singularities under the condition that energies and pressures remain positive. The effects of massless quantised fields on dust cloud collapse have also been calculated with qualitatively similar results[11]. It is found that both singularity free, 'bounce' solutions and singular solutions can be obtained, depending on the initial conditions.

Unfortunately, a closed form solution for the renormalised stress tensor does not exist for massive scalar fields in a Robertson–Walker background[12]. Studies suggest however that quantum effects may manifest themselves on a scale of the order of the inverse mass of the particle; there can be something of a 'resonance' effect here. For most of the known stable particles this is extremely small and hence unobservable, but if a light scalar such as has been considered so far existed then these interesting quantum effects could manifest themselves over much larger, even macroscopic, distances leaving them open to possible experimental verification.

Bounce behaviour at the order of the inverse mass of the scalar particle was exhibited in the paper of Parker and Fulling[13]. The object of this work was simply to see if the apparent inevitability of collapse to a singularity could be halted by quantum effects of any means. To do this the semiclassical Einstein equations for a closed Robertson–Walker universe were solved. The metric was treated as a classical function while the matter content, as represented by the energy momentum tensor, is a quantum field operator acting on a specific state. The methods used in this work were canonical quantization in the Heisenberg picture and the adiabatic regularization method to eliminate divergences from

[2]for the case κ=0. A classical dust term has also been included.

the ill-defined energy-momentum operator. The pressure and density terms were constructed from the tt and rr components of the canonical energy momentum tensor in the usual manner. The methods used fully took into account particle creation effects due to rapidly changing curved spacetime. When the scale factor varied very slowly no particle production took place, as perhaps one would naively expect.

The resultant equation of state for this quantum scalar gas behaved like an ideal gas for low velocities and as an extreme relativitic gas at high velocities.

The crucial part of this work was not in the methods used to construct the equation of state but in the *quantum state* which was used in the right hand side of the semiclassical equations. What Parker and Fulling did was to explicitly construct a quantum state that would give rise to negative pressure effects. The results they found were that the system would indeed bounce from such states but would collapse to a singularity for others. Again, the bounce occurs at spatial distance of the order of the Compton wavelength of the particle.

So, in that work singularity avoidance depended on the use of a special quantum state, the peculiarity or otherwise of which is open to speculation. The negative pressure produced in this case is a 'quantum coherence' effect between states with states with different particle numbers. States with definite particle number always formed singularities. What is more, this special state is not in any way intrinsically connected with general relatvity or curved space, it is completely general, and could possibly occur in many other situations. Parker and Fulling speculated that this state could be brought about during the collapse by some, (unspecified) interaction, in a somewhat similar manner to the superconducting BCS phase transition. This was because the special state they had constructed had a similarity to an excited superfluid state.

This is, altogether, a very interesting scenario, though, it must be said, very inconclusive. What makes it of relevance from the point of view of this thesis, and its primary emphasis on light scalars is that such exotic effects could manifest themselves over relatively large distances. Parker and Fulling when investigating scalar bounces had in mind the pion as a candidate particle. The pion has a Compton wavelength of around 10^{-15}cm. Observing the bounces of curved

spacetime over such small distances is clearly impossible, but if light scalars did exist, then there exists the possibility of witnessing these exotic and speculative quantum phenomena.

3.3 Exterior Solutions and Matching Conditions

Having found a representative sample of interior solutions and identifying novel and interesting qualitative featues in these, it is important that appropriate exterior solutions are found so that definite observational predictions may be made.

For instance it is well known that radial emitted photons in the Oppenheimer–Snyder model exhibit a characteristic redshift. What modifications to this picture will there be for collapsing objects with significant scalar component?

The surface of the star divides the spacetime into two regions; given a known interior which has been obtained previously by solving the Einstein equations, one must find a suitable exterior then match it smoothly to the interior at the star surface.

The form of the exterior that one might deem suitable depends on what matter content exists there. Normally there wouldn't be any, i.e. vacuum. This along with the assumptions of spherical symmetry leads uniquely to the Schwarzschild form for the exterior; this result is known as Birkhoff's theorem. If one envisaged the star to be radiating as it collapsed, but still maintaining spherical symmetry the simplest generalization of the Schwarzschild metric is that of Vaidya[21]. The Vaidya metric describes a non zero flux of incoherent massless radiation. These two metrics, the Schwarzschild and the Vaidya are therefore the two favoured candidates for matching to the collapsing Robertson-Walker interiors found in §3.2.

The Schwarzschild metric is

$$ds^2 = \left(1 - \frac{2m}{\bar{r}}\right) d\bar{t}^2 - \left(1 - \frac{2m}{\bar{r}}\right)^{-1} d\bar{r}^2 - \bar{r}^2 d\bar{\theta}^2 - \bar{r}^2 \sin^2(\bar{\theta}) d\bar{\phi}^2 \qquad (26)$$

where the barred coordinates are specifically Schwarzschild coordinates. Unbarred coordinates are the interior comoving coordinates. The Vaidya metric

is

$$ds^2 = \left(1 - \frac{2m(T)}{R}\right) + 2dTdR - R^2d\theta^2 - R^2\sin^2(\theta)d\phi^2 \qquad (27)$$

This is written in terms of radiative coordinates.

One possible difficulty that may arise is that because of the tailing of the scalar field, no sharp star boundary exists, so that instead of a well defined star surface one has a tail of interacting bosons and dust particles as was the case for the static configurations of chapter 1. This tail extends a distance of the order of the Compton wavelength of the scalar field, so the problem is more serious for lighter particles. On the other hand since the scalar field is massive and hence of finite range one would expect that at some suitably large radial distance the scalar tail will be negligible and then one may match at this 'effective' radius. This introduces a degree of arbitrariness into the problem; what is a 'suitable' effective radius? Is it that 99% of the star mass lies within this radius or 99.9%? Nevertheless, since the scalar range is finite, and assuming surface effects are unimportant, and the effective radius, whatever it is, is large enough, then matching to a simple Schwarzschild exterior should be possible with very little difficulty. Even if this is not the case one would expect that matching to a Vaidya metric possible since this takes into account mass loss from the star, and one might reasonably expect the some sort of radiative process is taking place simultaneously with the collapse.

It turns out that matching to Schwarzschild or Vaidya exteriors is *not* possible in this model. Nevertheless, it shall be shown explicitly why this is not possible, and later on some discussion will be spent on why, such an apparently reasonable thing to do, can't be done.

The two principal methods of matching are due to Lichnerowicz and Darmois respectively. These have been shown to be equivalent in the paper of Bonnor and Vickers[17], who also showed that other matching conditions due to Synge and O'Brien are inequivalent, being somewhat stronger.

The Lichnerowicz matching conditions are that the metric components and their first derivatives are continuous on the matching surface. This obviously requires that a single set of coordinates be used; so if the interior and exterior are not in the same coordinates, then a transformation has to be made. In this

case one would have to find the transformations taking one from the interior comoving coordinate system to the exterior Schwarzschild coordinates. Such a method is used by Weinberg in his treatment of the Oppenheimer–Snyder model. He matches the Robertson-Walker interior to the exterior Schwarzschild metric by using the following transformation

$$\overline{\theta} = \theta \quad \overline{\phi} = \phi \quad \overline{r} = r\,R \tag{28}$$

and

$$\overline{t}(t,r) = \left(\frac{1-\kappa a^2}{\kappa}\right)^{1/2} \int_{S(t,r)}^{1} \left(\frac{R}{1-R}\right)^{1/2} \frac{dR}{1-\frac{\kappa a^2}{R}} \tag{29}$$

where

$$S(t,r) = 1 - \left(\frac{1-\kappa r^2}{1-\kappa a^2}\right)^{1/2} (1 - R(t)) \tag{30}$$

Matching is accomplished by this means and relates the arbitrary constants of the two regions thus

$$m = \frac{\kappa a^3}{2} \tag{31}$$

The appearance of the collapsing star to a distant observer can now be calculated. Consider an external observer at radial coordinate $\overline{r}_o$ and photons being emitted radially from the surface of the star. Since for null geodesics, $ds^2 = 0$, in Schwarzschild spacetime one has

$$\frac{d\overline{t}}{d\overline{r}} = \left(1 - \frac{2m}{\overline{r}}\right)^{-1} \tag{32}$$

a photon emitted radially from the star surface $\overline{r}_s$, at a time $\overline{t}_s$, will arrive at the distant observer at a time $\overline{t}_o$, where

$$\overline{t}_o = \overline{t}_s + \int_{\overline{r}_s}^{\overline{r}_o} \left(1 - \frac{2m}{\overline{r}}\right)^{-1} d\overline{r} \tag{33}$$

$$= \overline{t}_s + \overline{r}_o - \overline{r}_s + 2m \log\left(\frac{\overline{r}_o - 2m}{\overline{r}_s - 2m}\right) \tag{34}$$

The redshift is defined as the fractional change in the observed and emitted wavelengths of the photons

$$z = \frac{\lambda' - \lambda_o}{\lambda_o} = \frac{d\overline{t}_o}{dt} - 1 \tag{35}$$

which is explicitly

$$z = \dot{\overline{t}}_s - aR\dot{R}\left(R - \frac{2m}{a}\right)^{-1} - 1 \tag{36}$$

This last equation gives the redshift as a function of the interior proper time. To convert this to the external coordinate time, one needs to use the coordinate transformation. (36) is in a very interesting form for it shows explicitly how the dynamics of the interior affect the external appearance; the redshift function is explicitly parametrized by the scale factor.

For (36) to be of any use it is necessary to transform the internal time dependence of the expression to a dependence upon the proper time of the external observer; since this observer is at a large distance from the collapsing star, his proper time will be the same as the coordinate time, $\bar{t}_s$. To do this conversion requires intricate manipulations with equations (29) and (34) on (36) and cannot be accomplished exactly. Instead, using the coordinate transformation one may identify two types of redshift behaviour, emanating from the 'early', initial radius much greater than Schwarzschild radius, and 'late' behaviour, when the star radius is nearly crossing the Schwarzschild radius.

For early times, R >> $\frac{2m}{a}$ since

$$\bar{t}_s \simeq t \tag{37}$$

$$\bar{t}_o \simeq t + \bar{r}_o \tag{38}$$

the redshift is approximately

$$z \simeq \sqrt{\frac{2m}{a}} \left(\frac{1 - R(\bar{t}_o - \bar{r}_o)}{R(\bar{t}_o - \bar{r}_o)} \right)^{1/2} \tag{39}$$

and for late times, R $\simeq \frac{2m}{a}$, since

$$\bar{t}_s \simeq -2m \log \left[1 - \frac{2m}{R} \right] + c_1 \tag{40}$$

$$\bar{t}_o \simeq -4m \log \left[1 - \frac{2m}{R} \right] + c_2 \tag{41}$$

where c_1, c_2 are some constants, one has

$$z \simeq \exp \left(\frac{\bar{t}_o}{2m} \right) \tag{42}$$

The usefulness of this way of treating the redshift, in that the interior dynamics explicitly appear, prompted an attempt to generalize the result (29), attempting to perform the matching in the manner of Lichnerowicz, so that through the

redshift formula (36), an easy interpretation of the interiors of §3.2 could be made. Naively, one might expect that when one has a 'bump', interior one would, making comparisons with the pure dust result, get power-law blue-shift followed by power-law red-shift, then finally exponential redshift. Certainly, if (37) and (38) still hold at early times, then this would be correct.

Generalizing the transformation proved in practice to be much more difficult than was initially envisaged and so was abandoned in favour of the Darmois method.

The Darmois[19] matching conditions are by far the neatest and most elegant matching conditions. They are highly geometric in nature, manifestly covariant and allow the use of different coordinates in the interior and exterior regions. This method is to be preferred since one need not worry about the admissibility of coordinate systems or actually calculating the coordinate transformation, which can rarely be found analytically.

The Darmois matching conditions are that the first and second fundamental forms of the matching surface calculated in each coordinate system must be identical. Let these be discussed in some greater detail[3].

One has a four dimensional spacetime M, divided into interior and exterior regions, M_I, M_E, which are separated by a three dimensional spherically symmetric timelike surface, Σ. The metrics on M_I, M_E are denoted ${ds_I}^2$, ${ds_E}^2$ respectively, whch are written in terms of the coordinates ${x_I}^\mu$, ${x_E}^\mu$. The first fundamental form is the intrinsic metric evaluated on Σ as seen from M_I, M_E. The second fundamental forms are the extrinsic curvatures K_I, K_E as seen from M_I, M_E. The matching surface is parametrized by parameters ξ^i, and described by the functions ${x_I}^\mu(\xi^i)$, ${x_E}^\mu(\xi^u)$ as seen from the interior and exterior regions.

The intrinsic metric of Σ in the interior is

$$ {ds_I}^2 = g_{I\mu\nu}\frac{\partial {x_I}^\mu}{\partial \xi^i}\frac{\partial {x_I}^\nu}{\partial \xi^j}d\xi^i d\xi^j \tag{43} $$

and the extrinsic curvature is

$$ K_I = -n_{I\mu}\left[\frac{\partial^2 {x_I}^\mu}{\partial\xi^i\partial\xi^j} + \frac{\partial {x_I}^\nu}{\partial\xi^i}\frac{\partial {x_I}^\sigma}{\partial\xi^j}\Gamma^\mu{}_{I\nu\sigma}\right]d\xi^i\xi^j \tag{44} $$

[3]The notation used here is that of [18]

where n_i is the unit outward normal of Σ as seen from M_i. Similar expressions hold for the exterior region.

The matching conditions are then

$$ds_I{}^2 \stackrel{\Sigma}{=} ds_E{}^2 \tag{45}$$

$$K_I \stackrel{\Sigma}{=} K_E \tag{46}$$

Matching using the Darmois method for dust collapse can be found in ref[20].

Here are the required geometric objects for the metrics that are under consideration

Robertson–Walker

$$ds^2 = dt^2 - \frac{R^2}{1-\kappa r^2}dr^2 - r^2R^2d\theta^2 - r^2R^2\sin^2(\theta)d\phi^2 \tag{47}$$

$$\xi = (t,\theta,\phi) \tag{48}$$

$$\Sigma = (t,a,\theta,\phi) \tag{49}$$

$$ds_\Sigma{}^2 = dt^2 - a^2R^2\left(d\theta^2 + \sin^2(\theta)d\phi^2\right) \tag{50}$$

$$n = \left(0, \frac{R}{\sqrt{1-ka^2}}, 0, 0\right) \tag{51}$$

$$K_{tt} = 0 \tag{52}$$

$$K_{\theta\theta} = aR\left(1-ka^2\right)^{1/2} \tag{53}$$

Schwarzschild

$$ds^2 = \left(1-\frac{2m}{\overline{r}}\right)d\overline{t}^2 + \left(1-\frac{2m}{\overline{r}}\right)^{-1}d\overline{r}^2 - \overline{r}^2d\overline{\theta}^2 - \overline{r}^2\sin^2(\overline{\theta})d\overline{\phi}^2 \tag{54}$$

$$\Sigma = \left(\overline{t}(t), \overline{r}(t), \overline{\theta}, \overline{\phi}\right) \tag{55}$$

$$n = \left[\frac{\overline{r}\,(\overline{r}-2m)}{(\overline{r}-2m)^2\dot{\overline{t}}^2 - \overline{r}^2\dot{\overline{r}}^2}\right]^{1/2}\left(-\dot{\overline{r}}, \dot{\overline{t}}, 0, 0\right) \tag{56}$$

$$ds_\Sigma{}^2 = \left[\left(1-\frac{2m}{\overline{r}}\right)\dot{\overline{t}}^2 - \left(1-\frac{2m}{\overline{r}}\right)^{-1}\dot{\overline{r}}^2\right]d\overline{t}^2 - \overline{r}^2\left(d\overline{\theta}^2 + \sin^2(\overline{\theta})d\overline{\phi}^2\right) \tag{57}$$

$$K_{tt} = \frac{m\dot{\overline{r}}^2\dot{\overline{t}}}{(\overline{r}-2m)^2} - \frac{2m^2\dot{\overline{r}}^2\dot{\overline{t}}}{\overline{r}(\overline{r}-2m)^2} + \frac{2m\dot{\overline{r}}^2\dot{\overline{t}}}{\overline{r}\,(\overline{r}-2m)} + \frac{2m\dot{\overline{t}}^3}{\overline{r}^3} - \frac{m\dot{\overline{t}}^3}{\overline{r}^2} - \dot{\overline{t}}\ddot{\overline{r}} + \dot{\overline{r}}\ddot{\overline{t}} \tag{58}$$

$$K_{\theta\theta} = \frac{\sqrt{\overline{r}}(\overline{r}-2m)^{3/2}\dot{\overline{t}}}{\left[(\overline{r}-2m)^2\dot{\overline{t}}^2 - \overline{r}^2\dot{\overline{r}}^2\right]^{1/2}} \tag{59}$$

$$ds^2 = \chi dT^2 + 2dTdR - R^2 d\Omega^2 \tag{60}$$

$$\Sigma = (T(t), R(t), \theta, \phi) \tag{61}$$

$$n = \left(\chi^2 + 2\dot{T}\dot{R}\right)^{-1/2}\left(-\dot{R}, \dot{T}, 0, 0\right) \tag{62}$$

$$ds_\Sigma{}^2 = \left(\chi\dot{T}^2 + 2\dot{T}\dot{R}\right)dt^2 - R^2 d\Omega^2 \tag{63}$$

$$K_{tt} = \frac{-\frac{1}{2}\dot{\chi}\dot{T}^3 - \dot{T}\ddot{R} + \dot{R}\ddot{T}}{\left(\chi\dot{T}^2 + 2\dot{T}\dot{R}\right)^{1/2}} \tag{64}$$

$$K_{\theta\theta} = \frac{R\dot{R} + \chi R\dot{T}}{\left(\chi\dot{T}^2 + 2\dot{T}\dot{R}\right)^{1/2}} \tag{65}$$

where $\chi = 1 - \frac{2m}{R}$, and m is a function of T.

The matching conditions for matching from the Robertson-Walker to the Schwarzschild exterior are

$$\bar{r} \overset{\Sigma}{=} aR \tag{66}$$

$$\left(1 - \frac{2m}{\bar{r}}\right)\dot{\bar{t}}^2 - \left(1 - \frac{2m}{\bar{r}}\right)^{-1}\dot{\bar{r}}^2 \overset{\Sigma}{=} 1 \tag{67}$$

$$\frac{\sqrt{\bar{r}}(\bar{r} - 2m)^{3/2}\dot{\bar{t}}}{\left((\bar{r} - 2m)^2\dot{\bar{t}}^2 - \bar{r}^2\dot{\bar{r}}^2\right)^{1/2}} \overset{\Sigma}{=} aR\left(1 - \kappa a^2\right)^{1/2} \tag{68}$$

$$\frac{m\dot{\bar{r}}^2\dot{\bar{t}}}{(\bar{r} - 2m)^2} - \frac{2m^2\dot{\bar{r}}^2\dot{\bar{t}}}{\bar{r}(\bar{r} - 2m)^2} + \frac{2m\dot{\bar{r}}^2\dot{\bar{t}}^2}{\bar{r}(\bar{r} - 2m)} + \frac{2m^2\dot{\bar{t}}^2}{\bar{r}^3} - \frac{m\dot{\bar{t}}^3}{\bar{r}^2} - \dot{\bar{t}}\ddot{\bar{r}} + \dot{\bar{r}}\ddot{\bar{t}} \overset{\Sigma}{=} 0 \tag{69}$$

The condition that is most useful here is (69). Upon simplification one gets

$$m = \frac{Ra^3}{2}\left(\kappa + \dot{R}^2\right) \tag{70}$$

If one has a dust solution one has

$$\dot{R}^2 = k\,(1/R - 1) \tag{71}$$

holding, and so one has as Weinberg (31).

For the more general interiors found in §3.2 (72) does no hold, and so matching is not possible since m and a are constants.

Why is matching not possible? The exterior is spherically symmetric and asymptotically static and there are no long range forces—perhaps the system is radiating, could one match to a Vaidya exterior? The answer is no, for as has been shown by [5] when the matching surface is comoving no radiation can take place and then the Vaidya metric reverts to Schwarzschild form.

This is a very puzzling result. Fayos et.al[18] have shown that matching a Robertson-Walker metric to a Vaidya metric is always possible if there exits a surface upon which the total radial pressure vanishes. For a massive scalar field as has been considered here, the total radial pressure indeed would *not* vanish, but it *would* become exponentially small at large radii. Surely this should be good enough for matching to take place??

One idea could be to try to match to a Vaidya metric with a non-comoving matching surface, but this, even if possible, results in difficulties of interpretation.

This state of affairs puts one in a frustrating position. From a very simple model interesting qualitative behaviour has been seen which differs from that of the pure dust case. Other arguments argue for extremely interesting behaviour connected with scalar fields, in phase transitions, particle production and quantum effects to occur in gravitational collapse. This simple model could be indicative of such possibilities. But any observation of such phenomena must be made by a distant observer in the exterior region; the failure to match to a suitable exterior spacetimes precludes the possibility of any definite identification of such phenomena.

The apparent naturalness of matching Robertson-Walker to Schwarzschild or Vaidya, and its apparent impossibility begs the question as to whether the problem is a fundamentally serious, physical problem, or merely some mathematical pathology. Physical intuition suggests the latter but then is confounded by the problem of understanding the precise nature of such a pathology, (if it exists).

The only way to settle this problem is to begin again, this time restoring the radial depedence in the field equations, and in doing so going down the way of numerically intensive general relativity. In this way one has to begin with clearly defined interior, exterior and boundary regions, and one may see how these all evolve during the collapse. To set down this road would be a very major

undertaking, which will not be attempted here.

In this approach one effectively 'undiscovers' the problems which have so far plagued the matching procedure. There is a very big jump in complexity in going from the simple methods of this chapter to numerically intensive general relativity, but this is the only way to go to settle the problem. This is not a glib remark; one may think that by 'tweaking' around with the Schwarzschild metric it may be possible to get an appropriate exterior, and indeed one can, but this approach subsequently becomes as difficult as the numerically intensive approach as will be demonstrated below.

Taking a more general exterior metric, which reduces to the Schwarzschild case for pure dust collapse, and the usual Robertson-Walker exterior, the matching conditions will be derived along with necessary steps to make firm observational predictions about the model.

The exterior metric is

$$ds^2 = B(\bar{t},\bar{r})d\bar{t}^2 - A(\bar{t},\bar{r})d\bar{r}^2 - \bar{r}^2 d\Omega^2 \tag{72}$$

where

$$B(\bar{t},\bar{r}) = \left(1 - \frac{2m}{\bar{r}} + \delta B(\bar{t},\bar{r})\right) \tag{73}$$

$$A(\bar{t},\bar{r}) = \left(1 - \frac{2m}{\bar{r}} + \delta A(\bar{t},\bar{r})\right)^{-1} \tag{74}$$

The functions δA, δB therefore represent the deviations from the Schwarzschild metric.

The curvature forms are then

$$ds_\Sigma{}^2 = \left(B\dot{\bar{t}}^2 - A\dot{\bar{r}}^2\right)d\bar{t}^2 - \bar{r}^2 d\Omega^2 \tag{75}$$

$$\begin{aligned} K_{tt} = & \left(AB\sqrt{B\dot{\bar{t}}^2 - A\dot{\bar{r}}^2}\right)^{-1}(AB\dot{\bar{t}}\ddot{\bar{r}} - AB\ddot{\bar{r}}\dot{\bar{t}} \\ & + \frac{1}{2}B\dot{\bar{r}}^2\dot{\bar{t}}A' - AB'\dot{\bar{r}}^2\dot{\bar{t}} + \frac{1}{2}BB'\dot{\bar{t}}^3 - \frac{1}{2}A\dot{\bar{r}}^3\dot{A} \\ & + B\dot{A}\dot{\bar{r}}\dot{\bar{t}}^2 - \frac{1}{2}AA'\dot{\bar{r}}\dot{\bar{t}}^2 - \frac{1}{2}A\dot{B}\dot{\bar{r}}\dot{\bar{t}}^2) \end{aligned} \tag{76}$$

$$K_{\theta\theta} = -\frac{\sqrt{B}\bar{r}\dot{\bar{t}}}{\sqrt{A}\left(B\dot{\bar{t}}^2 - A\dot{\bar{r}}^2\right)^{1/2}} \tag{77}$$

Applying the first two matching conditions gives

$$\bar{r} \overset{\Sigma}{=} aR \tag{78}$$

$$\dot{\bar{t}}^2 \overset{\Sigma}{=} B^{-1}\left(1 + a^2 A \dot{R}^2\right) \tag{79}$$

The third matching condition gives

$$\delta A \overset{\Sigma}{=} -2a^2 \dot{R}_o \delta \dot{R} - a^2 \delta \dot{R}^2 \tag{80}$$

upon assuming (72) for R_o, (31) and setting

$$R(t) = R_o(t) + \delta R \tag{81}$$

The form of δA makes for a very easy interpretation in terms of the known solutions of §3.1. Bearing in mind that R_o is in some sense the dust solution that is most closely related to the actual solution, it is obvious that the deviation from Schwarzschild must be fairly small when the scalar field results in only a slight 'bump' in the scale factor, as in figure 3.3, but very large when the scalar field causes a vast expansion, as in figure 3.5.

The last matching condition is altogether more tricky, but can in principle be integrated to give δB on the star surface, since the other three matching conditions provide the unknown functions of t.

The matching conditions provide initial data for the full Einstein equations for the exterior; these have then to be integrated, perhaps with some scalar field content, to provide the metric functions over the whole exterior region. Once these are constructed one may check that the deviation functions, δA, δB tend to zero at large values of the radial coordinate and become time-independent at large times. These conditions satisfied, one may conclude that the exterior is indeed the correct one, and then go on to analyse the null geodesics of this exterior, so finding out how the collapsing star will appear to some distant observer. The work is then finished. The drawback is that integrating the exterior equations and analyzing the null geodesics must be done numerically, which is not significantly easier than adopting this approach from the beginning.

3.4 Conclusion

In this chapter the Oppenheimer–Snyder model has been extended to include a classical scalar field. The solutions found differ qualitatively from the pure dust solutions of the Oppenheimer–Snyder model. The significance of these solutions was discussed in relation to more sophisticated treatments and phenomena, the main conclusion of which being is that the scalar field is of interest since it may lead to bounce behaviour. Of course, treatment of the gravitational collapse problem is as yet in an early state of development, since even for simple fluid models, integrating the Einstein equations is notoriously difficult and computationally expensive—which is to say nothing of the problems of providing a rigorous field-theoretic treatment.

Gravitational collapse has been described as *the* ultimate problem of theoretical physics, and its eventual resolution must require solution of the backreaction problem for quantum fields in curved space. This is perhaps the most difficult problem of theoretical physics. Study of scalar fields in this context has primarily been in the sense of constructing 'toy' models, purely to gain an insight into the technical aspects of the problem. This work may yet find phenomenological applications, since for some time now, as detailed in the introduction, there has been no shortage of candidate scalar particles.

Hence, in this chapter, after discussing such possibilities, the emphasis has been on finding appropriate exterior solutions and so in trying to tie down some observational predictions. In this sense the work is only partially successful. Matching was not performed, but the problem was discussed, identified and, I hope, clarified; the difficulties encountered related to known work[5, 18] in the area, and offering, perhaps, a useful critique. The most probable cause of the difficulties encountered is that the scalar field causes a sharp star boundary to become impossible. This is precisely related to the problem of scalar tailing which was mentioned in chapter one, and which subsequently caused the calculations of which, to be so very time consuming.

Originally it was hoped that matching would be performed, allowing the redshift function to be precisely calculated as a function of the external observers time and of the collapse parameters themselves, i.e. the dust density, and the

scalar mass, coupling and initial density. To do this requires a significantly more sophisticated approach, as is described in §3.3 . The most it is possible to say at present is that in the late stages of collapse, the scalar field will give rise to a very similar redshift as the pure dust solution, but in the early stages there may be the possibility of a blue-shift.

One aspect so far unconsidered is that of the importance of scalar radiation during collapse. Light scalars would be copiously produced during the collapse and could in certain circumstances carry off significant amounts of mass, perhaps leading to singularity avoidance by allowing the star to shrink or fragment into small enough pieces that a black hole would not be formed. A study of this type, though prohibitvely difficult, would link up with the work of chapter two, and could lead to significant bounds on the allowed values of the scalar field parameters.

Figure Captions

Figure 3.1: Pure dust collapse; scale factors corresponding to initial expansion, contraction and stationarity.

Figure 3.2: Pure scalar collapse; scale factor.

Figure 3.3: Pure scalar collapse; time dependence of scalar field corresponding to scale factor of figure 3.2 .

Figure 3.4: Pure scalar collapse; scale factors showing variation with changing scalar mass.

Figure 3.5: Pure scalar collapse; scale factors showing effect of varying initial scalar density .

Figure 3.6: Pure scalar collapse; evolution of scalar field corresponding to largest scale factor of figure 3.5 .

Figure 3.7: Pure scalar collapse; scale factor .

Figure 3.8: Pure scalar collapse; evolution of scalar field corresponding to scale factor of figure 3.7 .

Figure 3.9: Combined scalar/dust collapse; scale factors showing variation with yukawa coupling .

Figure 3.10: Pure scalar collapse; scale factors showing variation with quartic coupling .

References

1. S.Weinberg, 'Gravitation and Cosmology' (1972)
2. C.W.Misner, K.S.Thorne, J.A.Wheeler, 'Gravitation' (1972)
3. J.R.Oppenheimer, H.Snyder, Phys.Rev 56 455 (1939)
4. G.J.Benson, R.G.Moorhouse, A.B.Henriques, GUTPA 92/5/1
5. F.Fayos, X.Jaén, E.Llanta, J.M.M.Senovilla, Class.Quantum Grav. 8 2057 (1991)
6. N.D.Birrell, P.C.W.Davies 'Quantum Fields in Curved Space'
7. P.C.W.Davies, S.A.Fulling, S.M.Christensen, T.S.Bunch, Annals of Physics 109 108 (1977)
8. P.C.W.Davies, Phys.Lett B68 402
9. M.V.Fischetti, J.B.Hartle, B.L.Hu, Phys.Rev D20 1757 (1979)
10. P.Anderson, Phys.Rev D28 271 (1983)
11. G.Kennedy, A.F.Keith, J.H.Sanders, Class.Quantum Grav. 6 1697 (1989)
12. T.S.Bunch, S.M.Christensen, S.A.Fulling, Phys.Rev D18 4435 (1978)
13. L.Parker, S.A.Fulling, Phys.Rev D7 2357 (1973)
14. M.A.Sher, Phys.Rev D22 2989 (1980)
15. D.A.Kirzhnits, A.Linde, Phys.Lett B42 471 (1972)
16. R.P.Sinha, A.R.Prasanna, Phys.Lett B174 40 (1986)
17. W.B.Bonnor, P.A.Vickers, Gen.Rel.Grav 13 29 (1981)
18. F.Fayos, X.Jaén, E.Llanta, J.M.M.Senovilla, Phys.Rev D22 (1980) 2989
19. G.Darmois, 'Memorial des Sciences Mathematiques' vol.25

20. A.P.Lightman, W.H.Press, R.H.Price, S.A.Teukolsky, 'Problem Book in Relativity and Gravitation'

21. P.C.Vaidya, Phys.Rev 83 10 (1951)

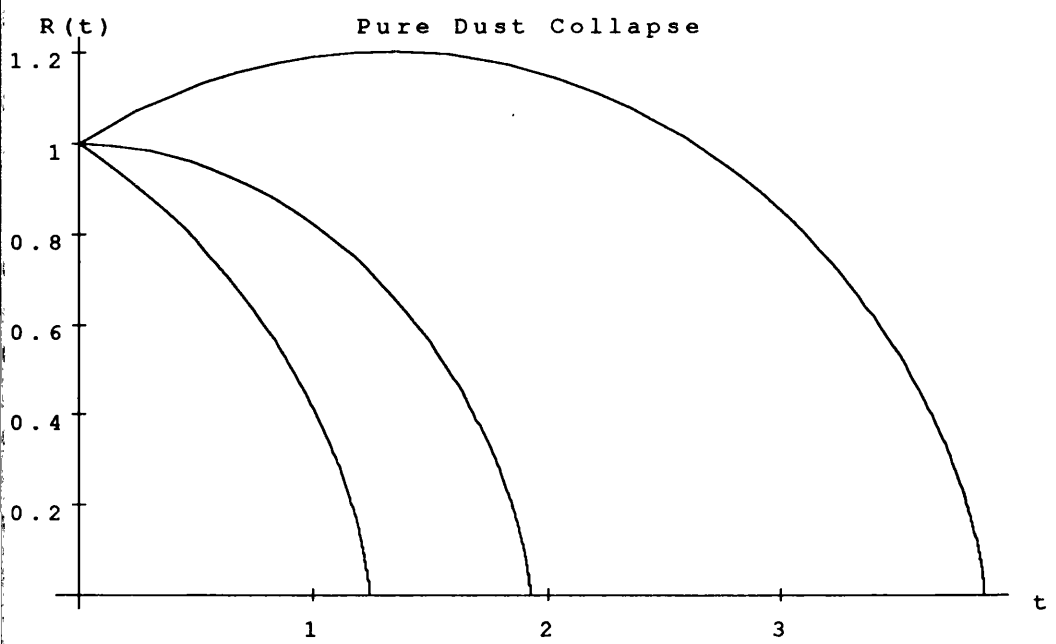

Figure 3.1

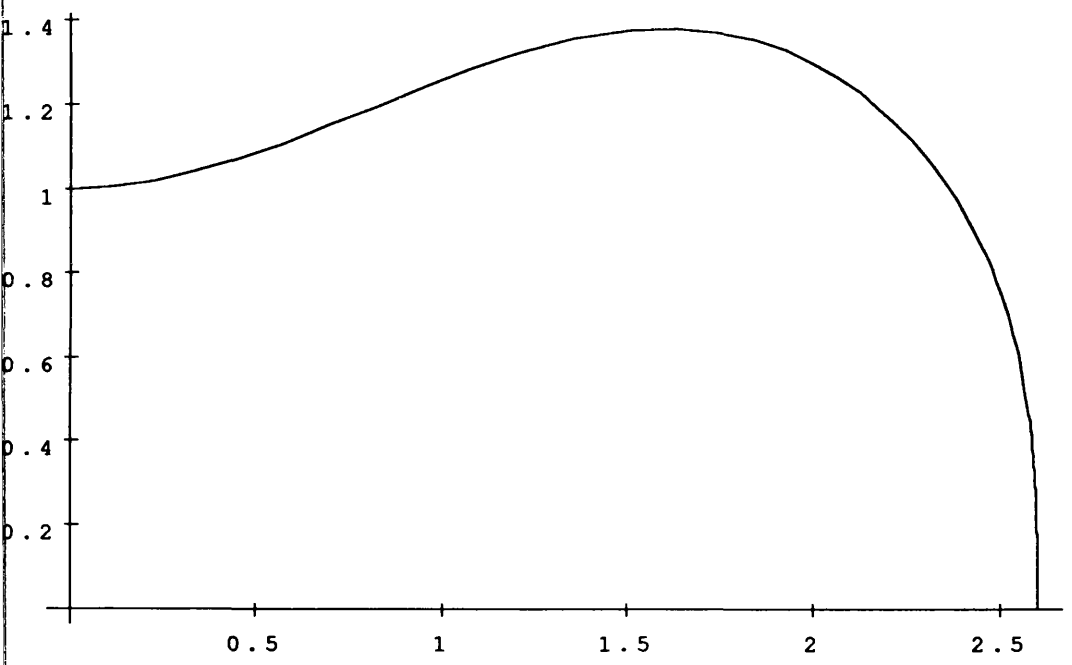

Figure 3.2

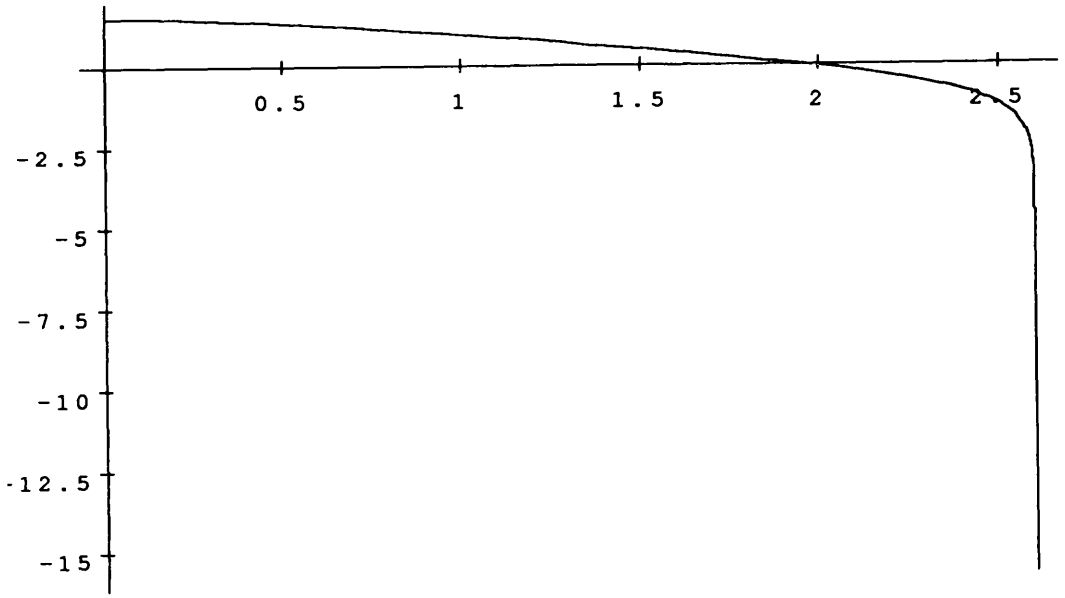

Figure 3.3

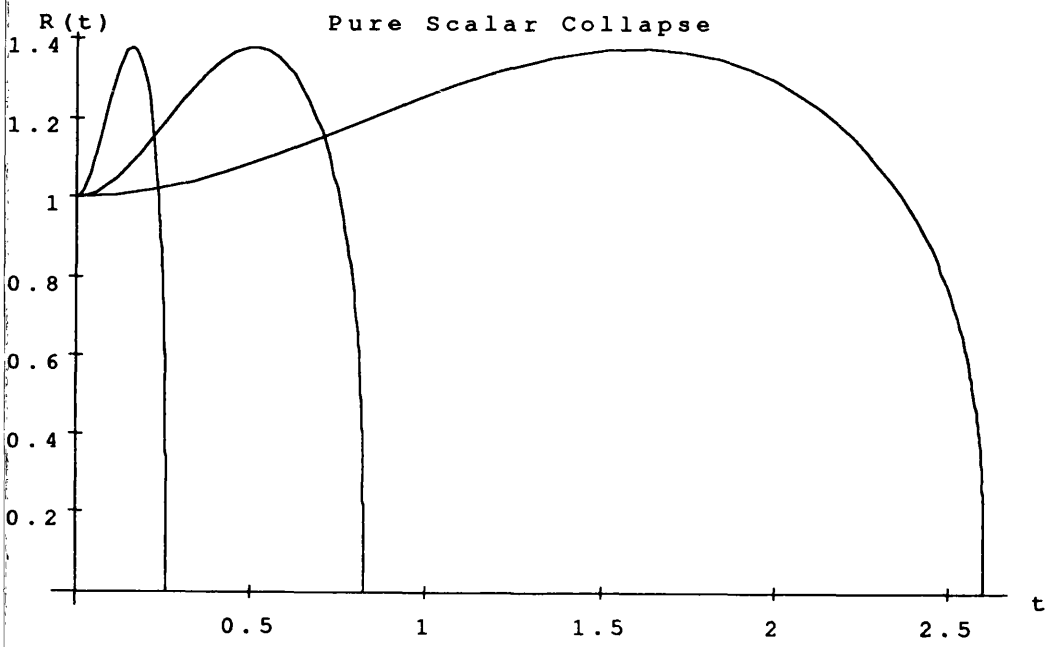

Figure 3.4

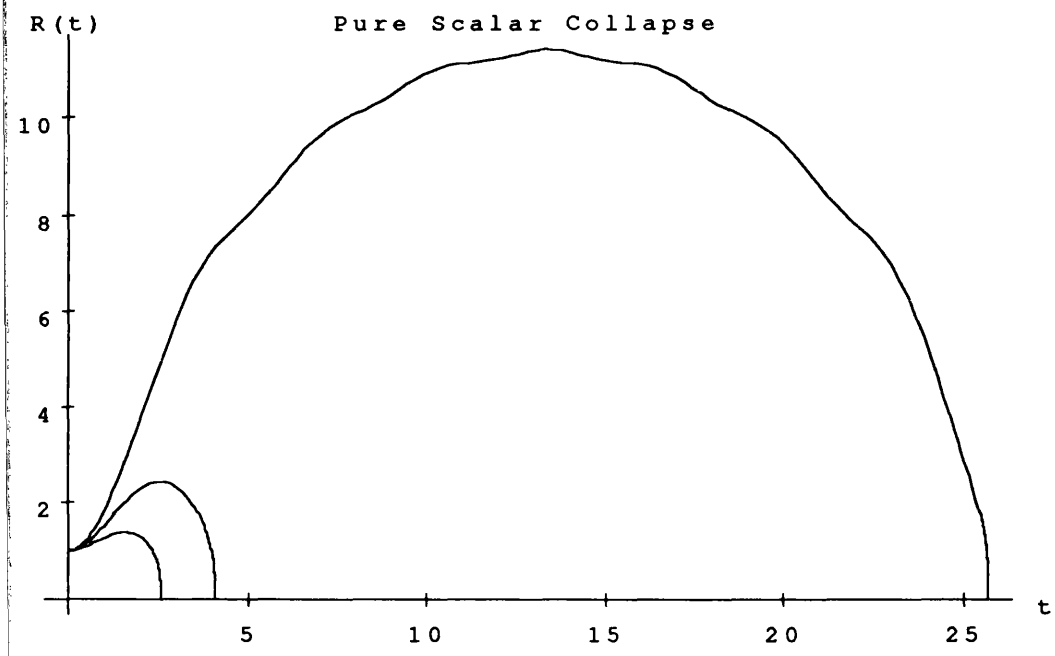

Figure 3.5

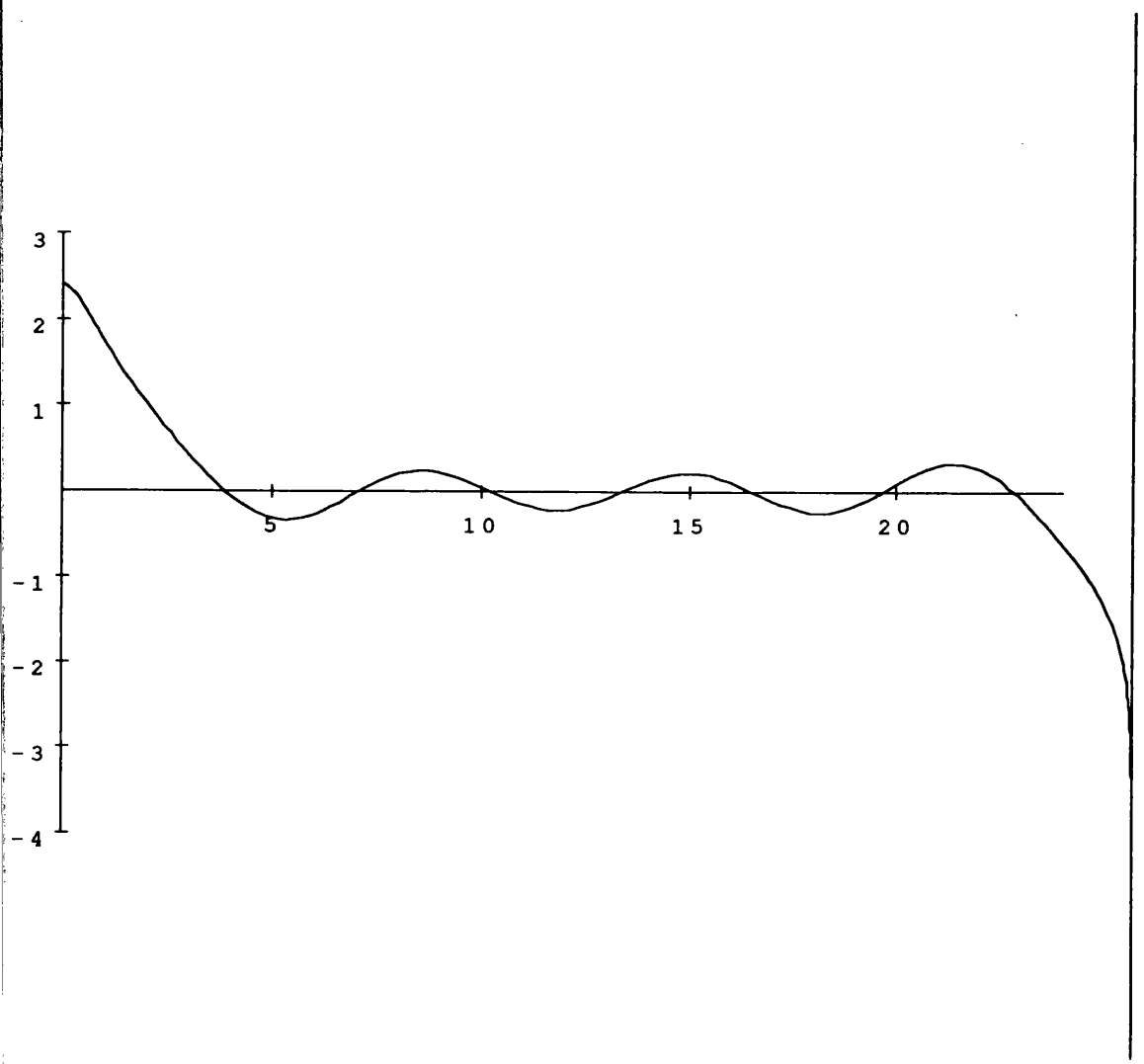

Figure 3.6

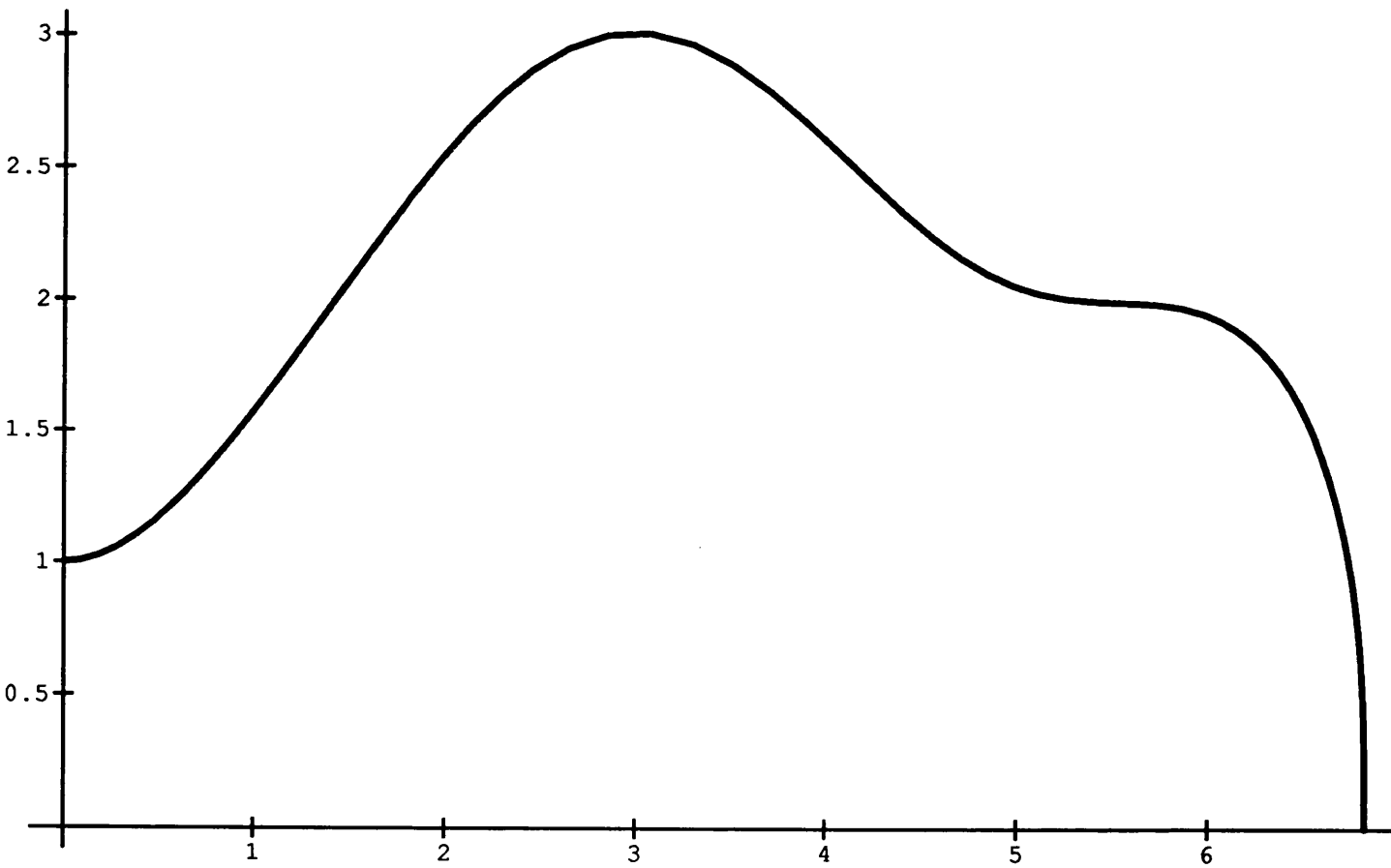

Figure 3.7

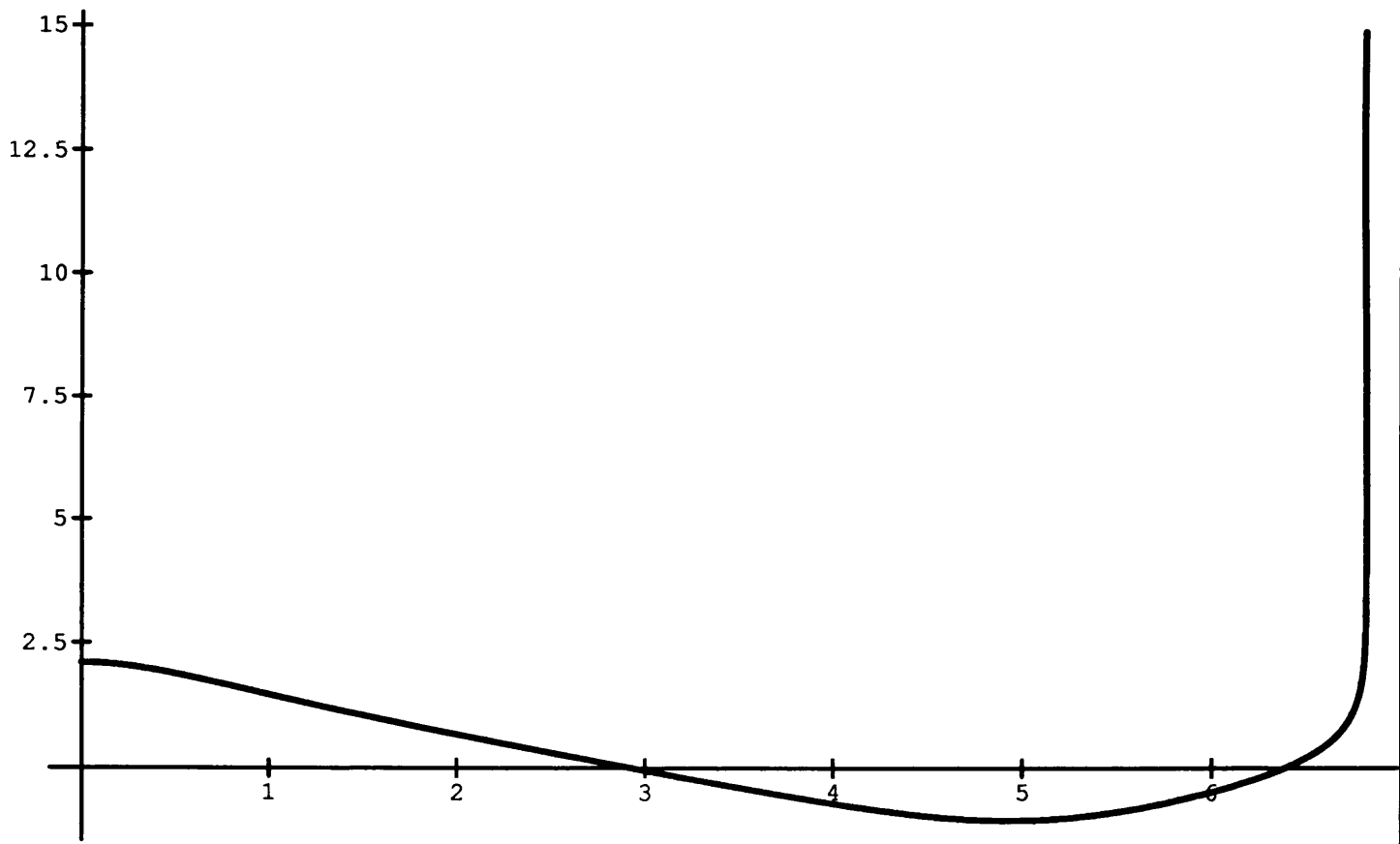

Figure 3.8

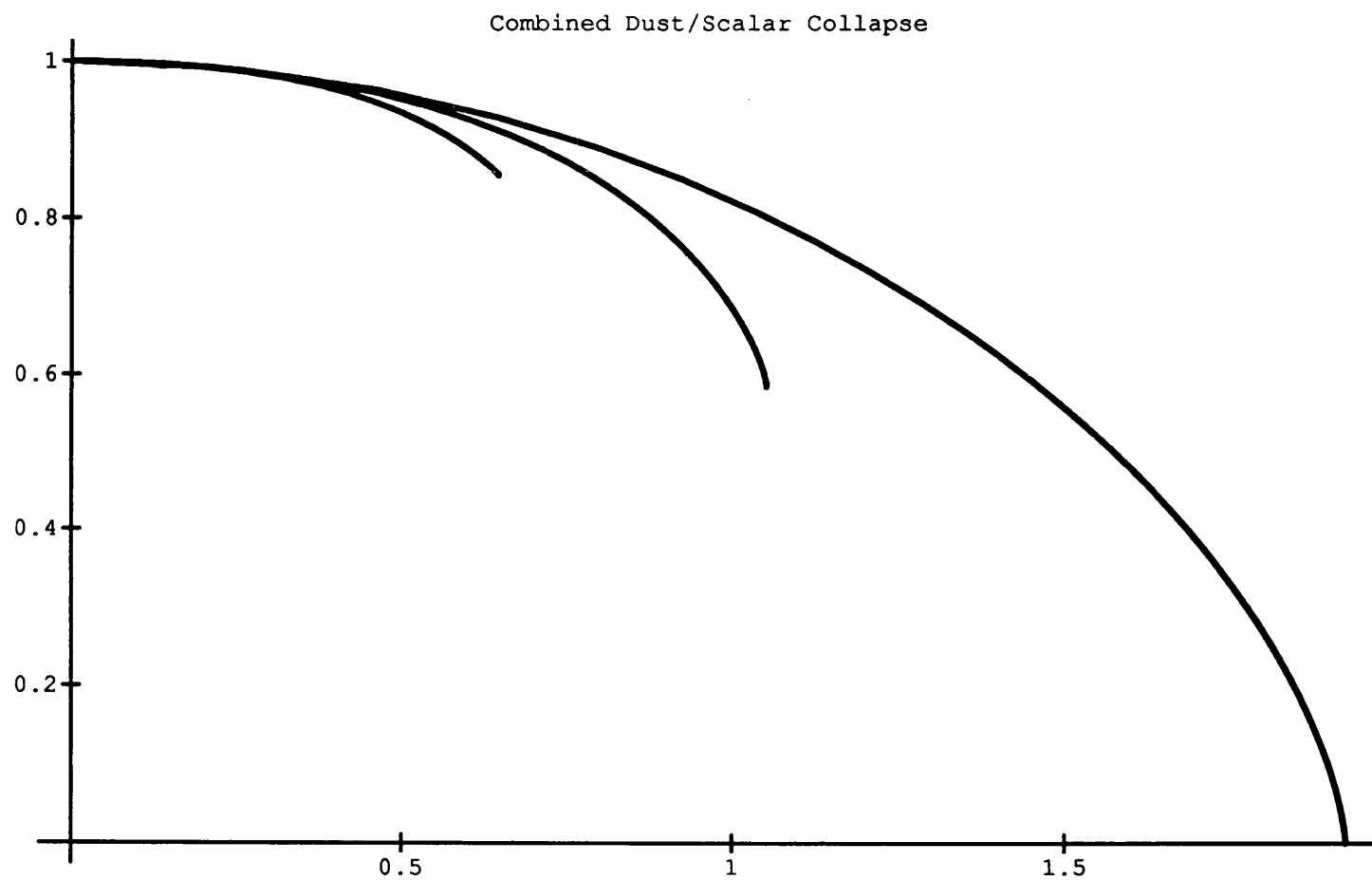

Figure 3.9

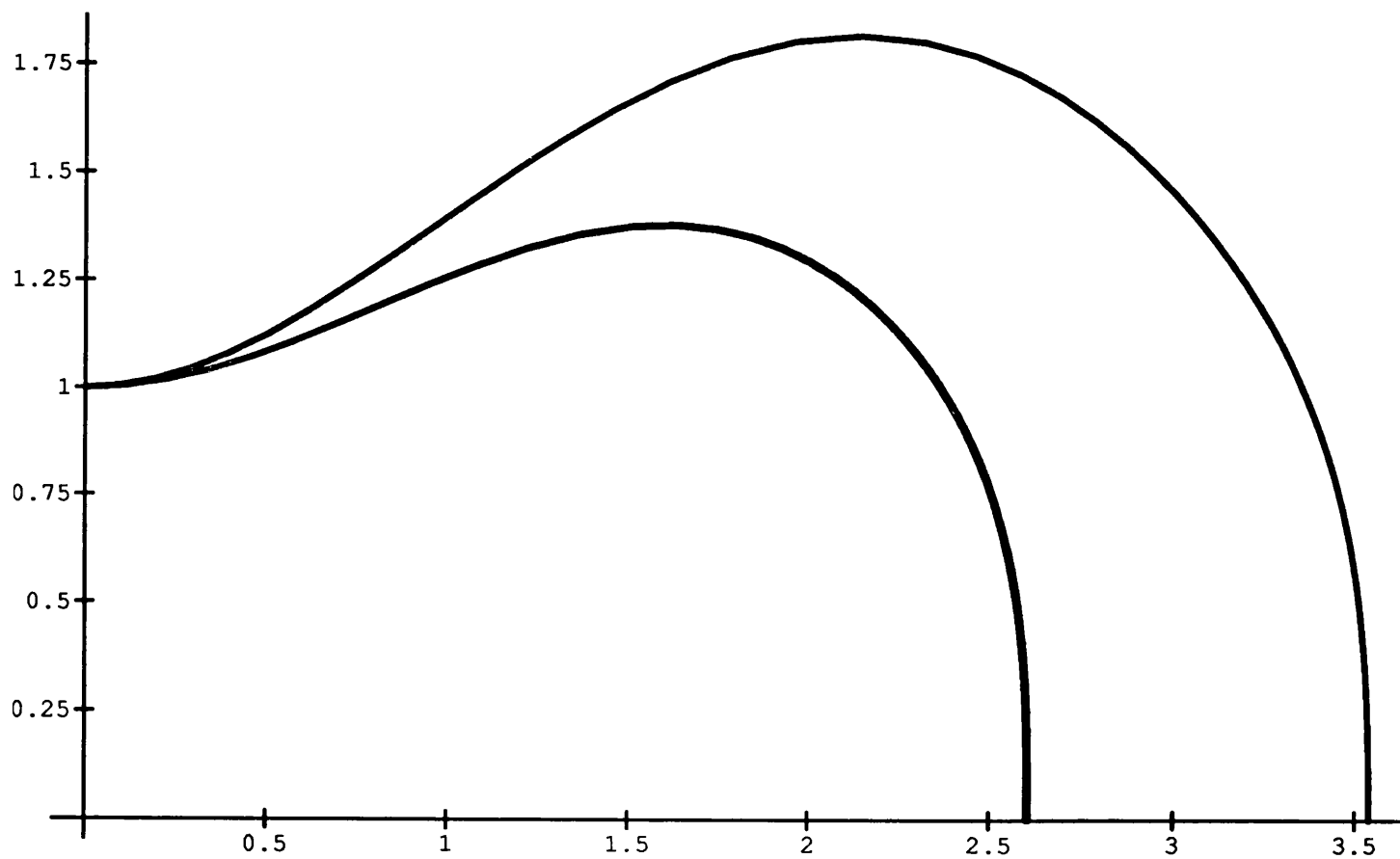

Figure 3.10

Overview and Conclusion

The object of this thesis was to consider what effects certain postulated fundamental fields could have on the constitution and dynamics of collapsed or collapsing stars. Since these postulated particles, whose origins were explained in the introduction, have a very great uncertainty amongst their defining parameters, it was thought useful to consider the possible modifications to known and surmised properties of neutron star and gravitational collapse models as a function of these parameters. This made for a great deal of labour, examining such alterations over many orders of magnitude of parameter space, but was necessary in enabling a thorough job to be done.

The models considered in this thesis increase rapidly in difficulty as firstly, static, then pulsating, then time-dependent models were considered. The simplest case, that considering the effects of light scalars on static neutron star configurations was examined carefully and thoroughly, though even in this, the easiest case, there were found to be significant difficulties due to the tendency of the scalar field to tail-off over large distances. This 'tailing' behaviour is the most serious and recurrent problem which affects any exhaustive study of the scalar field over very light mass ranges.

The study of the pulsations did not require the intense numerical treatment that was carried out in chapter one, luckily, by consideration of the radiation condition and comparison with works on stability for neutron stars and boson stars, it was possible to work out the possible behaviour of the configurations in the various parameter regions.

The last model considered was that of gravitational collapse itself. Due to the innate difficulty of this study, only a very simple model was considered, though it was hoped that this would be a reliable indicator of any significant modifications due to scalar fields. Interior solutions were and their possible relevance discussed. Here the success was only partial; a rigorous, quantitative interpretation of these solutions was not achieved because of the inability to match the interior solutions to an appropriate exterior. In lieu of this, a critical appraisal of the matching problem was given. The conclusion to this part of the work was that, again, the problem was probably due to scalar 'tails', and that to progress further a more

sophisticated computational approach was required.

To have difficulty with the collapse problem is perhaps unsurprising, it is after all, a very active and challenging field of research; gravitational collapse is the work of a lifetime, not merely a thesis.